# UC Berkeley
## UC Berkeley Electronic Theses and Dissertations

**Title**

Controlling Ring-Opening Alkyne Metathesis Polymerization as a Pathway Toward Conductive Polymers

**Permalink**

https://escholarship.org/uc/item/7sp898jh

**Author**

Bellone, Donatela Elsa

**Publication Date**

2016

Peer reviewed|Thesis/dissertation

Controlling Ring-Opening Alkyne Metathesis Polymerization as a Pathway Toward Conductive
Polymers

By

Donatela Elsa Bellone

A dissertation submitted in partial satisfaction of the

requirements for the degree of

Doctor of Philosophy

in

Chemistry

in the

Graduate Division

of the

University of California, Berkeley

Committee in charge:

Professor Felix R. Fischer, Chair
Professor Robert G. Bergman
Professor T. Don Tilley
Professor Ana C. Arias

Fall 2016

Abstract

Controlling Ring-Opening Alkyne Metathesis Polymerization as a Pathway Toward Conductive Polymers
by

Donatela Elsa Bellone

Doctor of Philosophy in Chemistry

University of California, Berkeley

Professor Felix R. Fischer, Chair


Although alkene metathesis has found a wide range of applications since its discovery in the mid-1960s, alkyne metathesis has only recently become the focus of attention. Despite recent synthetic advances toward highly functionalized ring-strained alkynes, the application of ring-opening alkyne metathesis polymerization (ROAMP) to the field of polymer synthesis has remained limited due to the lack of commercially available well-behaved catalysts. Previous attempts at synthesizing polymers using ring-opening of strained alkynes showed polydispersities ranging from 1.1 to 7.0. Polymers resulting from these catalysts tend to have higher molecular weights than predicted on the basis of the monomer to catalyst loading.

The pseudo-octahedral molybdenum benzylidyne complex [TolC≡Mo(ONO)(OR)]·KOR (R = CCH$_3$(CF$_3$)$_2$), featuring a stabilizing ONO pincer ligand, initiates the controlled living polymerization of strained dibenzocyclooctynes at T > 60 °C to give high molecular weight polymers with exceptionally low polydispersities (PDI ~ 1.02). Kinetic analyses reveal that the growing polymer chain attached to the propagating catalyst efficiently limits the rate of propagation with respect to the rate of initiation ($k_p/k_i$ ~ 10$^{-3}$). The reversible coordination of KOCCH$_3$(CF$_3$)$_2$ to the propagating catalyst prevents undesired chain-termination and -transfer processes. The ring-opening alkyne metathesis polymerization with 1 has all the characteristics of a living polymerization and enables, for the first time, the controlled synthesis of amphiphilic block copolymers via ROAMP.

Semiconducting π-conjugated polymers have been widely explored as functional materials in advanced electronic devices. Among these materials, poly(phenylene ethynylenes) (PPEs), a class of conjugated polymers featuring a pattern of alternating aromatic rings and triple bonds, have stood out for their stability, moderate fluorescence quantum yields, and readily tunable band gap. The classical syntheses of PPEs rely on step-growth polymerizations based on either transition-metal-catalyzed cross-coupling

reactions or alkyne cross-metathesis (ACM). While these strategies benefit from readily accessible monomers, they lack the precise control over degree of polymerization (Xn), molecular weight, end-group functionality, and polydispersity index (PDI) unique to a controlled ring-opening alkyne metathesis polymerization (ROAMP) mechanism.

Molybdenum carbyne complexes [RC≡Mo(OC(CH$_3$)(CF$_3$)$_2$)$_3$] featuring a mesityl (R = Mes) or an ethyl (R = Et) substituent initiate the living ring-opening alkyne metathesis polymerization of the strained cyclic alkyne, 5,6,11,12-tetradehydrobenzo[a,e][8]annulene, to yield fully conjugated poly- (o-phenylene ethynylene). The difference in the steric demand of the polymer end-group (Mes vs Et) transferred during the initiation step determines the topology of the resulting polymer chain. While [MesC≡Mo(OC(CH$_3$)(CF$_3$)$_2$)$_3$] exclusively yields linear poly(o-phenylene ethynylene), polymerization initiated by [EtC≡Mo- (OC(CH$_3$)(CF$_3$)$_2$)$_3$] results in cyclic polymers ranging in size from n = 5 to 20 monomer units. Kinetic studies reveal that the propagating species emerging from [EtC≡Mo(OC(CH$_3$)(CF$_3$)$_2$)$_3$] undergoes a highly selective intramolecular backbiting into the butynyl end-group.

As the field of ring-opening alkyne metathesis polymerization continues to grow, there is an increase in interest for controlling terminations, and understanding undesirable ones. Attaching a desirable end-group expands the potential applications of the polymerization by adding a new degree of functionalization. Addition of water to the alkylidynes studied herein results in the formation of free radicals, leading to a variety of products. In order to control the termination, ynamines may be used for the regioselective termination of molybdenum benzylidyne catalysts, such as [RC≡Mo(OC(CH$_3$)(CF$_3$)$_2$)$_3$] (R = Tol, Mes) and [TolC≡Mo(ONO)(OR)]·KOR (R = CCH$_3$(CF$_3$)$_2$). Quantitative termination is accomplished and proper functionalization of the polymers is achieved.

# Table of contents

To my family,
who constantly supported me
and sacrificed everything for my future,
and, specially,
to Alumine,
who is our guardian angel

# Acknowledgments

Our accomplishments have not been achieved due to our sole efforts. I believe that every success can be attributed to the ongoing support of role models, family, teachers, and friends. In particular, the principal investigator in the research project serves as an advisor, supporter, guidance, and inspiration. My PhD advisor, Professor Felix R. Fischer, has surpassed my expectations as a dissertation chair and mentor. It is not common for an untenured professor to support their student's full exploration of subjects and careers, inside and outside of the lab. He supported my research in the electrical engineering department, and transition into the job world. I am thankful to have had Felix as my P.I.

Secondly, I am thankful to Professors Robert G. Bergman, T. Don Tilley, and Ana C. Arias, for kindly agreeing to be my dissertation committee and being part of my qualifying exam committee. They have provided direction throughout my PhD career, and have served as ongoing sources of encouragement.

A large portion of your PhD career involves working closely with other people. I am thankful for the support and companionship of Justin Bours and Patrick Gorman, who became much more than colleagues. Moreover, every member of the Fischer group at one point or another has helped me with an instrument, a concept, or a material. It is this kind of teamwork that allows graduate students to succeed.

Finally, like many people, I wouldn't be where I am without the ongoing support of my family: my parents who made the sacrifice of leaving their home country to give me a better future; my sister for being a warrior in life and a source of inspiration; and my husband for excelling at being present when I need him the most. Their encouragement and ongoing understanding is present whenever I need it. Your belief in me is all I need.

# 1 Introduction

## 1.1 Alkyne Metathesis Chemistry and *Poly*(phenylene ethynylene)s

Conjugated polymers containing C≡C in their backbone have gained interest due to their potential application in organic light-emitting diodes (OLEDs), organic photovoltaic devices (OPVs), thin-film transistors (TFT), foldamers, and sensors.[1] A notable group of polymers are poly(phenylene ethynylene)s (PPEs) which are constituted of acetylenic links between aromatic groups in a π-conjugated system. These polymers possess air and photophysical stability, and moderate fluorescence both in film and in solution.[2] Poly(arylene ethynylene)s have been synthesized by Pd-Cu-catalyzed coupling reactions and Heck-Cassar-Sonogashira-Hagihara reaction of diethynylbenzenes and dihaloarenes since 1975.[1,3-6] Some complications associated with such reactions were the low control over the molecular weight dependent on solvent, formation of back-to-back ethynyl moieties even under strict air-free conditions, several termination reactions, dehalogenation, ill-defined end-groups, and the presence of phosphorus and palladium impurities. Additionally, due to the step-growth nature of this reaction, the polydispersity indices (PDIs) may be as high as 1.3 to 7.8.[3] It was not until 1997 that Weiss et al. proved that PPE may be synthesized by the alkyne metathesis of triple bonds via acyclic diyne metathesis (ADIMET) using Schrock's alkylidyne catalyst **1** (Scheme 1-1).[7] Although larger molecular weights may be achieved by ADIMET, certain challenges still remain. The catalyst was unselective due to its inability to energetically distinguish between the monomer alkynes to those in the polymer backbone. As a result, termination side reactions and scrambling of the chain result in cyclic polymers and polydisperse samples with PDIs as large as 1.3 to 6.9.[1,3,8,9]
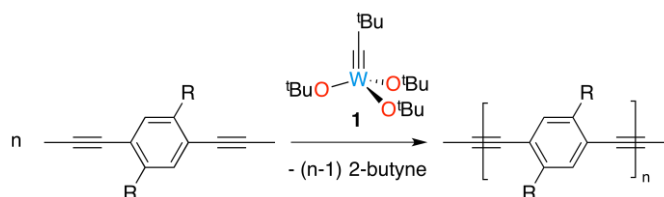


**Scheme 1-1.** Acyclic diyne metathesis may be employed to synthesize PAEs.[10]

Recently, the synthesis of PPE via living ring-opening alkyne metathesis polymerization (ROAMP) has been demonstrated.[11] Unlike ring-opening metathesis polymerization of strained alkenes, ROAMP has not been as well established due to the scarcity of catalysts, limited amount of synthetically accessible substrates, and poor understanding of the mechanism. Although some noteworthy catalysts have been studied, Schrock's tungsten alkylidyne and Fürstner's complexes remain the only commercially available catalysts to date. Recently, a new wave of strained cyclic alkynes have been synthesized, opening a path to novel polymeric materials.[12-15] Although alkyne metathesis is almost 50 years old, ROAMP has only recently been proven to proceed in the well behaved way required for the synthesis of complex polymers.[16]

This chapter will cover the area of synthesis via ROAMP, development of catalysts, and new mechanistic perspectives. We will discuss alkyne metathesis in its relation to ROAMP, historically, synthetically, and mechanistically. We will focus on the chronological progression of ROAMP, from its discovery to the well-awaited living ROAMP and its applications. Finally, we will summarize the key mechanistic and thermodynamic aspects of the reaction, finishing with the outlook for ROAMP.

## 1.2 History of Alkyne Metathesis

### 1.2.1. Early Discoveries of Heterogeneous and Homogeneous Catalysts

Although alkyne metathesis is not as well established as olefin metathesis, it has proven to be useful for a wide variety of applications including alkyne cross metathesis (ACM), ring-closing alkyne metathesis (RCAM), acyclic diyne metathesis (ADIMET), and ring-opening alkyne metathesis polymerization (ROAMP). Fürstner demonstrated the wide applicability of RCAM in the synthesis of natural products containing a cyclic alkyne or alkene in E or Z geometry after reduction of the alkyne.[17] Bunz, Moore, and Zhang have reported the synthesis of conducting polymers, solvophobic foldamers, cages, and sensors by applying ADIMET.[2,3,7-9,18-24]

However, it was almost 50 years ago that alkyne metathesis by a heterogeneous tungsten system was discovered. Pennella et al. reported the alkyne metathesis of pent-2-yne by tungsten oxide supported on silica in 1968 (Scheme 1-2).[25] They observed the presence of but-3-yne and hex-3-yne in a ratio of 1.0 to 1.2 and polymeric materials with a loading of 6 to 8% catalyst on silica in cyclohexane at 200 to 400 °C. This catalyst required activation in dry air at 600 °C. With the current knowledge we have of group 6 metals bound to alcohols, one may consider this activation to be pertinent in order to form the nitrido complex of tungsten(VI) on silica which in turn was reactive for alkyne metathesis.[26-28]
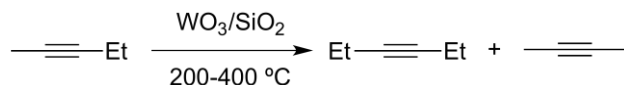


**Scheme 1-2.** Alkyne metathesis by Pennella's heterogeneous system.

It was not until six years later that the first homogeneous alkyne metathesis was reported. Mortreux et al. showed that the mixture of molybdenum hexacarbonyl and phenol was effective as the catalyst for the alkyne metathesis of aromatic alkynes (Scheme 1-3).[29] In a typical reaction, p-tolylphenylacetylene was added to molybdenum hexacarbonyl (1 eq.) and resorcinol (6 eq.) in decalin and heated to 160 °C. After 3 hours, the approximate equilibrium composition of products was observed with the ratio of p-

tolylphenylacetylene : diphenylcetylene : di-p-tolylacetylene being 55:23.5:21.5. The reaction showed dependence on the amount of resorcinol used, and was possible with α-naphthol. This system was widely used due to the availability of its "off the shelf" reagents, though it is still limited by low functional group tolerance and high temperatures.[9]
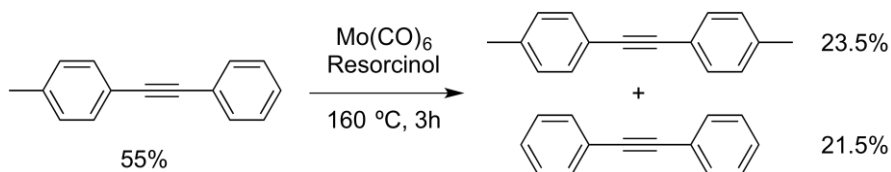


**Scheme 1-3.** Mortreux's off the shelf alkyne metathesis catalyst.


*1.2.2 First Well-Defined Homogeneous System and Isolation of the Metallacyclobutadyene*

In 1981, Wengrovius et al. reported the first instance of alkyne metathesis by a well-defined tungsten alkylidyne catalyst [Me$_3$C≡W(OCMe$_3$)$_3$] **1**.[30] This study confirmed that the activity of these complexes was analogous to that of Schrock alkene metathesis catalysts. Indeed, alkyne metathesis was possible using alkylidyne complexes, supporting the notion that previous ill-defined systems may at one point proceed via reactive alkylidyne species. The metathesis of various aromatic and alkyl acetylenes was confirmed with rates in the range of 0.017 to 300 min$^{-1}$ (Scheme 1-4). Those alkynes containing two aromatic groups were the slowest at alkyne metathesis while 3-heptyne was the fastest. Perhaps this was the first hint of the reactivity of tungsten alkylidyne catalysts having a strong preference for sterically unhindered alkyl acetylenes over aromatic substrates. Finally, Wengrovious et al. reported the selectivity for these catalysts for alkynes over alkenes, a reactivity that is to this day still highly desired as it allows for a the stereospecific synthesis of alkenes.[31]
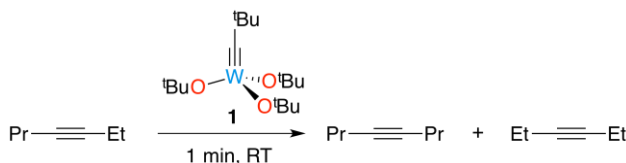


**Scheme 1-4.** First well-defined alkylidyne alkyne metathesis catalyst.


Soon after, McCullough and Schrock discovered alkyne metathesis catalyzed by [Me$_3$C≡Mo(OMe(CF$_3$)$_2$)$_3$(DME)].[32] The molybdenum analog of the previously reported tungsten catalyst, [Me$_3$C≡Mo(OCMe$_3$)$_3$], did not react with 3-heptyne to give alkyne metathesis. Instead, early products were polymers formed via the ring expansion of a metallacyclobutadiene intermediate. Unfortunately, it was necessary to activate the catalyst by incorporating electron withdrawing alkoxides such as OMe(CF$_3$)$_2$. Although

4

the metallacyclobutadiene formed from [EtC≡Mo(2,6-C$_6$H$_3$($^i$Pr)$_2$)$_3$] was observed by $^1$H NMR, it was not until a year later that the material was isolated and characterized by X-ray crystallography.[33] These noteworthy papers, which appeared at the same time as contributions by Churchill et al. and Freudenberger et al., demonstrated that addition of excess of 3-hexyne to [Me$_3$C≡W(O-2,6-C$_6$H$_3$($^i$Pr)$_2$)$_3$] and [Me$_3$C≡W(OCH(CF$_3$)$_2$)$_3$] formed the metallacyclobutadienes [Et$_3$C$_3$W(2,6-C$_6$H$_3$($^i$Pr)$_2$)$_3$] and [Et$_3$C$_3$W(OCH(CF$_3$)$_2$)$_3$], respectively.[33,34] The X-ray structure of the trigonal bypyramid/square pyramidal intermediate [Et$_3$C$_3$W(O-2,6-C$_6$H$_3$($^i$Pr)$_2$)$_3$] shows an asymmetric metallacyclobutadiene W(1)C(1)C(2)C(3) with bond lengths of 1.949(9), 1.433(14), 1.467(14), and 1.883(10) for W(1)–C(1), C(1)–C(2), C(2)–C(3), and C(3)–W(1), respectively. Finally, mechanistic experiments revealed the decay of [Et$_3$C$_3$W(O-2,6-C$_6$H$_3$($^i$Pr)$_2$)$_3$] in the presence of 3-hexyne. A positive ΔS$^‡$ suggests that the rate determining step is the cycloreversion of the metallacyclobutadiene.

Up to this point, only high-valent Schrock alkylidyne catalysts had been shown to be active in alkyne metathesis. In contrast, formal Fischer type carbynes such as [PhC≡WBr(CO)$_4$] were unreactive.[35,36] The interest in alkyne metathesis waned until Laplaza et al. reported the cleavage of dinitrogen by Mo[N(R)Ar]$_3$, (R = C(CD$_3$)$_2$CH$_3$, Ar = 3,5-C$_6$H$_3$Me$_2$) (**2**) in 1996.[28] Three years later, Fürstner investigated these systems and their reactivity towards alkynes.[37] Although the trisamido complex did not participate in alkyne metathesis, one of the many products that result from its addition to dichloromethane did result in the disproportionation of alkyl and aromatic acetylenes. The article supported the claim that ClMo[N(R)Ar]$_3$ (**3**) and not HC≡Mo[N(R)Ar]$_3$ is responsible for the reactivity of the mixture. Several molecules were ring-closed with 60–91% yields.

### 1.2.3. Reductive Recycling Synthesis of Trisamido Alkylidyne Complexes

In the following years, researchers from the group of Cummins published new syntheses of alkylidyne complexes from a known metallaaziridine-hydride complex, Mo(H)($\eta^2$- Me$_2$CNAr)(N[$^i$Pr]Ar)$_2$ (Ar = 3,5-C$_6$H$_3$Me$_2$), that proved to be efficient as alkyne metathesis initiators. [38,39] However, it was Zhang and Moore's study on reductive recycling that built a pathway for new catalysts.[40] The synthesis of EtC≡Mo[N(R)(Ar)]$_3$ (**4**), (R = tBu, Ar = 3,5-C$_6$H$_3$Me$_2$) was reported in 91% yield with the use of 2 equiv. of 1,1-dichloropropane in the presence of excess magnesium (Scheme 1-5). The alkaline earth metal was used as a reductant that reverted the byproduct **3** back to the starting material **2**. Upon addition of trifluoro-*o*-cresol or perfluoro-*tert*-butyl alcohol, a catalytically active complex was formed.
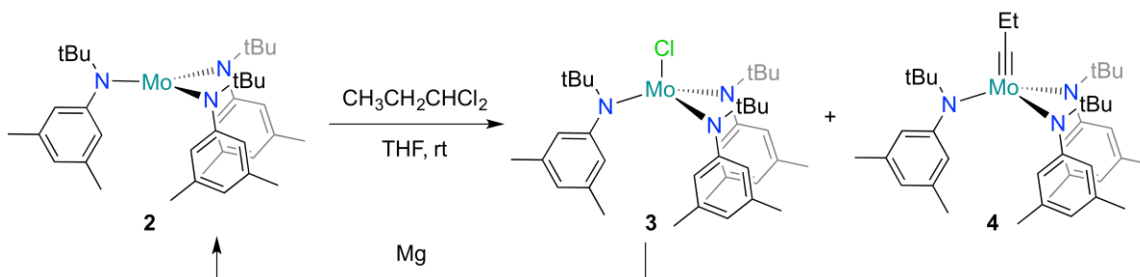
**Scheme 1-5.** Reductive recycling enabled large-scale synthesis of precatalyst **4**.

Soon after, Zhang et al. reported the alkyne metathesis by trialkoxymolybdenum(VI) alkylidyne complexes and the effect of alkynyl substituents, ligands, and substrates.[41] As expected, the presence of sterically bulky alkynyl substituents resulted in lower yields, with no yield from the attempted metathesis of 4-(3,3-dimethylbut-1-yn-1-yl)benzonitrile. Additionally, the rate of the reaction was enhanced by the presence of nitro groups in the phenol ligand, while it was deterred by trifluoromethyl-substituents. Finally, electron donating alkynes were metathesized with a greater yield. The Mo(VI) catalyst is an electrophile, and thus electron rich substrates result in higher yields. It is worth mentioning that the cross alkyne metathesis of 2,2′-dithienylethynylene was achieved with 91% yield by employing p-nitrophenol as a ligand. This reactivity opened pathways to a variety of electronically interesting thiophene polymers. Zhang et al. published the synthesis of poly(2,5-thienyleneethynylene)s with 97–98% yield and a PDI of 2.0 – 2.7. [42] Soon afterwards, the multigram synthesis of arylene ethynylene macrocycles driven by the precipitation of arylene byproducts was reported from the same group.[19]

### 1.2.4. Podand Phenoxide Ligands

The synthesis of a highly active alkyne metathesis catalyst employing a podand ligand motif was reported from the group of Wei Zhang.[43-45] Addition of the chelating ligand **5** to **4** afforded the dimer [EtC≡MoL]$_2$ and 6 equiv. of the amine [N(tBu)(3,5-(CH$_3$)$_2$C$_6$H$_3$)] (Scheme 1-6). Additionally, exploration of ligands with methylated nitrogen and with H or Br in place of the nitro group served to provide further understanding of the catalysis. The complex with the methylated ligand, [EtC≡Mo(OC$_6$H$_4$CH$_2$)$_3$NCH$_3$I]$_2$ resulted in the highest functional group tolerance and reactivity in the alkyne metathesis of 4-nitropropynylbenzene reaching 64% conversion, an improvement from catalysts bearing bromine and unsubstituted ligands.
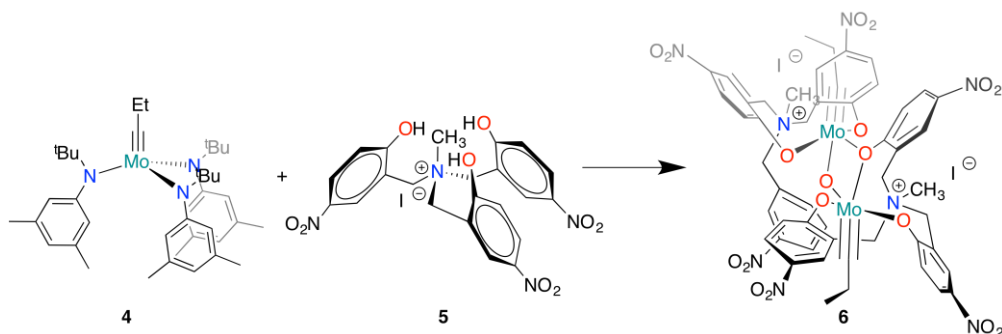
**Scheme 1-6.** Synthesis of catalyst with a podand moiety **6**.

With a catalyst loading of 3 mol%, the ring-closing alkyne metathesis of di(pent-3-yn-1-yl)adipate and the alkyne cross metathesis of 1-methoxy-4-(prop-1-yn-1-yl)benzene was achieved in 95% and 94% yield, respectively. It was no surprise that the presence of electron withdrawing groups in the propynylbenzene alkynes resulted in lower yield compared to those with electron donating groups. Originally, it was hypothesized that the coordination of the central nitrogen in the tetrapodal ligand effectively blocks a binding site, and thus prevents side reactions such as alkyne polymerization by chain expansion reported as early as 1984.[32] However, the catalysts with methylated amine groups resulted in the greatest yields, and instead, the authors claimed that the podand motif, rather than the coordinating amine, is responsible for the high selectivity. This may be attributed to the entropy driven chelating effect of the ligand and/or the steric blockage of substrates. In the presence of a large excess of 2-butyne no alkyne polymerization was observed. Furthermore, the monodentate analogue of **6** was not as stable and became inactive within the first few hours of metathesis with 4-propynylanisole. Although no explanation was provided in the article about the enhanced group tolerance of the quaternized complex, the improvement in reactivity was thought to be caused by the decrease in electron density at the metal center. Future studies investigating the increase in group tolerance would provide valuable insights to further tune alkyne metathesis catalysts.

### 1.2.5. Push-Pull Ligand Sphere in Alkyne Metathesis

A new catalyst design utilizing an imidazolin-2-imide ligand in conjunction with 1,1,1,3,3,3-hexafluoro-2-(trifluoromethyl)propan-2-oxides was reported by Beer et al.[46] Complete conversion in the RCAM of 6,15-dioxaeicosa-2,18-diyne (**7**) was achieved in 120 min at a 2 mol% loading of catalyst **8** (Scheme 1-7). Computational studies of the system suggest that the rate-limiting step is the cycloaddition of the alkyne with the alkylidyne. In comparison, the rate determining step for Schrock's [EtCW(O-2,6-C6H3(iPr)$_2$)$_3$] catalyst was the cycloreversion of the metallacycle.
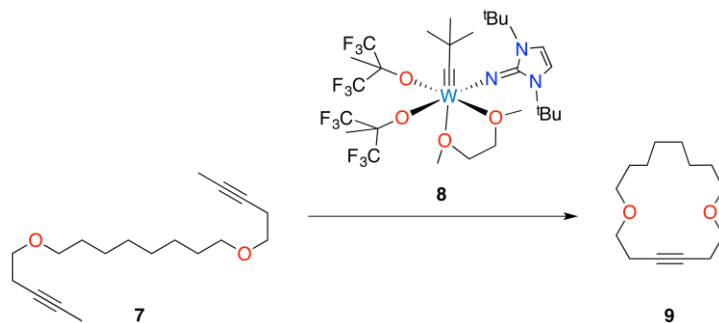
**Scheme 1-7.** Ring-closing alkyne metathesis with catalyst **8**.

According to DFT calculations, the inclusion of the imidazolin-2-imide effectively lowers the activation barrier of the metathesis of 2-butyne by 6.8 kcal/mol. The authors claim that such a difference was mostly an enthalpic effect, and the pertinence of having a push (imidazolin-2-imide) and a pull (1,1,1,3,3,3-hexafluoro-2-(trifluoromethyl)propan-2-oxides) ligand to ensure highly active alkyne metathesis catalysts. Recent studies into the nature of the W≡C bond with push-pull chelating ligands suggest that such a ligand sphere increases the nucleophilicity of the α-carbon.[47] Although monodentate donating ligands tend to donate to the $d_{xy}$ orbital, tridentate ligands donate directly to the W≡C bond. Furthermore, the complex **8** was proven to be an efficient alkyne metathesis catalyst of 1-phenylpropyne in hexane under reduced pressure (300 mbar).[48]

### 1.2.6. Active Nitrido Complexes and Bench-Top Stable Pre-Catalysts

In 2007, Geyer et al. reported an improved nitrile alkyne cross metathesis (NACM), compared to those of Schrock's and Chisholm's.[27,49-51] Synthesis of symmetrical alkynes was achieved with up to 100% yield by exposing the tungsten catalyst **10** to benzonitriles in conjunction with excess 3-hexyne. After removing volatiles from the solution, further activity of the reaction mixture resulted in the formation of 3-hexyne and subsequent alkyne polymerization.
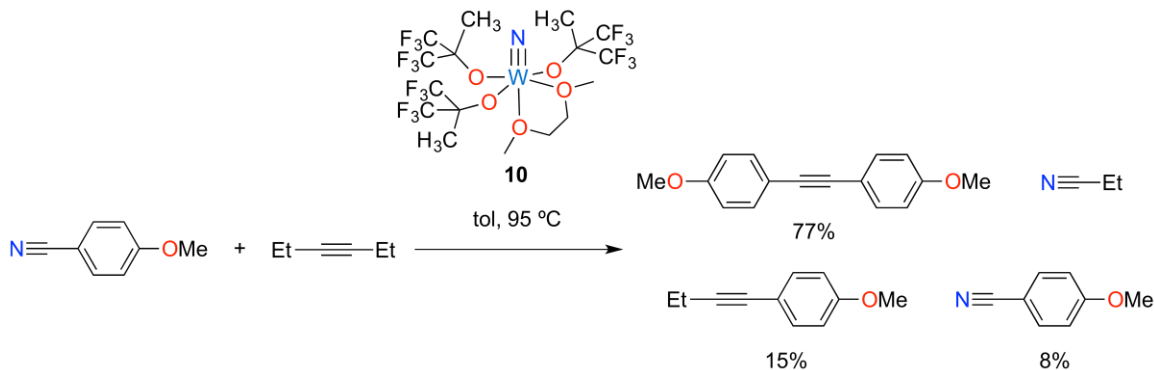


**Scheme 1-8.** Nitrile-Alkyne Cross-Metathesis of 4-methoxybenzonitrile by **10**.

It is worth noting that such reactivity is possible in the presence of electron donating alkoxide. High valent group(VI) nitrido complexes tend to be unreactive for alkyne metathesis due to their high stability. Using alkoxides with lower electron donating capabilities, the relative thermodynamic energies of the alkylidyne and nitride complexes are almost equivalent. Another approach to alkyne metathesis by nitrido complexes was reported by Finke et al.[52] Alkyne metathesis of 1-phenylbutyne was achieved by $N\equiv Mo(OSiPh_3)_3$ activated with the borane $B(C_6F_5)_3$.

In 2009, Fürstner reported a group of novel nitrido catalysts which were significantly more reactive than the widely used Schrock catalyst $(^tBuO)_3WCCMe_3$ (**1**).[53-55] Adducts of $N\equiv Mo(OSiPh_3)_3(L)$ (L = pyridine, 1,10- phenanthroline, 2,2'-bipyridine) (**11**) were minimally active for alkyne metathesis unless they were activated with $MnCl_2$ or another Lewis acid, while the weakly bound diethyl ether adduct required no Lewis acid activation (Scheme 1-9). These complexes possess high stability ($N\equiv Mo(OSiPh_3)_3(phen)$ is indefinitely bench-top stable) and functional group tolerance. An exception is their reactivity with aromatic aldehydes, which react in a stoichiometric "redox metathesis" to form aromatic nitriles. The nitride complexes are not believed to be active species, but, in turn, they act as a reservoir of inactivated catalyst which allows these complexes to remain active at 80 ºC over several days. Moreover, the use of 5 Å sieves further increases their reactivity by sequestering 2-butyne byproducts resulting in yields in the range of 84 – 99% for alkyne cross metathesis. Overall, the triphenylsilanolate ligands are thought to be ideal for ACM as their large size prevents chain growth alkyne polymerization and bimolecular termination. Their high Mo-O-Si angle flexibility allows for facile reorganization of the ligand sphere and adjustment of electron donation. Furthermore, their weakly donating capabilities allow for the catalyst to be electrophilic enough, and are an improvement from the commonly used (fluorinated) alkoxides.
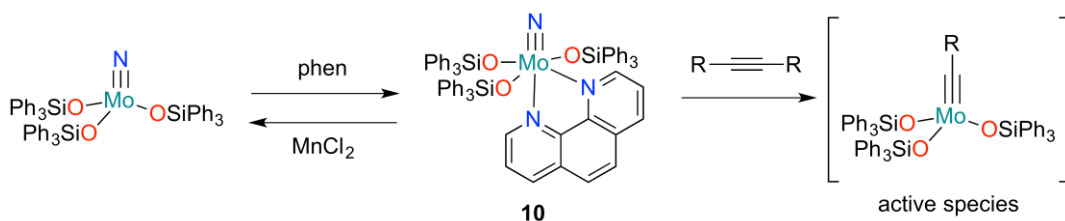


**Scheme 1-9.** Activation of precatalyst **10** by a Lewis acid and an alkyne leads to the active species.

Triphenylsilanolate were also employed in the synthesis of complexes of the type $ArC\equiv Mo(OSiPh_3)_3(L)$ (L = bipy, phen, 2,2'-bipyrimidine) where activation of the nitride group is avoided.[55] Incorporation of a *p*-methoxybenzylidyne group allows for the large scale synthesis of $MeOC_6H_4C\equiv Mo(OSiPh_3)_3$ upon slow addition of $KOSiPh_3$ to

MeOC$_6$H$_4$C≡MoBr$_3$(DME). Such a selectivity was not seen in the synthesis of PhC≡Mo(OSiPh$_3$)$_3$ where a significant portion of the ate complex was observed. Perhaps this is a crucial aspect of the synthesis of alkoxide carbyne complexes, where even in a stoichiometric reaction the ate-complex is formed. However, the presence of the electron donating methoxy group on the aromatic carbyne results in a strong trans influence. Additionally, the donor free complex significantly outperforms the ate-complex and leveled off after 20 min with over 50% conversion. Heppekausen et al. reported that all complexes of the type [(X≡Mo(OSiR'$_3$)$_3$] (X = N, CR; R = aryl, alkyl, R' = aryl) can be stabilized as the 1,10-phenanthroline,2,2'-bipyridine adduct. These complexes are unreactive toward air and do not participate in alkyne metathesis, but may be activated with Lewis acids such as ZnCl$_2$ and MnCl$_2$ as bipyridine sequestrators. The alkyne metathesis of phenylpropyne yielded tolane in 99% yield with preactivated 5 mol% MeOC$_6$H$_4$C≡Mo(OSiPh$_3$)$_3$(phen) with 5 mol% of MnCl$_2$, and 5 Å sieves at ambient temperature. Nitrido complexes, N≡Mo(OSiPh$_3$)$_3$, and pyridine adducts, ArC≡Mo(OSiPh$_3$)$_3$(L), allow to the synthesis of air-stable and user-friendly catalysts to expand the scope of alkyne metathesis.

## 1.3 Synthesis of Relevant Alkyne Metathesis Catalysts

This section will cover the synthesis of the most prominent alkyne metathesis catalysts. An example of an alkylidyne complex synthesized via the high-valent route is Schrock's alkyne metathesis catalyst **1**.[56-60] This catalyst may be accessed by first incorporating the alkylidyne via the addition of neopentyl Grignard to trimethoxytungsten(VI) chloride (**11**) forming **12**. Addition of hydrochloric acid forms the trihalide complex **13**. Finally, ligand exchange with lithium tert-butoxide yields alkyne metathesis catalyst **1**. Alternatively, one may access this catalyst by forming the dimer **15** by ligand exchange from **14**, and then cleaving the W≡W bond via alkyne metathesis.
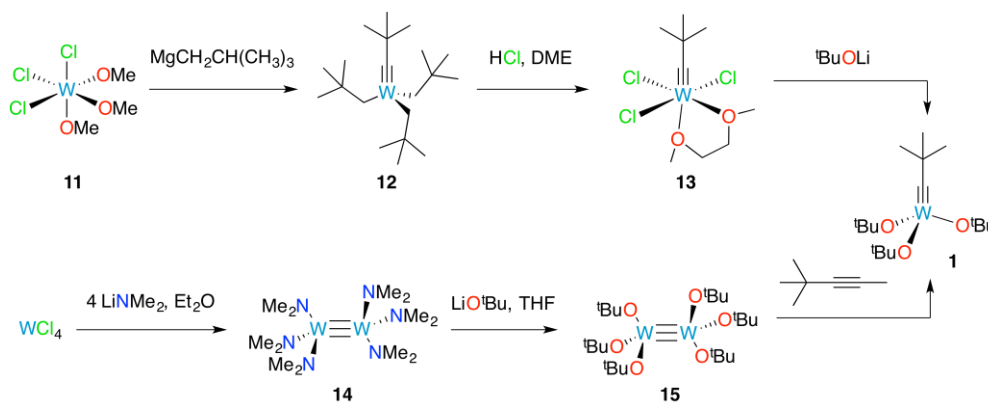


**Scheme 1-10.** Two routes for the synthesis of Schrock's catalyst **1**.

Another well-established route starts from the readily available molybdenum hexacarbonyl and proceeds through a low-oxidation state route.[61-64] The acyl complex **16** is oxidized with oxalyl bromide and bromine, leading to intermediate **17**, which is not active in alkyne metathesis. Ligand exchange with potassium alkoxides gives rise to an active alkyne metathesis catalyst **18**. The low-oxidation state route allows for facile modification of the benzylidyne and alkoxide, and access to catalysts with heteroleptic ligand spheres. The later route is more atom economic, easier to prepare, and pertinent for the synthesis of molybdenum and tungsten complexes.
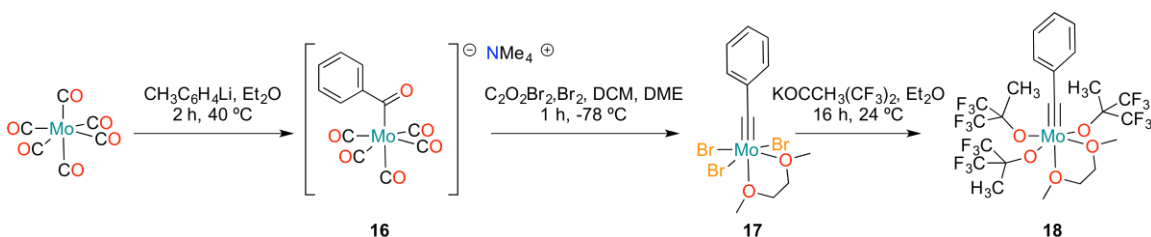


**Scheme 1-11.** Low oxidation route to alkyne metathesis catalyst **18**.

It is worth noting that catalyst **18** may be further modified by exchanging the alkoxides for other ligands, as long as these are more electron donating or chelating.[16,46] A surge in the interest of alkylidyne catalysts for alkyne metathesis in the mid-2000s arose from the newly discovered synthesis of the alkylidyne-tris-amido complex **4**.[12,15,37,38,40,65] The precatalyst formed from **19** allowed for facile ligand exchange with an off-the-shelf alcohol, driven by the thermodynamic stability of the product. However, the active catalyst and the variety of products from the addition of the alcohol to the complex are not well-defined. Moreover, the synthesis is challenging, and intermediate **2** is sensitive to air, water, and nitrogen.[28] However, it played an active role in the advancement of ROAMP.
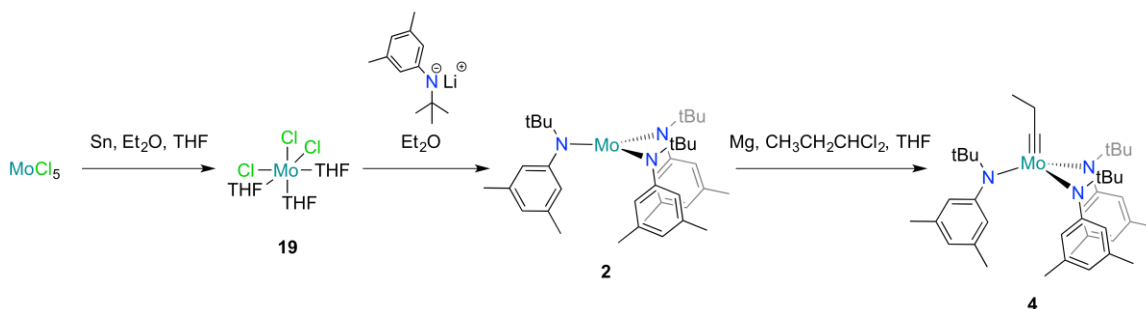


**Scheme 1-12.** Synthetic route to precatalyst **4** via reductive recycling of complex **2**.

A large scale and easily accessible route to alkyne metathesis catalysts was reported by Gdula et al.[66] Complex **20** was first reported by Schrock et al. as an alkyne metathesis catalyst via the route shown in Scheme 1-13.[67] However, the route reported by the Johnson group was facile, scalable, and reliable.[66] The alkyne metathesis required to form the product from the nitrido complex **21** proceeds over several days at high temperatures yielding **20** in 62% yield.
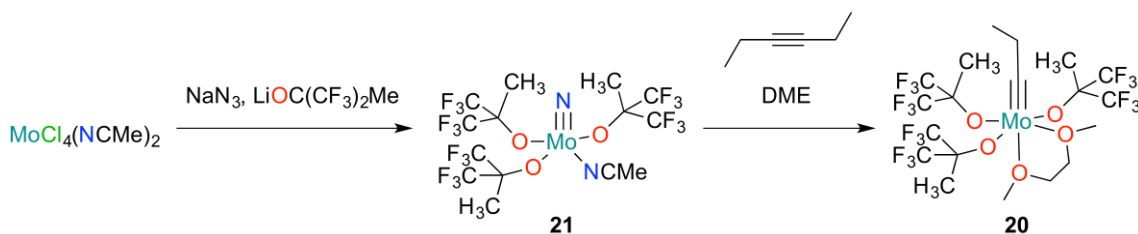


**Scheme 1-13.** Scalable synthesis of propylidyne **20**, a catalyst with an active role in the development of ROAMP.

Finally, the synthesis of the air stable precatalyst **10** was reported by Heppekausen et al.[55] The presence of the phenanthrine as an active site blocker, and the nitride instead of the alkylidyne, makes this catalyst indefinitely bench-stable. It requires a Lewis acid such as MnCl$_2$ to activate the precatalyst for alkyne metathesis.
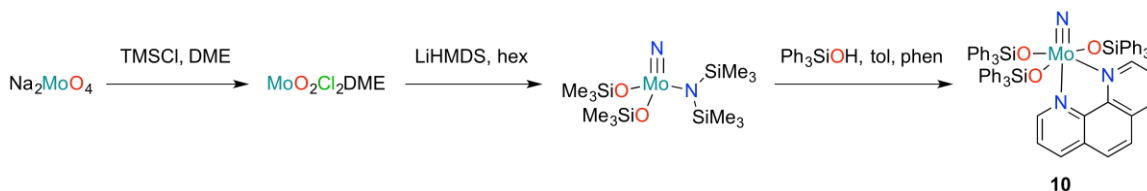


**Scheme 1-14.** Synthesis of air stable precatalyst **10**.

Alkyne metathesis catalysts are accessible via several routes, those we thought to be less pertinent to ROAMP or the field of alkyne metathesis have been excluded from this chapter. Recent advances in the synthesis of air stable, high functional group tolerance, and heteroleptic catalysts have opened the doors for the advancement of ROAMP.

## 1.4 Mechanism of Alkyne Metathesis

In 1975, Katz et al. proposed the mechanism of alkyne metathesis that has been confirmed since then by isolation of intermediates, kinetic studies, and mechanistic investigations.[68] In an editorial letter, Katz suggested that the mechanism of alkyne

metathesis was analogous to that of alkene metathesis as described by Hérisson, and Chauvin.[69] A metal-carbon triple bond and an alkyne proceed through a formal [2+2] addition forming of a metallocyclobutadiene as the key intermediate. Cycloreversion of this intermediate results in a new alkyne and a catalytically active complex which may continue reacting (Scheme 1-15).
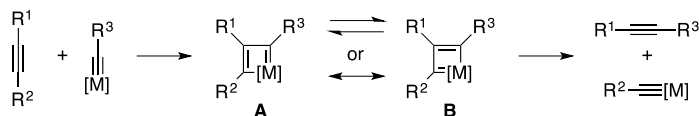


**Scheme 1-15.** Reaction mechanism for alkyne metathesis.

## 1.5 Alkyne Metathesis and Ring-Opening Alkyne Metathesis Polymerization For the Synthesis of Alkyne Containing Polymers

### 1.5.1. Poly-phenylene Ethynylenes via Alkyne Cross Metathesis

Poly(arylene ethynylene)s (PAEs) are a class of polymers with diverse applications in foldamer dynamics, organic light-emitting devices, thin-film transistors, and optical sensors.[70-78]Although these polymers may be accessed by Heck-Cassar-Sonogashira coupling, alkyne metathesis facilitates the synthesis of large molecular weight polymers and presents an alternative for Pd-coupled reactions.[3,8] Great accomplishments in the synthesis of PAEs via alkyne metathesis come from the groups of Swager, Bunz, and Moore.[7,8,24,78,79] Although acyclic diyne metathesis (ADIMET) polymerization proved to be an improvement from the metal-coupled synthesis of PAE, this method lacks control over molecular weight and regioselectivity. Furthermore, the step-growth of polymers via ADIMET results in a wide range of molecular weights. Living ring-opening alkyne metathesis polymerization is a powerful alternative for a well-controlled synthesis of PAEs. The following sections discuss all the reports of ROAMP to date. Table 1-1, located at the end of the chapter, summarizes the key results.

### 1.5.2 First Instance of Ring-Opening Alkyne Metathesis Polymerization

The synthesis of a polycyclooctyne was first reported in 1989 by Krouse et al.[80] Similarly to living ROMP of alkenes, the group of Schrock aimed at discovering the right catalyst for the alkyne analogue. The complex of choice was the dimer **15** due to its ease of synthesis and alkyne metathesis reactivity. Addition of 5-100 equiv. of cyclooctyne to **15** at room temperature resulted in a gelatinous polymer (Table 1-1). The polymeric product was quenched with benzoic acid and methanol. The product was insoluble in toluene, DCM, 1,3,5-trichlorotoluene, 2-dichlorobenzene, and THF, and a characterizable sample was obtained by using 20 equiv. of cyclooctyne. The C≡C resonance in the $^{13}$C NMR shifts from 94.5 to 80.4 ppm. The disappearance of the strained C≡C was further confirmed by IR spectroscopy. Addition of unreacted **15** to the polymer collected resulted

in breakdown and an increase in solubility caused by the alkyne metathesis of the internal triple bonds.

Due to its high insolubility, hydrogenation of the polymer with Rh(PPh$_3$)Cl at 40 ℃ in 60 psig H$_2$ for 16 h in toluene was carried out to yield polyethylene. This polymer was analyzed by size exclusion chromatography and the results are summarized in Table 1-1. A correlation between the equiv. of monomer added and the molecular weight was found, suggesting that the polymerization exhibits a living character. The high polydispersities may be due to hydrogenolysis, slow initiation, chain backbiting, or other modes of quenching of the active species. By mass spectrometry of oligomers, only cyclic polymers were observed.

In order to achieve living ROAMP, the authors attempted using a catalyst with lower metathesis activity, such as PrC≡Mo(O$^t$Bu)$_3$ (**22**). Addition of 15 equiv. of cyclooctyne to catalyst **22** resulted in the presence of the initiated catalyst Pr[C(CH$_2$)$_3$C]$_n$≡Mo(O$^t$Bu)$_3$. The active chains are quenched with 20-fold excess of phenylacetylene. However, the recovered polymeric product consisted mainly of macrocyclic polymers if quenched after more than 2 min. This was not surprising as these catalysts are reactive with unstrained internal alkynes, and are likely react with internal triple bonds along the polymer chain once the monomer has been consumed. The macrocycles observed follow a distribution according to Jacobson-Stockmayer model.[90] Catalyst PrC≡Mo(O$^t$Bu)$_3$ (**22**) was also activate for the ROAMP of cyclohexadecadiyne.

Finally, a new catalyst $^t$BuC≡W(ODIPP)$_3$ (**23**) (DIPP = 2,6-diisopropylphenyl) was tested for the ROAMP of cyclooctyne. Upon isolation of the polymer product, red crystals were isolated which correspond to the metallacyclobutadiene **24** (Scheme 1-16). No further reaction was observed upon adding more monomer to the cyclobutadiene, suggesting that it is a thermodynamic minimum rather than an intermediate.
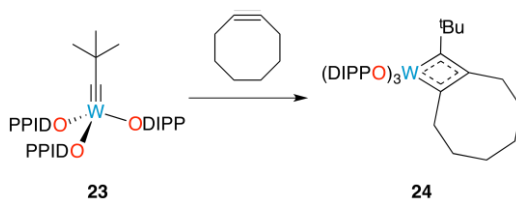


**Scheme 1-16.** Formation of cyclobutadiene thermodynamic sink **24**.

The article by Krouse et al. teaches the first lesson of ROAMP: catalysts active for alkyne metathesis are not suitable for living ROAMP due to their innate nature to react with unstrained alkynes, such as those found in the polymer backbone.

## 1.5.3. Ring-Opening Alkyne Metathesis Polymerization of 1,2,5,6-tetrasilacycloocta-3,7-diynes

In 1994, Zhang et al. reported the synthesis of several poly(disilanylene ethynylene)s (PDSEs) via alkyne metathesis.[81] Polymers of the PDSE type may be conductive after doping with $SbF_5$ vapor, stable under air, and soluble in organic solvents. At the time, the main method for synthesis of PDSE involved anionic ring-opening polymerization of 1,2,5,6-tetrasilacycloocta-3,7-diynes with alkyl lithium reagents. Although high molecular weight polymers may be achieved by this method, usually the molecular weight range obtained was broad.
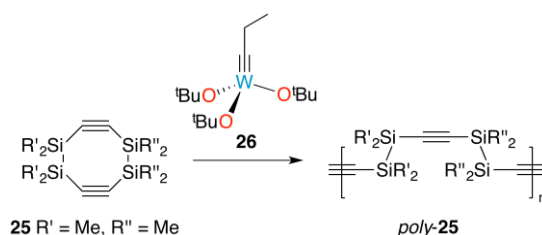


**Scheme 1-17.** Synthesis of PDSE

Alkyne metathesis of 5 equiv. of monomer **25** by $EtC{\equiv}W(O^tBu)_3$ (**26**) reached completion after 30 h at room temperature (Scheme 1-17). However, use of the dimer $W_2(OCF_3Me_2)_6$ (**27**) with 3 equiv. of the monomer **25** resulted in full consumption over 3 h and the formation of *poly*-**25**. The authors claim that qualitatively, the consumption of monomer was faster than that of catalyst, suggesting a slow initiation. Catalysts **26** and **27** were not reactive for the metathesis of bulky monomer **28** (R' = Et, R'' = Et). Instead, in order to minimize steric hindrance, the authors opted to polymerize monomer **28**. Addition of 1.2 equiv. of 2-butyne activates catalyst $W_2(OCF_3Me_2)_6$ (**27**) forming $MeC{\equiv}W(OCF_3Me_2)_3$ (**30**). Alkyne metathesis of **28** with **30** led to *poly*-**28** with an average molecular weight of 4,300 and a modest PDI of 1.4. The significant kinetic effect of the bulky silyl substituents was exploited to regioselectively synthesize a head-to-tail polymer.

Catalyst **30** was added to the substrate **31** (R' = Et, R'' = Me) forming a regioregular soluble PDSE *poly*-**31** as characterized by ^{1}H, ^{13}C, and ^{29}Si NMR. The relative narrow PDI suggests that the reaction is moderately living, but that side reactions such as chain backbiting occur. It may be concluded that the bulkier *poly*-**28** possesses a narrower PDI for its molecular weight, and a more predictable degree of polymerization due to the steric control over backbiting and chain scrambling. Zhang et al. reported a significant sensitivity to steric effects on ROAMP, a lesson that will persist throughout this chapter.

## 1.5.4. Awakened Interest in Ring-Opening Alkyne Metathesis Polymerization

While alkene metathesis has been extensively investigated, the analogous forty-year-old alkyne metathesis is not as well established. The lack of widely available air-stable monomers and commercially available catalysts have hindered the advancement of the ROAMP field. Fourteen years after the initial report of Zhang et al. ROAMP was once again studied. In 2008, Carnes et al. reported the alkyne metathesis of (5Z,11E)-Dibenzo[a,e]cyclooctatetraene (**32**).[82] The reaction proceeded upon addition of catalyst **1** to the substrate **32** and was confirmed by the shift of the alkyne carbon from 108 ppm to 93 ppm in the ^{13}C NMR. Consumption of the monomer **32** was faster than that of **1** in experiments with large catalyst loadings, supporting the notion that the initiation was slower than the propagation. After stirring overnight and quenching with methanol, the polymer was characterized by NMR and GPC. The authors claim that the presence of a *cis* alkyne *ortho* to the alkyne prevents further backbiting into the chain. This suggests that the broad PDI arises from the slow initiation of the catalyst.

## 1.5.5. Ring-Opening Alkyne Metathesis Polymerization by Ruthenium Complex

Almost all of the ring-opening alkyne metathesis polymerization catalysts are exclusively Mo or W; however, in 2009, there was a report of polymerization by Ru.[83] Dr. Macnaughtan published her thesis claiming that $[PCy_3(I)_3Ru{\equiv}CTol]$ (**33**), upon activation with thallium trifluoromethanesulfonate, was capable of polymerizing cyclooctyne. Although, no details were disclosed with regards to the nature of such polymerization, we thought it was worth mentioning to incite interest in group 8 ROAMP catalysts.

## 1.5.6. Ring-Opening Alkyne Metathesis Polymerization by a Push-Pull Complex

In the 2010s, several articles on heteroleptic alkyne metathesis catalysts and imidazolin-2-iminato ligands were published by Tamm.[46,48,64,84-89] In 2010, Lysenko et al. reported the ROAMP, albeit not living, of catalysts **33** and **34**. The reactions were carried out in toluene, n-hexane, or neat.[90] Table 1-1 summarizes what is considered to be the best results. A solution of cyclohexane was added to a solution of catalyst **34** and the resulting mixture was stirred for 16 h at room temperature, followed by quenching with methanol. However, when carried out neat, the reaction was done within 15 min. The products were characterized by size exclusion GPC. Both **33** and **34** perform similarly in neat solutions at 1 mol% with PDIs of 1.4 and 1.6, and yields of 70% and 80%, respectively. Yields as high as 95% were obtained for catalyst loadings of 5 mol%. When the reaction was carried out in toluene, the percent yield dropped significantly, but achieved a PDI of 1.2. However, at concentrations as low as 0.02 M no polymers were obtained. Like many reports up to this point, the polymeric material contains both linear polymers and cyclic polymers following Jacobson-Stockmayer (JS) theory. The data supported the notion in JS theory that at lower concentrations formation of cyclic polymers is favored.
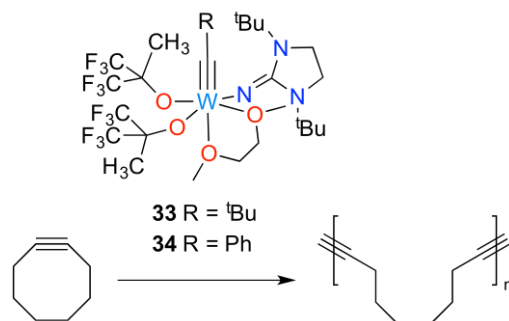
**Scheme 1-18.** Ring-opening alkyne metathesis polymerization of cyclooctyne by the heteroleptic catalysts **33** and **34**.

While it is curious to see this concentration dependence, it calls to attention the subtle balance between yield and selectivity for most ROAMP catalysts. It is expected that at low concentrations, the catalyst is less likely to react with another polymer chain, and instead back-bites into its own chain, resulting in a larger relative amount of cyclic polymers. The shutdown of ROAMP activity at concentrations lower than 0.03 M may be a sign of either slow kinetics (unlikely based on the alkyne metathesis reactivity of this catalyst for alkyne metathesis), decomposition of the active species by trace air/water, or termination due to side reactions such as alkyne polymerization and ring chain-growth.[91] A word of caution should be mentioned when interpreting these results. The polymers, to our knowledge, were never characterized by NMR, and therefore ring-opening may not be the mode of polymerization. However, based on our experiments with analogous complexes, we believe that cyclooctyne was indeed ring-opened.

*1.5.7. Living Ring-Opening Alkyne Metathesis Polymerization*

In 2010, Fischer et al. published the first report of living ROAMP.[12] In this article, a variety of catalysts and activating ligands were studied systematically to inspect the kinetic and thermodynamic principles of ROAMP. Furthermore, the authors described the scalable synthesis of an accessible, soluble, and easily functionalizable cyclocctyne, 3,8-dihexyloxy-5,6-dihydro-11,12-didehydrodibenzo[a,e][8]annulene (**35a-c**), (Scheme 1-19). According to DFT calculations, the HOMO and the LUMO of **35** lies in the plane of the phenyl ring. It is suggested that the catalyst will attach on the face of the alkyne, and not on its side.

Initially, the authors investigated the alkyne metathesis of **35** with the standard catalyst for alkyne metathesis, Schrock's alkylidyne **1**. Catalyst **1** quantitatively ring-opens **35a-c** instantaneously forming *poly*-**35a-c**. This reaction led to high molecular weight polymers with PDIs of 1.4 − 2.6. The degree of polymerization exceeds the equiv. by ~6 − 10 times, indicating a slow initiation. However, the polymerization exhibits a

linear relationship between molecular weight and the conversion of the monomer, suggesting the expected chain-growth behavior for substrates **35b-c**.
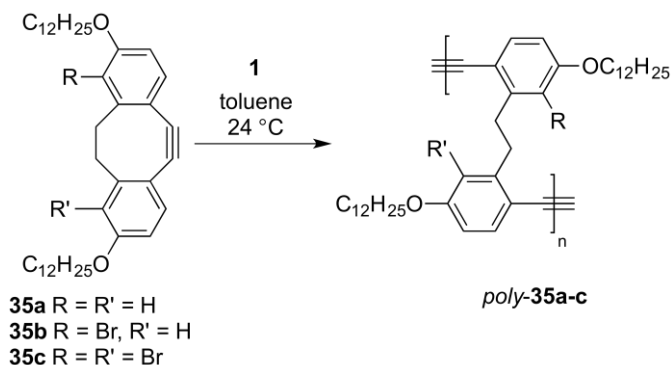


**Scheme 1-19.** Living ROAMP of substrates **35a-c** by **1**.

With the synthesis of the precatalyst EtC≡Mo[N(R)(Ar)]$_3$ (**4**), (R = tBu, Ar = 3,5-C$_6$H$_3$Me$_2$), the authors sought to study ROAMP using 19 different activating alcohols with **35c** in a 1:5:3 **4/35c**/alcohol ratio. The molecular weights obtained range from 19,300-1,020,000 and the PDIs from 1.1 to 3.1. The best catalysts according to narrow PDIs were those activated with 2-nitrophenol (**36**), 3-nitrophenol, and 3,5-bis(trifluoro-methyl)phenol (Table 1-1). In particular, the catalytic mixture (**36**) formed from the precursor and 2-nitrophenol possessed the smallest molecular weight of 19,300, suggesting a smaller discrepancy between the rates of initiation and propagation. Considering that upon addition, it was not guaranteed that all of the complexes formed were active, this may suggest that the propagation was slower than the initiation. Furthermore, the PDI and molecular weight of the polymers in the reaction mixture do not change over time, supporting the notion that this is a living system without any chain back biting or scrambling. To further test their hypothesis, the authors performed ROAMP with **36** by adding additional monomer **35c** in 40 s intervals, and taking intermediate aliquots to characterize the reaction mixture. They observed an incremental increase in molecular weight and decrease in PDI, as it is expected for a living system.

Although no direct correlation between the pKa of these alcohols and the PDI was found, one may conclude that more acidic alcohols, considered more electron withdrawing, result in narrower PDIs overall. Perhaps this is a result of fast initiation, although some possess high molecular weight and low PDIs, suggesting the opposite. The active species is unknown, and based on experiments conducted in our lab, there are several alkylidyne species present in solution upon activation, resulting in smaller catalyst loadings. Moreover, no correlation was observed between the molecular weights and the acidity of the alcohols. Finally, we believe that the catalytic mixture **36** which was activated by 2-nitrophenol gives a better PDI than that one activated by 3-

nitrophenol due to bonding by the oxygen in the nitro group. Such a chelating effect may block an active site preventing termination reactions, or sterically hindering alkyne polymerization.

### 1.5.8. Chelating Ligands for Ring-Opening Alkyne Metathesis Polymerization Catalysts

A second article was published from the Nuckolls group further exploring the living ROAMP of dibenzocyclooctynes.[15] The presence of a chelating electron withdrawing alcohol enhanced the selectivity of ROAMP catalysts by stabilizing the molybdenum propagating species and preventing alkyne cross metathesis. In the 2012 paper, Sedbrook et al. discuss the importance of the chelating nature of the ligand and the nature of the monomer.

Their first set of experiments involved using various alcohols to understand the kinetics of the ROAMP. In the typical experiment, the catalytic mixture (1:3 **4**/alcohol) was added to the octyne monomer at –78 ºC, and the reaction reached completion within the first 30 s. When summarizing this article, we will first compare the catalyst formed by the activating alcohols' functional groups and substitution pattern. The tris-amido molybdenum alkylidyne complex **4** was activated with 2-nitrophenol, (*E*)-2-((phenylimino)methyl)phenol, and o-cresol (catalysts **36**, **37**, **38**) followed by addition to monomer **39** (Scheme 1-20). The stark difference in reactivity between these was the significant difference in molecular weight and PDIs between **38**, and **36** and **37**. While the polymers formed by **36** and **37** had a molecular weight of 3,800 and 3,900 (and PDIs of 1.4 and 1.2), those formed by **38** had a molecular weight of 62,000 (PDI = 4.3). This observation suggested that the presence of chelating ligands with donating capabilities may suppress a fast propagation by stabilizing the resting state, therefore preventing incomplete initiation. Secondly, the PDI of the polymers formed by **37** was lower than that of **36**, probably due to the enhanced donating capabilities of salicylimine compared to the oxygen in a nitro group. Similar to the report by Fischer et al., iterative addition of monomer resulted in an increase in molecular weight, implying that the catalytic centers remain living even after full monomer consumption. It is worth noting that the GPC of the polymers formed by **36** and **37** exhibit a multimodal distribution which the authors attribute to the resolution of the GPC column, but which is usually seen in the presence of cyclic polymers. Mass spectrometry supports their claim.

**35c** R = R' = Br, R" = C$_{12}$H$_{25}$
**39** R = R' = H, R" = TIPS

*poly*-**35c**
*poly*-**39**
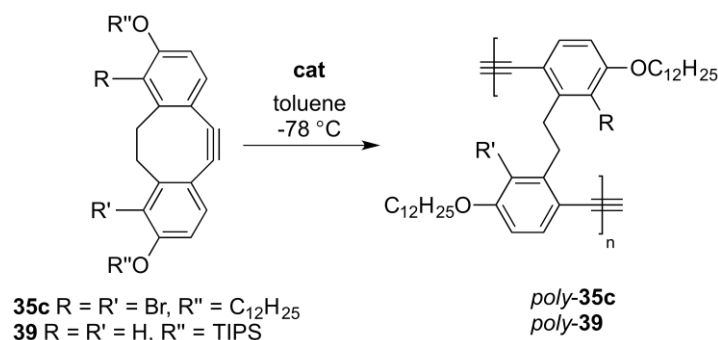
**Scheme 1-20.** ROAMP of monomers **35c** and **39** by various catalysts **36**, **37**, **38**, **40**, and **41**.

The catalysts **40** and **41** formed by adding activating alcohols 4-nitrophenol and (*E*)-4-((phenylimino)methyl)phenol, respectively, with different substitution patterns were also studied. Both of these showed inferior performance by molecular weight (27,000 and 137,000) and PDI (1.5 and 2.2) compared to **37** and **38**. Catalyst **40** outperforms **41**, implying the necessity for an electron withdrawing ligand for fast initiation.

When the reaction was run at room temperature instead of –78 °C, all of the polymers have higher molecular weight except those formed by catalyst **37**. Even at higher temperatures, the salicylimine group inhibited undesirable side reactions after the monomer was consumed.

Finally, the reactivity of all catalysts with a new monomer ((1*R*,8*S*)-bicyclo[6.1.0]non-4-yn-9-yl)methyl 4-methoxybenzoate **42** was studied. Upon addition of the catalysts, **42** was consumed within 5 seconds. The ring opening of **42** was faster than that of **39**, either due to the reactive nature of alkylidyne compared to benzylidyne or larger monomer strain in **42**. After completion, the propagating species for all catalysts except **37** continued reacting and the molecular weight changed over time. This supports once again the hypothesis of the importance of a chelating donating ligand. The PDIs obtained compare to those found with monomer **39**.

In this report, the importance of a donating chelating ligand, and not merely steric hindrance substantially increases the selectivity of the catalysts.
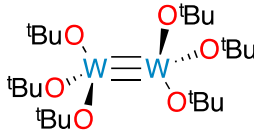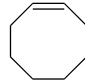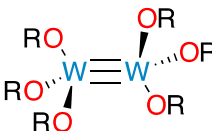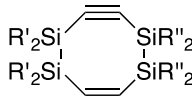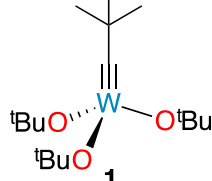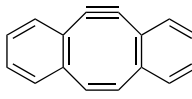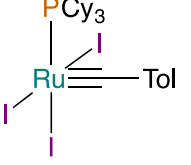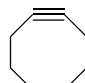
### 1.5.9. Alcohol Promoted Ring-Opening Alkyne Metathesis Polymerization
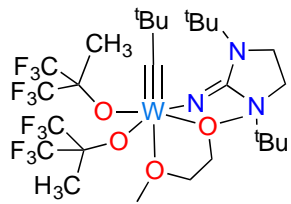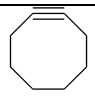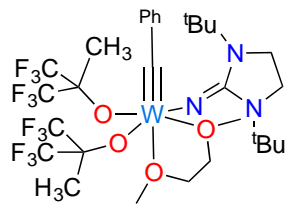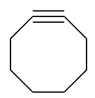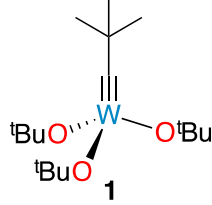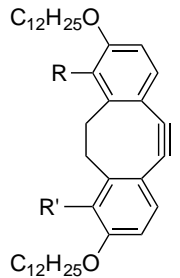
Thus far, all reports of ROAMP have described the use of air and water sensitive catalysts. Interest in air stable catalysts was rising, and Paley et al. reported the first known ROAMP catalyst that is active in wet protic solvents.[65] As mentioned earlier in this chapter, Jyothish et al. reported the synthesis of a dimeric alkyne metathesis catalyst with a chelating ligand.[43] The ROAMP catalyst was synthesized by addition of (tris(2-hydroxybenzyl)amine to **4** to form a dimer **43**. Purified samples of **43** are not as reactive as those with impurities, giving an insight into the reactivity characteristics of this dimer.

20
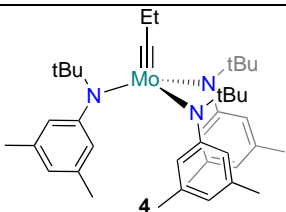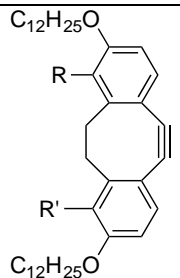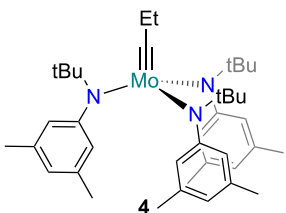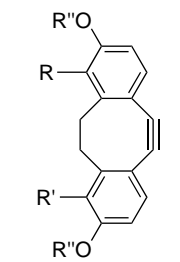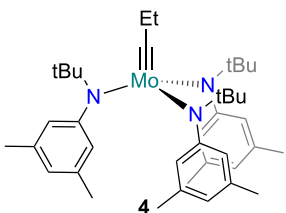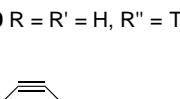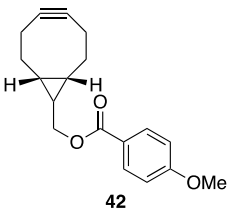
In a solution of toluene/methanol, the complex **43** immediately reacts with the substrate **39** and the catalytic activity does not significantly diminish for 8 h. As compared to Jyothish's system (**6**), **43** does not exhibit molecular weight broadening and larger molecular weights than expected. In methanol, **43** dissociates to form a monomer species bound to methanol (**43a**), amongst others caused by metallocyclobutadiene side reactions, as confirmed by ^{1}H NMR. Moreover, upon concentration of the mixture of **43**, **43a**, and other uncharacterized species, **43** is recovered in 96% yield. Upon addition of a pegylated monomer in methanol, **43a** in solution is instantaneously consumed, although only 55% were initiated. The rest 45%, the authors claim, may be due to side reaction of the metallocyclobutadiene intermediate. Alkyne cross metathesis by **43** was not observed, although the catalyst was consumed.
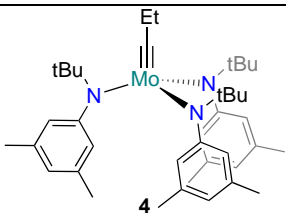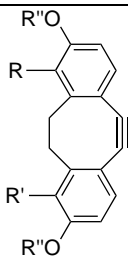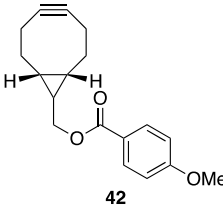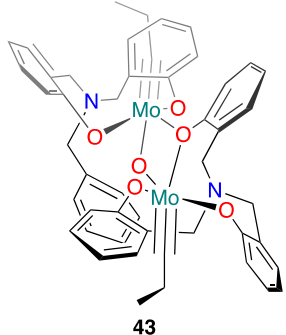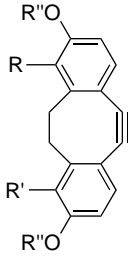
This article changes our notion that alkylidyne catalysts are sensitive to air and water. No sign of protonation is observed. Moreover, this system requires a protic solvent to dissociate, as other σ-donating solvents such as THF do not work. It is difficult to discern what provides **43** its air stability. One may propose that the presence of a donating amine blocks and active site, preventing decomposition.

**Table 1-1.** *GPC analysis was performed on the hydrogenated polycyclooctyne. ** Extrapolated from PDI = Mw/Mn. ***Equiv. to the monomeric dissociated species.

| Entry | Year | Ref. | Catalyst | Monomer | Equiv. | $M_w$ | $M_n$ | $X_n$ | PDI |
|---|---|---|---|---|---|---|---|---|---|
| 1* | 1989 | [80] | **15** | | 250 | 26,000 | 4,300 | 40 | 6.1 |
| | | | | | 350 | 33,000 | 7,500 | 69 | 4.4 |
| | | | | | 500 | 60,000 | 8,600 | 556 | 7.0 |
| 2 | 1994 | [81] | R = CCF$_3$Me$_2$ + butyne **30** | **25** R' = Me, R" = Me | 3 | - | 5,200 | 19 | - |
| | | | | **28** R' = Et, R" = Et | 10 | 6,000** | 4,300 | 11 | 1.4 |
| | | | | **31** R' = Et, R" = Me | - | 43,400** | 31,000 | 92 | 1.4 |
| 3* | 2008 | [82] | **1** | **32** | 36 | 20,330 | 8,470 | 100 | 2.4 |
| 4 | 2009 | [83] | **33** | | - | - | - | - | - |

| | | | | | | | | | |
|---|---|---|---|---|---|---|---|---|---|
| 5 | 2010 | [90] |  **33** |  | 100 | 46,800 | 33,000 | 306 | 1.4 |
| | | |  **34** |  | 100 | 26,400 | 41,300 | 382 | 1.6 |
| 6 | 2010 | [12] |  **1** |  **35b** R = Br, R' = H | 10<br>5<br>2 | 169,300**<br>31,400**<br>18,600** | 65,100<br>19,600<br>13,300 | 100<br>30<br>20 | 2.6<br>1.6<br>1.4 |

| | | | | | | | | | |
|---|---|---|---|---|---|---|---|---|---|
| | | |  **4** +2-nitrophenol **36** |  **35b** R = Br, R' = H | 5 | 21,300 | 19,300 | 30 | 1.1 |
| 7 | 2012 | [15] |  **4** + **37** |  **39** R = R' = H, R" = TIPS | 5 | - | 3,900 | 7 | 1.2 |
| | | | |  **42** | 5 | - | 8,400 | 30 | 1.8 |

| | | | | | | 5 | - | 3,800 | 7 | 1.4 |
|---|---|---|---|---|---|---|---|---|---|---|

Et

tBu—N—Mo····N—tBu

**4**
+2-nitrophenol

**36**

R"O
R

R'

R"O

**39** R = R' = H, R" = TIPS

|  | | | | | | 5 | - | 5,600 | 20 | 1.4 |

H  H

O

OMe

**42**

| 8 | 2013 | [65] | | | | 5*** | - | 5,200 | 9 | 1.6 |

N—Mo—O
O

O—Mo—N
O

**43**

R"O
R

R'

R"O

**39** R = R' = H, R" = TIPS

## 1.6 Conclusion and Outlook

In this chapter, we reviewed the history of alkyne metathesis, with a focus on ring-opening alkyne metathesis polymerization. Unlike alkene ROMP, ROAMP has not received much attention due to the scarcity of substrates and catalysts. There are various ways of synthesizing benzylidyne or alkylidyne complexes active for alkyne metathesis and ROAMP, including the high-oxidation state and low-oxidation state routes.

We reviewed several mechanistic trends of ROAMP. The foremost concept is that of a catalyst that may differentiate between strained and unstrained alkynes, thus being selective and reactive at the same time. First, molybdenum catalysts are less reactive than tungsten catalysts, thus making Mo the metal of choice for ROAMP. Second, we described that alkylidynes tend to be more reactive than benzylidynes. Furthermore, we outline several aspects of the alcohols that play a part in the kinetics of ROAMP. While catalysts with electron withdrawing phenols are more reactive, they also result in faster initiation, and thus narrower PDIs. However, a chelating ligand with a σ donor prevents side reactions such as chain backbiting and decomposition. We found that ROAMP of dibenzocyclooctynes is better behaved than other cyclooctynes.

Since its discovery in 1989, ROAMP has gotten farther away from alkyne metathesis and closer to being its own field. ROAMP catalysts are currently designed to be selective for strained alkynes and unreactive for alkyne metathesis. It was not until 2010 that this shift in design strategy took place. In merely six years, the first well-defined and well-behaved living ROAMP with PDIs as low as 1.02 was discovered.[16] However, several improvements are underway. First, a living ROAMP catalyst that is stable in protic solvents under air conditions at room temperature with low PDIs have yet not been reported. Moreover, we are still in search of a well-behaved catalyst for the living ROAMP of cyclic alkynes other than dibenzocyclooctynes. Finally, we need to discover more synthetically accessible cyclic alkynes and catalysts, to not only expand the understanding of ROAMP, but also its applications. In the six years since the first report of a catalyst designed specifically for ROAMP, much progress has been made and will be made in the years to come.

## 1.7 References

(1)     Blankenburg, L.; Bunz, U. H. F.; Klemm, E.; Moore, J. S.; Pautzsch, T.; Ray, C. R.; Swager, T. M.; Voskerician, G.; Weder, C.; Yamaguchi, I.; Yamamoto, T.; Yasuda, T.; Zheng, J. Poly(arylene ethynylene)s: From Synthesis to Application; Weder, C., Ed.; Springer: Berlin, 2005.

(2)     Bunz, U. *Macromol. Rapid Commun.* **2009**.

(3)     Bunz, U. H. F. *Chem. Rev.* **2000**, *100* (4), 1605.

(4)     Dieck, H. A.; Heck, F. R. *J. Organomet. Chem.* **1975**, *93* (2), 259.

(5)     Sonogashira, K.; Tohda, Y.; Hagihara, N. *Tetrahedron. Lett* **1975**, *50*, 4467.

(6)     Cassar, L. *J. Organomet. Chem.* **1975**, *93*, 253.

(7)     Weiss, K.; Michel, A.; Auth, E. M.; Bunz, U. *Angew. Chem. Int. Ed.* **1997**, *36* (5), 506.

(8)     Bunz, U. H. F. *Acc. Chem. Res.* **2001**, *34* (12), 998.

(9)     Yang, H.; Jin, Y.; Du, Y.; Zhang, W. *J. Mater. Chem. A* **2014**, *2* (17), 5986.

(10)    Weiss, K.; Michel, A.; Auth, E. M.; Bunz, U. H. F.; Mangel, T.; Müllen, K. *Angew. Chem. Int. Ed. Engl.* **1997**, *36* (5), 506.

(11)    Kugelgen, von, S.; Bellone, D. E.; Cloke, R. R.; Perkins, W. S.; Fischer, F. R. *J. Am. Chem. Soc.* **2016**, *138* (19), 6234.

(12)    Fischer, F. R.; Nuckolls, C. *Angew. Chem. Int. Ed.* **2010**, *49* (40), 7257.

(13)    McGrath, N. A.; Raines, R. T. *Chem. Sci.* **2012**, *3* (11), 3237.

(14)    Gordon, C. G.; Mackey, J. L.; Jewett, J. C.; Sletten, E. M.; Houk, K. N.; Bertozzi, C. R. *J. Am. Chem. Soc.* **2012**, *134* (22), 9199.

(15)    Sedbrook, D. F.; Paley, D. W.; Steigerwald, M. L.; Nuckolls, C.; Fischer, F. R. *Macromolecules* **2012**, *45* (12), 5040.

(16)    Bellone, D. E.; Bours, J.; Menke, E. H.; Fischer, F. R. *J. Am. Chem. Soc.* **2015**, *137* (2), 850.

(17)    Fürstner, A.; Davies, P. W. *Chem. Commun.* **2005**, No. 18, 2307.

(18)    Zhang, W.; Brombosz, S. M.; Mendoza, J. L.; Moore, J. S. *J. Org. Chem.* **2005**, *70* (24), 10198.

(19)    Zhang, W.; Moore, J. S. *J. Am. Chem. Soc.* **2004**, *126* (40), 12796.

(20)    **2016**, 1.

(21)    Sisco, S. W.; Moore, J. S. *J. Am. Chem. Soc.* **2012**, *134* (22), 9114.

(22)    Ghosh, K.; Moore, J. S. *J. Am. Chem. Soc.* **2011**, *133* (49), 19650.

(23)    Stone, M. T.; Moore, J. S. *Org. Lett.* **2004**, *6* (4), 469.

(24)    Zhang, W.; Moore, J. S. *Adv. Synth. Catal.* **2007**, *349* (1-2), 93.

(25)    Pennella, F.; Banks, R. L.; Bailey, G. C. *Chem. Commun.* **1968**, *23*, 1548.

(26)    Geyer, A. M.; Holland, M. J.; Gdula, R. L.; Goodman, J. E.; Johnson, M. J.; Kampf, J. W. *J. Organomet. Chem.* **2012**, *708*, 1.

(27)   Geyer, A. M.; Wiedner, E. S.; Gary, J. B.; Gdula, R. L.; Kuhlmann, N. C.; Johnson, M. J. A.; Dunietz, B. D.; Kampf, J. W. *J. Am. Chem. Soc.* **2008**, *130* (28), 8984.

(28)   Laplaza, C. E.; Johnson, M. J. A.; Peters, J. C.; Odom, A. L.; Kim, E.; Cummins, C. C.; George, G. N.; Pickering, I. J. *J. Am. Chem. Soc.* **1996**, *118* (36), 8623.

(29)   Mortreux, A.; Blanchard, M. *J. Chem. Soc., Chem. Commun.* **1974**, No. 19, 786.

(30)   Wengrovius, J. H.; Sancho, J.; Schrock, R. R. *J. Am. Chem. Soc.* **1981**, *103* (13), 3932.

(31)   Fürstner, A. *Angew. Chem. Int. Ed. Engl.* **2013**, *52* (10), 2794.

(32)   McCullough, L. G.; Schrock, R. R. *J. Am. Chem. Soc*. **1984**, *106*, 4067.

(33)   Freudenberger, J. H.; Schrock, R. R.; Churchill, M. R.; Rheingold, A. L.; Ziller, J. W. *Organometallics* **1984**, *3* (10), 1563.

(34)   Churchill, M. R.; Ziller, J. W.; Freudenberger, J. H.; Schrock, R. R. *Organometallics* **1984**, *3* (10), 1554.

(35)   Mayr, A. *Comment. Inorg. Chem.* **1990**, *10* (4-5), 227.

(36)   Fischer, H.; Hofmann, P.; Kreissl, F. R.; Schrock, R. R.; Schubert, U.; Weiss, K. *Carbyne Complexes*; Wiley-VCH Verlag GmbH, 1988.

(37)   Fürstner, A.; Mathes, C.; Lehmann, C. W. *J. Am. Chem. Soc.* **1999**, *121* (40), 9453.

(38)   Tsai, Y.-C.; Diaconescu, P. L.; CUMMINS, C. C. *Organometallics* **2000**, *19* (25), 5260.

(39)   James, M.; Figueroa, J. S.; Stephens, F. H.; Cummins, C. C. *Organometallics* **2003**, *22* (17), 3351.

(40)   Zhang, W.; Kraft, S.; Moore, J. S. *Chem. Commun.* **2003**, No. 7, 832.

(41)   Zhang, W.; Kraft, S.; Moore, J. S. *J. Am. Chem. Soc.* **2004**, *126* (1), 329.

(42)   Zhang, W.; Moore, J. S. *Macromolecules* **2004**, *37* (11), 3973.

(43)   Jyothish, K.; Zhang, W. **2011**, *50* (15), 3435.

(44)   Jyothish, K.; Wang, Q.; Zhang, W. *Adv. Synth. Catal.* **2012**, *354* (11-12), 2063.

(45)   Jyothish, K.; Zhang, W. *Angew. Chem. Int. Ed. Engl.* **2011**, *50* (37), 8478.

(46)   Beer, S.; Hrib, C. G.; Jones, P. G.; Brandhorst, K.; Grunenberg, J.; Tamm, M. *Angew. Chem. Int. Ed. Engl.* **2007**, *46* (46), 8890.

(47)   O'Reilly, M. E.; Ghiviriga, I.; Abboud, K. A.; Veige, A. S. *J. Am. Chem. Soc.*

**2012**, 120626162210009.

(48)     Beer, S.; Brandhorst, K.; Hrib, C. G.; Wu, X.; Haberlag, B.; Grunenberg, J.; Jones, P. G.; Tamm, M. *Organometallics* **2009**, *28* (5), 1534.

(49)     Schrock, R. R.; Listemann, M. L.; Sturgeoff, L. G. *J. Am. Chem. Soc.* **1982**, *104* (15), 4291.

(50)     Chisholm, M. H.; Folting, K.; Lynn, M. L.; Tiedtke, D. B.; Lemoigno, F.; Eisenstein, O. *Chem. Eur. J.* **1999**, *5* (8), 2318.

(51)     Andrea M Geyer; Robyn L Gdula; Eric S Wiedner, A.; Johnson, M. J. A. *J. Am. Chem. Soc.* **2007**, *129* (13), 3800.

(52)     Finke, A. D.; Moore, J. S. *Chem. Commun.* **2010**, *46* (42), 7939.

(53)     Bindl, M.; Stade, R.; Heilmann, E. K.; Picot, A.; Goddard, R.; Fürstner, A. *J. Am. Chem. Soc.* **2009**, *131* (27), 9468.

(54)     Heppekausen, J.; Stade, R.; Goddard, R.; Fürstner, A. *J. Am. Chem. Soc.* **2010**, *132* (32), 11045.

(55)     Heppekausen, J.; Stade, R.; Kondoh, A.; Seidel, G.; Goddard, R.; Fürstner, A. *Chem. Eur. J.* **2012**, *18* (33), 10281.

(56)     Clark, D. N.; Schrock, R. R. *J. Am. Chem. Soc.* **1978**, *100* (21), 6774.

(57)     Freudenberger, J. H.; Schrock, R. R. *Organometallics* **1985**, *4* (11), 1937.

(58)     Schrock, R. R. *Chem. Commun.* **2005**, 2773.

(59)     Schrock, R. R. *Chem. Commun.* **2013,** *49*, 5529.

(60)     Schrock, R. R. *Acc. Chem. Res.* **1986**, *19* (11), 342.

(61)     Mayr, A.; McDermott, G. A. *J. Am. Chem. Soc.* **1986**, *108* (3), 548.

(62)     McDermott, G. A.; Dorries, A. M.; Mayr, A. *Organometallics* **1987**.

(63)     Fischer, E. O.; Massböl, A. *Chem. Ber* **1967**, *100*, 2445.

(64)     Tamm, M. *chimica oggi/Chemistry Today* **2010**.

(65)     Paley, D. W.; Sedbrook, D. F.; Decatur, J.; Fischer, F. R.; Steigerwald, M. L.; Nuckolls, C. *Angew. Chem. Int. Ed.* **2013**, *52* (17), 4591.

(66)     Gdula, R. L.; Johnson, M. J. A. *J. Am. Chem. Soc.* **2006**, *128* (30), 9614.

(67)     McCullough, L. G.; Schrock, R. R.; Dewan, J. C. *J. Am. Chem. Soc.* **1985**, *107*, 5987.

(68)     Katz, T. J.; McGinnis, J. *J. Am. Chem. Soc.* **1975**, *97* (6), 1592.

(69)    Jean Louis Hérisson, P.; Chauvin, Y. *Makromolekul. Chem.* **1971**, *141* (1), 161.

(70)    Zhu, N.; Hu, W.; Han, S.; Wang, Q.; Zhao, D. *Org. Lett.* **2008**, *10* (19), 4283.

(71)    Zhu, N.; Yan, Q.; Luo, Z.; Zhai, Y.; Zhao, D. *Chem. Asian J.* **2012**, *7* (10), 2386.

(72)    Banno, M.; Yamaguchi, T.; Nagai, K.; Kaiser, C.; HECHT, S.; Yashima, E. *J. Am. Chem. Soc.* **2012**, *134* (20), 8718.

(73)    Jiang, J.; Slutsky, M. M.; Jones, T. V.; Tew, G. N. *New J. Chem.* **2009**.

(74)    Smaldone, R. A.; Moore, J. S. *J. Am. Chem. Soc.* **2007**, *129* (17), 5444.

(75)    Neil G Pschirer; Tzenka Miteva; Una Evans; Rhonda S Roberts; Alan R Marshall; Dieter Neher; Michael L Myrick, A.; Bunz, U. H. F. *Chem. Mater.* **2001**, *13* (8), 2691.

(76)    Breen, C. A.; Tischler, J. R.; Bulović, V.; Swager, T. M. *Adv. Mater. Weinheim* **2005**, *17* (16), 1981.

(77)    Xu, Y.; Berger, P. R.; Wilson, J. N.; Bunz, U. H. F. *Appl. Phys. Lett.* **2004**, *85* (18), 4219.

(78)    Swager, T. M.; Zheng, J. *Adv. Polym. Sci* **2005**, *177*, 151.

(79)    Gross, D. E.; Zang, L.; Moore, J. S. *Pure Appl. Chem.* **2012**, *84* (4), 869.

(80)    Krouse, S.; Schrock, R. *Macromolecules* **1989**, *22* (6), 2569.

(81)    Zhang, X. P.; Bazan, G. C. *Macromolecules* **1994**, *27* (16), 4627.

(82)    Carnes, M.; Buccella, D.; Siegrist, T.; Steigerwald, M. L.; Nuckolls, C. *J. Am. Chem. Soc.* **2008**, *130* (43), 14078.

(83)    Macnaughtan, M. L. Ruthenium-Catalyzed Metathesis with Directly Functionalized Olefins. Ph.D. Thesis, University of Michigan, 2009.

(84)    Wu, X.; Tamm, M. *Beilstein J. Org. Chem.* **2011**, *7*, 82.

(85)    Tamm, M.; Petrovic, D.; Randoll, S.; Beer, S.; Bannenberg, T.; Jones, P. G.; Grunenberg, J. *Org. Biomol. Chem.* **2007**, *5* (3), 523.

(86)    Wu, X.; Tamm, M. *Coordin. Chem. Rev.* **2014**, *260*, 116.

(87)    Lysenko, S.; Volbeda, J.; Jones, P. G.; Tamm, M. *Angew. Chem. Int. Ed. Engl.* **2012**, *51* (27), 6757.

(88)    Haberlag, B.; Freytag, M.; Daniliuc, C. G.; Jones, P. G.; Tamm, M. *Angew. Chem. Int. Ed. Engl.* **2012**.

(89)    Lysenko, S.; Haberlag, B.; Daniliuc, C. G.; Jones, P. G.; Tamm, M. *ChemCatChem* **2011**, *3* (1), 115.

(90)    Lysenko, S.; Haberlag, B.; Wu, X.; Tamm, M. *Macromol. Symp.* **2010**, *293* (1), 20.

(91)    Haberlag, B.; Wu, X.; Brandhorst, K.; Grunenberg, J.; Daniliuc, C. G.; Jones, P. G.; Tamm, M. *Chem. Eur. J.* **2010**, *16* (29), 8868.

# 2 Ring-Opening Alkyne Metathesis Polymerization of 3,8-dihexyloxy-5,6-dihydro-11,12-didehydrodibenzo[a,e][8]annulene

## 2.1 Introduction: Living Ring-Opening Alkyne Metathesis

Since its discovery in the mid-sixties, the development of stable, well-defined, and functional group tolerant olefin metathesis catalysts has greatly influenced the fields of organic synthesis, polymer and materials science.[1,2] Although alkene metathesis has found a wide range of applications, alkyne metathesis has only recently become the focus of attention.[3-10] Moreover, living ring-opening olefin metathesis polymerization (ROMP) has had a great impact in the areas of biomimetic synthetic polymers, self-assembled nanomaterials, and monolithic supports.[1] Despite recent synthetic advances towards highly functionalized ring-strained alkynes,[11a–d] the application of ring-opening alkyne metathesis polymerization (ROAMP) to the field of polymer synthesis has remained limited due to the lack of commercially available well-behaved catalysts.[12–17]

Presently, poly(arylene ethynylene)s, used in applications ranging from molecular photonics, electronics, to sensing, can be accessed through acyclic diyne metathesis (ADIMET) polymerization of diynes using highly active molybdenum and tungsten catalysts.[18–22] However, this step-growth process provides only very limited control over the polydispersity, length, and modality of the polymer product. Previous attempts at synthesizing polymers using ring-opening of strained alkynes showed polydispersities ranging from 1.1–7.0.[12,14,23] While polymers with polydispersities as low as 1.1 have been obtained, the active catalyst species is poorly defined and the reaction requires low temperatures and rigorous air-free conditions.[15] Polymers resulting from these catalysts tend to have higher molecular weights than predicted based on the monomer to catalyst loading. ^{1}H NMR experiments show that only a fraction of the catalyst is activated and contributes to the linear chain growth, indicating that the rate of propagation is larger than the rate of initiation ($k_p/k_i > 1$). The poor selectivity of alkyne metathesis catalysts for strained over unstrained alkynes in the growing polymer chain leads to significant broadening of the PDI through chain-transfer processes and back-biting to form cyclic structures.
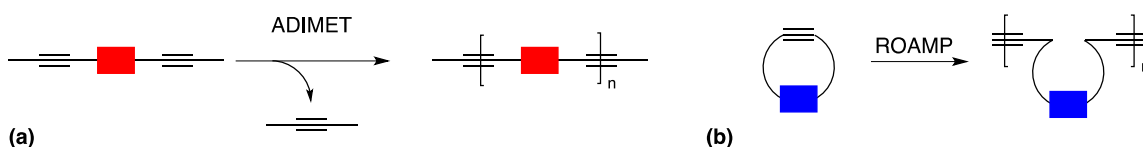


**Scheme 2-1.** Synthesis of polymers containing alkynes in their backbone by (a) acyclic diyne metathesis (ADIMET) polymerization and by (b) ring-opening alkyne metathesis polymerization (ROAMP).

In this chapter, we report the synthesis and the detailed mechanistic investigation of the first molecularly-defined living ring-opening alkyne metathesis catalyst [TolC≡Mo(ONO)(OR)]•KOR (R = CCH$_3$(CF$_3$)$_2$, ONO = 6,6'-(pyridine-2,6-diyl)bis(2,4-di-*tert*-butylphenolate)) **1**. In solution, a rapid equilibrium between the -ate complex **1** and the pentacoordinate 14-electron complex **2** is observed (electron count does not

include potential π-donation of electron density from alkoxide lone pairs). While the reversible association of a free alkoxide prevents undesired side reactions, the dissociation of **1** does not represent a rate-limiting step during the propagation. Kinetic studies reveal that the growing polymer chain efficiently limits the rate of propagation with respect to the rate of initiation ($k_p/k_i \sim 10^{-3}$). We herein demonstrate the outstanding control over molecular weight and polydispersity achieved in living ROAMP with **1** and the first synthesis of block-copolymers through alkyne metathesis.

## 2.2 Design of Ring-Opening Alkyne Metathesis Polymerization via the Incorporation of a Pincer Ligand

### 2.2.1. Design and Synthesis of 3,8-dihexyloxy-5,6-dihydro-11,12-didehydrodibenzo[a,e][8]annulene

To study a well-controlled ROAMP, we synthesized strained cyclic alkyne 3,8-dihexyloxy-5,6-dihydro-11,12-didehydrodibenzo[a,e]-[8]annulene (**2a**). Previous studies have shown that ring-opening alkyne metathesis polymerization of similar monomers have resulted in a chain-growth polymerization with PDIs as low as 1.1.[15] Moreover, this monomer is synthetically accessible, easily modifiable, and highly soluble. The monomer was synthesized analogous to literature procedures (Scheme 2-2).
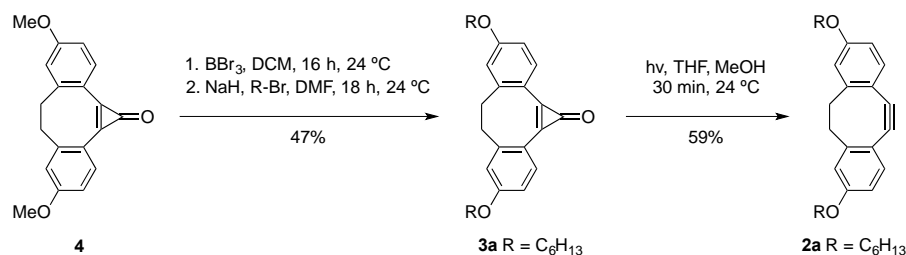


**Scheme 2-2.** Synthesis of strained alkyne **2a**.

Cyclopropenone **4** was synthesized according to literature procedures.[15] Deprotection of the methoxy groups in cyclopropenone **4** with boron tribromide, followed by deprotonation and alkylation with 1-bromohexane yielded **3a** in 47% yield. Photochemical decarbonylation of the cyclopropenone **3a** afforded the solubilized ring-strained monomer **2a**.

Figures 2-1 and 2-2 show ORTEP diagrams derived from the crystal structures of **3a** and **2a**. Refinement of the diffraction data from a single crystal of **3a** required disorder modeling of the unit cell. Each asymmetric cell contains two molecules of **3a**. One of the disordered hexyl-chain adopts two conformations with a 56:44 positional distribution.
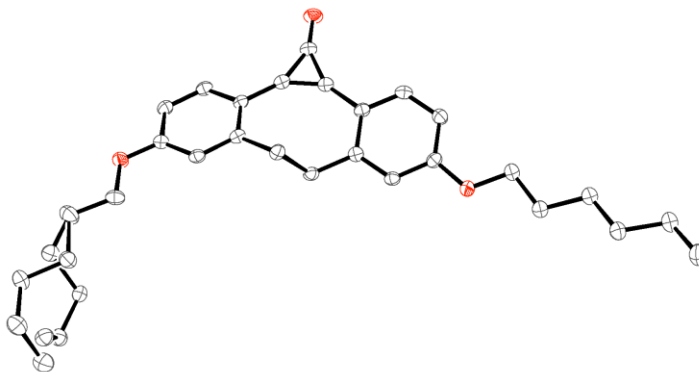
**Figure 2-1.** ORTEP representation of the X-ray crystal structure of **3a**. Thermal ellipsoids are drawn at the 50% probability level. Color coding: C (gray), O (red). Hydrogen atoms are omitted for clarity.
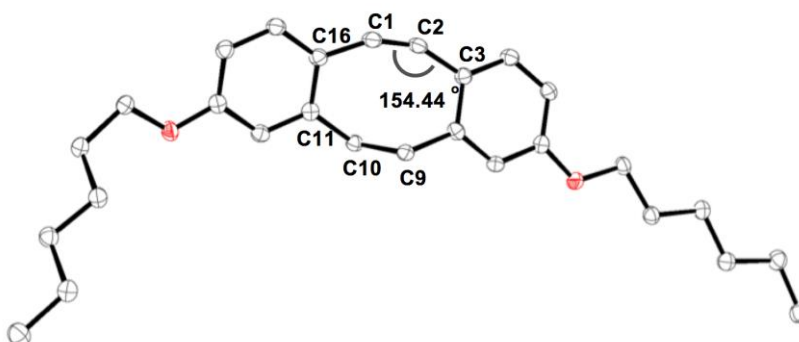


**Figure 2-2.** ORTEP representation of the X-ray crystal structure of **2a**. Thermal ellipsoids are drawn at the 50% probability level. Color coding: C (gray), O (red). Hydrogen atoms are omitted for clarity.

As shown in Figure 2-2, there is a significant amount of strain in the cyclooctyne ring in **2a**. The C(16)−C(1), C(1)−C(2), C(9)−C(10), and C(10)−C(11) bond lengths are 1.4327(17) Å, 1.2038(19) Å, 1.5687(17) Å, and 1.5141(18) Å, respectively. The C(1)≡C(2)−C(3), and C(11)-C(10)-C(9) bond angles (154.44(13)° and 116.19(11)°) greatly deviate from the 180° and 109.5° expected for a linear and tetrahedral bonding angle. The elongated C(10)−C(9) bond, and bond angle distortions give rise to the strain in the molecule. The release of this strain represents the driving force for the ROAMP reaction and balances the entropic penalty associated with the formation of a polymer from the monomer precursor.

In order to prove the living ROAMP of **2a**, we ought to synthesize a new monomer to make block copolymers. In analogy to the synthesis of **2a**, a water-soluble monomer **2b** was prepared from cyclopropenone **3b** (Scheme 2-3).
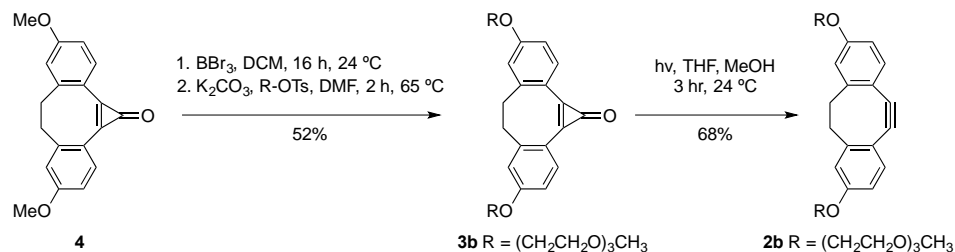
**Scheme 2-3.** Synthesis of strained alkyne **2b**.

### 2.2.2. Design and Synthesis of [TolC≡Mo(ONO)(OR)]•KOR (R = CCH₃(CF₃)₂, ONO = 6,6'-(pyridine-2,6-diyl)bis(2,4-di-tert-butylphenolate))

In order to synthesize a catalyst that is selective towards strained alkynes, we sought to incorporate tunable chelating phenoxide ligands as reported by Fischer et al.. Herein, we report the use of a bulky chelating ligand that blocks an active site and potentially limits undesired side reactions such as alkyne polymerization. While structurally related 12-electron molybdenum and tungsten complexes have been reported as catalysts for alkyne cross-metathesis and ring-closing metathesis, these highly active complexes are unsuitable for controlled ROAMP. Extensive chain transfer reactions lead to undesired broad weight distributions (PDI > 2).[6,14,28–35] In an effort to increase the selectivity of our catalyst for the activation of strained monomers over unstrained alkynes in the growing polymer chain, we incorporated a permanent electron donating, sterically demanding ONO pincer ligand **9**.[24,36a–f] This tridentate ligand stabilizes the high oxidation state of the molybdenum benzylidyne complex, prevents its dimerization in solution,[12] and irreversibly blocks one of the catalyst's active sites.[37,38]

Catalyst **1** was synthesized through ligand exchange from the trisalkoxy molybdenum benzylidyne complex [TolC≡Mo(OR)₃(dme)] **5**.[24–27] The synthesis of catalyst **1** is detailed in Scheme 2-4. Following the procedure by Fischer it al., molybdenum hexacarbonyl **6** was reacted with *p*-tolyl lithium affording the orange acyl complex **7**.[25] Oxidation of **7** with oxalyl bromide and bromine in the presence of DME yielded the brown Mo(VI) complex **8**. The ligand exchange of **8** with potassium 1,1,1,3,3,3-hexafluoro-2-methyl-2-propanoxide is driven by the precipitation of potassium bromide and the thermodynamic stability of the alkoxide complex **5**. Deprotonation of the ONO pincer ligand **6** with potassium benzyl followed by addition to [TolC≡Mo(OR)₃(dme)] in toluene quantitatively converted **5** to the desired product **1**, by ¹H and ¹⁹F NMR spectroscopy. Isolation of **1** was accomplished by recrystallization from a saturated diisopropyl ether or pentane solution.
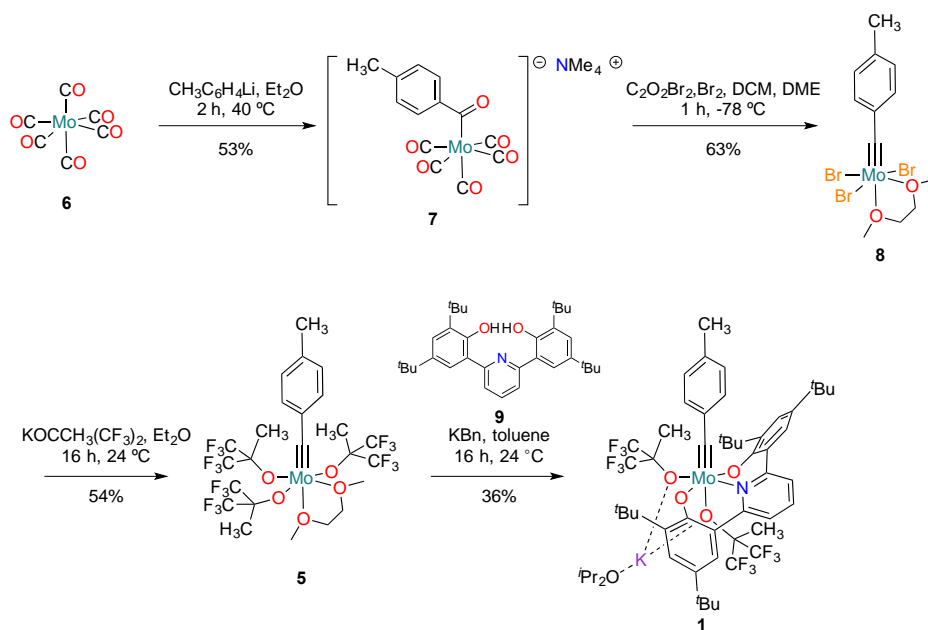
**Scheme 2-4.** Synthesis of ROAMP catalyst **1**.

Dark brown crystals of **1** were isolated in 36% yield after recrystallization from diisopropyl ether at –35 °C. The geometry at the metal center is pseudo-octahedral. X-ray crystallography of **1** (Figure 2-3) confirms the presence of a C(1)≡Mo(1) triple bond with bond length of 1.760(2) Å and C(2)–C(1)–Mo(1) angle of 176.91(19)°. The tridentate ONO pincer ligand adopts a skewed conformation featuring typical Mo(1)–O(1) and Mo(1)–O(3) distances of 1.9876(16) Å and 2.0010(16) Å, respectively. The Mo(1)–N(1) distance of 2.2227(19) Å corresponds to a neutral L-type N–Mo bond, indicating the presence of an interaction between the lone pair of the pyridine ring and the metal center. The presence of two alkoxides and one potassium cation in the crystal structure of **1** confirms that only one alkoxide in **3** has been displaced by the ONO pincer ligand. The Mo–O distances are 2.0038(16) Å and 2.2475(16) Å for the hexafluoro-*tert*-butoxide *cis*, Mo(1)–O(2), and *trans*, Mo(1)–O(4), to the carbyne, respectively. The elongated Mo(1)–O(4) bond for the alkoxide *trans* to the carbyne suggests a weak interaction with an oxygen lone pair.
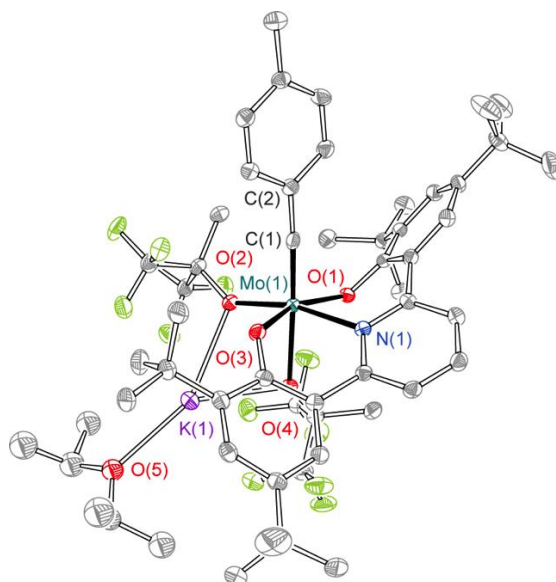
**Figure 2-3.** ORTEP representation of the X-ray crystal structure of **1**. Thermal ellipsoids are drawn at the 50% probability level. Color coding: C (gray), O (red), N (blue) F (green), Mo (turquoise), K (purple). Hydrogen atoms are omitted for clarity. Diisopropyl ether was refined isotropically.

### 2.2.3. Dissociation Equilibrium in Solution of the –ate Complex 1

Crystals of **1** are stable in dry air for hours and can be stored for indefinite time under an atmosphere of nitrogen. In the absence of moisture and air, a solution of **1** in toluene-$d_8$ shows less than 5% decomposition after one month at 24 °C. In toluene-$d_8$, the pseudo-octahedral -ate complex **1** is in dynamic equilibrium with the dissociated pentacoordinate complex [TolC≡Mo(ONO)(OR)] (R = CCH$_3$(CF$_3$)$_2$) **10** (Figure 2-4). This dissociation equilibrium is evident in the $^{19}$F NMR of the complex **1**. As shown in Figure 2-4 the octahedrally coordinated complex **1** shows two distinctive fluorine resonances at −77.80 and −78.26 ppm for the equatorial and axial hexafluoroalkoxide ligands. The dissociated complex **10** only shows one coordinated ligand at −76.79 ppm and the free alkoxide at −81.18 ppm. The dissociation equilibrium is a crucial component to the reactivity of the catalyst. While the presence of the alkoxide provides stability in the solid state, its dissociation in solution opens a free coordination site for the association with the ring-strained monomer.

**Figure 2-4.** $^{19}$F NMR (470 MHz) spectrum of **1** in Tol-$d_8$. In Tol-$d_8$ **1** is in equilibrium with **10** and KOCCH$_3$(CF$_3$)$_2$. (* trifluorotoluene)

In THF-$d_8$ the alkoxide *trans* to the carbyne is replaced by the solvent, and only a single species, corresponding to a THF bound hexacoordinate complex, is observed by $^1$H and $^{19}$F NMR (Figure 2-5).
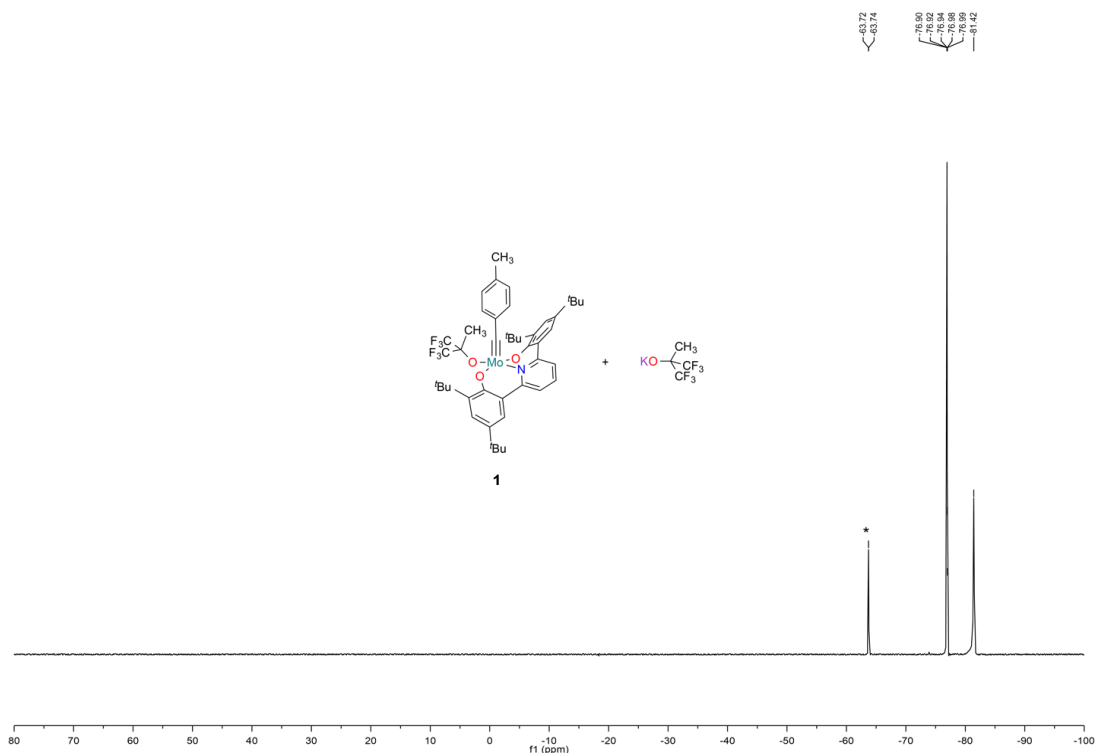
**Figure 2-5.** $^{19}$F NMR (470 MHz) spectrum of **1** in THF-$d_8$. In THF-$d_8$ **1** completely dissociates to **10** and KOCCH$_3$(CF$_3$)$_2$.  (* trifluorotoluene)

We studied the equilibrium between complex **1** and the free dissociated species **10** in Tol-$d_8$. At elevated temperatures (T > 60 °C) a rapid equilibrium is established between the -*ate* complexes **1** and the dissociated complex **10** (Figure 2-5). The dissociation constant of **1** ($K_{diss}$) at selected temperatures is summarized in Table 2-1. Van't Hoff analysis reveals that the change in standard free enthalpy and entropy associated with the dissociation of KOR from **1** is $\Delta H° = 9.5 \pm 0.5$ kcal mol$^{-1}$, $\Delta S° = 16.8 \pm 2.1$ eu, respectively (Figure 2-6).
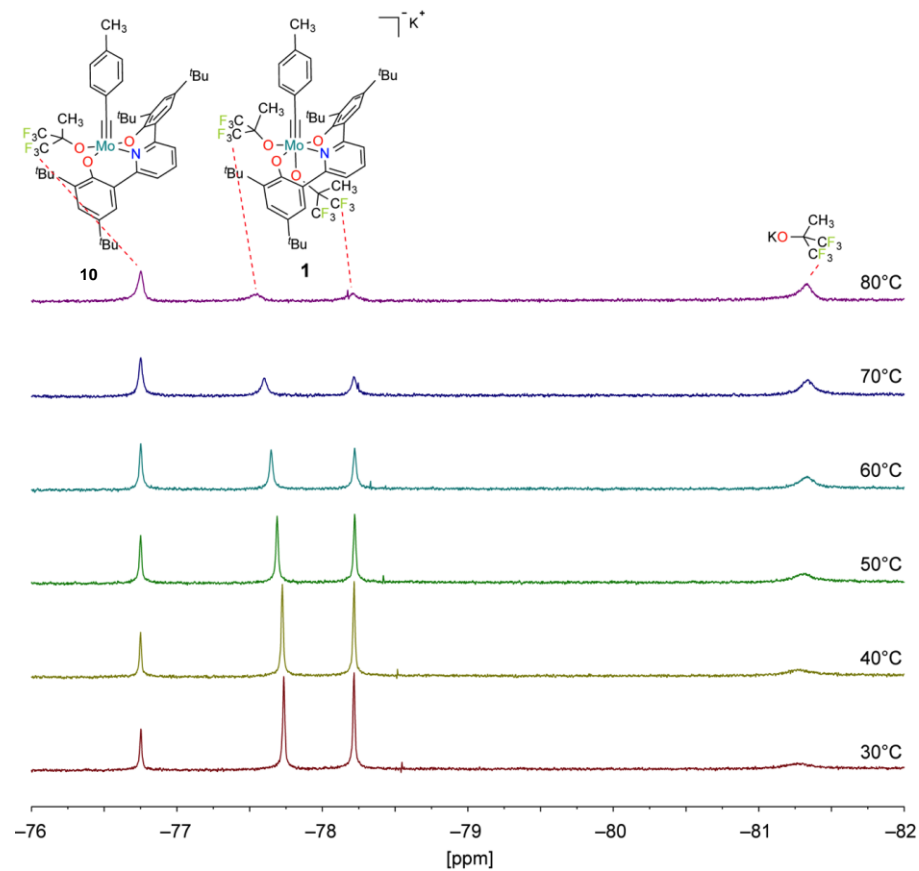
**Figure 2-4.** $^{19}$F NMR of the dissociation equilibrium between **1** and **10** in Tol-$d_8$.

**Table 2-1.** Dissociation constant ($K_{diss}$) and selected rate constants ($k_1$) for **1** different temperatures. [a] The resonance signals in the $^{19}$F NMR are broadened and could not be inverted for SIR experiments.

| T (°C) | $K_{diss}$ (M) | $k_1$ (s$^{-1}$) |
|---|---|---|
| 30 | $0.78 \cdot 10^{-3}$ | 7.9 |
| 40 | $1.22 \cdot 10^{-3}$ | 15.1 |
| 50 | $1.98 \cdot 10^{-3}$ | 27.7 |
| 60 | $3.40 \cdot 10^{-3}$ | 43.2 |
| 70 | $4.66 \cdot 10^{-3}$ | $-$[a] |
| 80 | $6.84$ | $-$[a] |
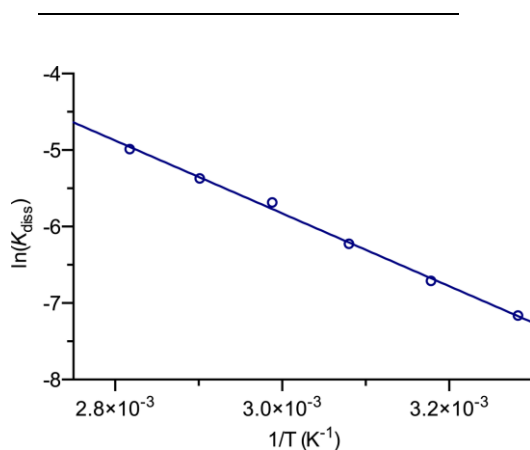
**Figure 2-6.** Van't Hoff plot of $K_{diss}$ of **1** between 30 °C and 80 °C. $R^2 = 0.998$.

The rates of dissociation ($k_1$) at various temperatures were measured by Selective Inversion Recovery (SIR) $^{19}F$ NMR experiments (Table 2-1, Figures 2-6 and 2-7).[40,41] The standard activation enthalpies for the dissociation of **1** ($\Delta H^{\ddagger} = 10.4 \pm 0.6$ kcal mol$^{-1}$) was derived from Eyring plots (Figure 2-8).
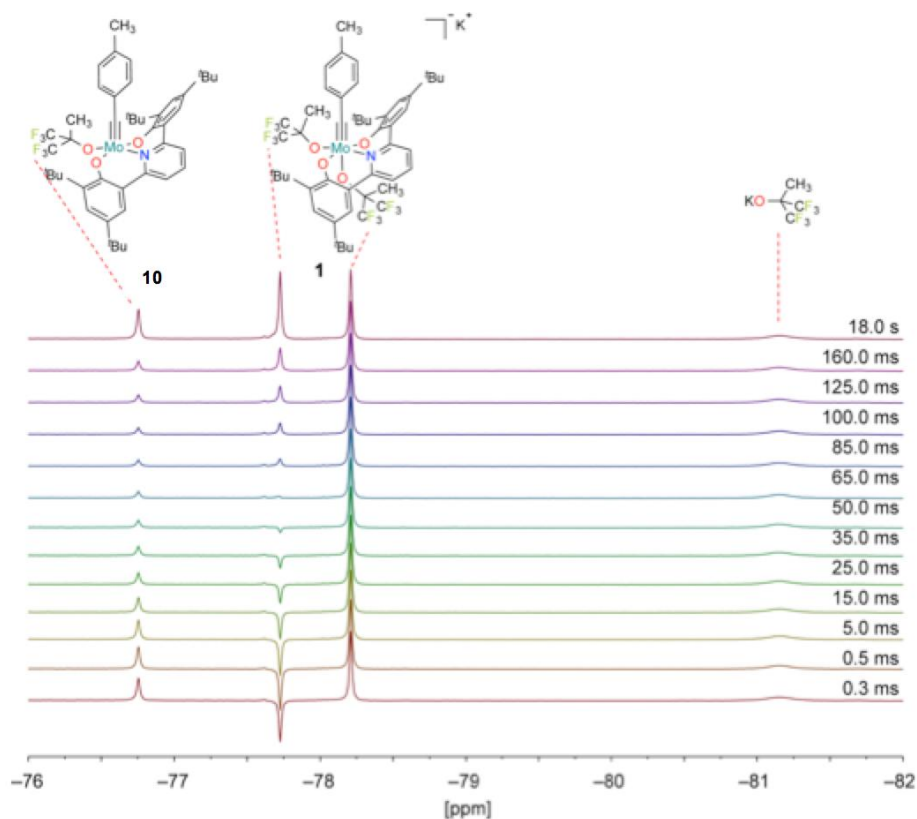
**Figure 2-6.** SIR $^{19}$F NMR experiments of **1** at 30 °C in Tol-$d_8$. The hexafluoro-*tert*-butoxide ligand *cis* to the benzylidyne was inverted at $t = 0$ ms.
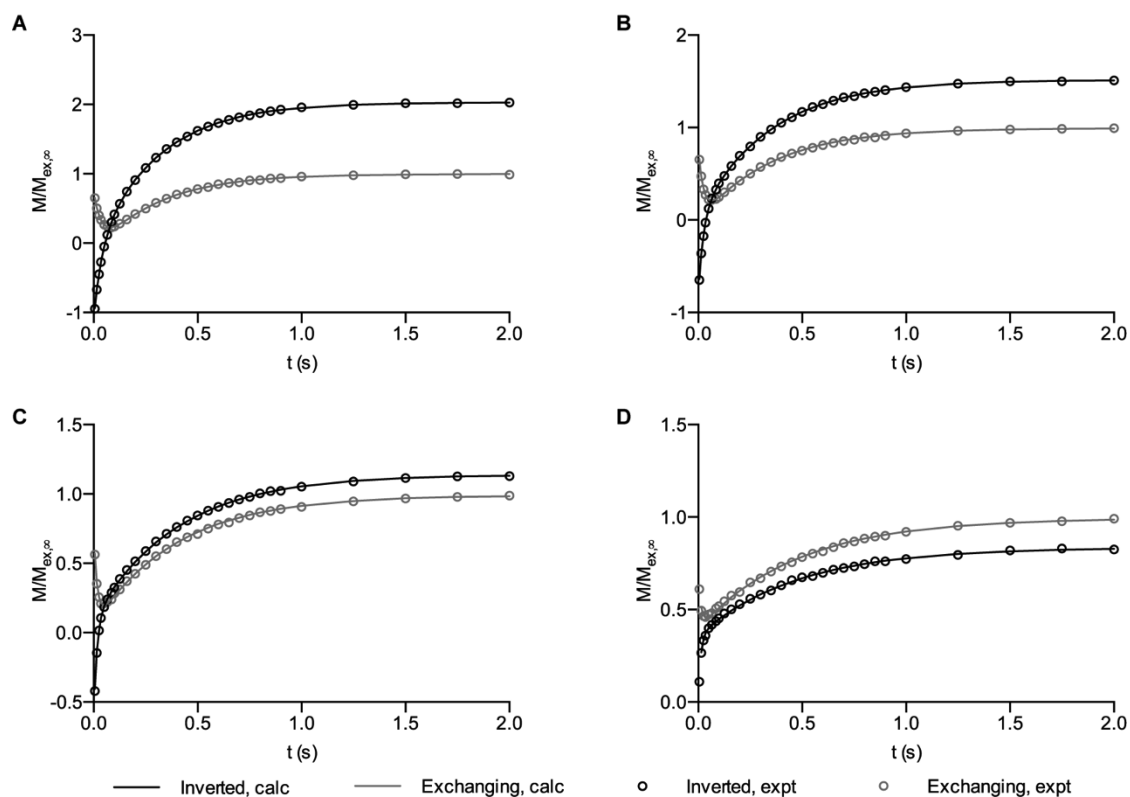


**Figure 2-7.** SIR experiments of the dissociation of **1** at (A) 30 °C, (B) 40 °C, (C) 50 °C, and (D) 60 °C.
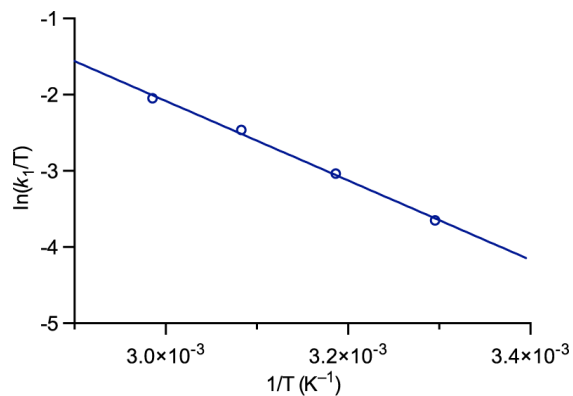


**Figure 2-8.** Eyring plot for the rate of dissociation ($k_1$) of **1**. ($R^2 = 0.996$).

## 2.3 Ring-Opening Alkyne Metathesis Polymerization Reactivity of Complex 1

### 2.3.1 Ring-Opening Alkyne Metathesis Polymerization by Complex 1

We studied the ROAMP of 3,8-dihexyloxy-5,6-dihydro-11,12-didehydrodibenzo[*a,e*][8]annulene (**5a**) (Scheme 2-5), a readily accessible highly solubilized ring-strained alkyne, with **1**.
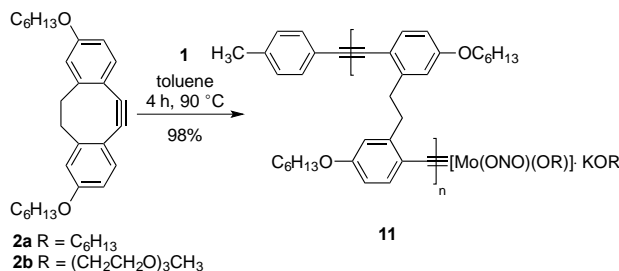


**Scheme 2-5.** ROAMP of **2a,b** with catalyst **1**.

Addition of **1** to a solution of **2a** in toluene ([**2a**]/[**1**] = 10) at 24 °C does not lead to the formation of polymeric species within 24 h. $^1$H and $^{19}$F NMR indicate that the ROAMP catalyst **1** quantitatively initiates with a half-life of $t_{1/2} < 5$ min with 1 equiv. of **2a** to form the initiated complex **11** (n = 1) (Scheme 2-5). At 90 °C, however, the initiation reaction is instantaneous and the living ROAMP of monomer **2a** (10 equiv.) in toluene is completed in less than 2 h, as determined by $^1$H NMR spectroscopy. In the absence of monomer, the molybdenum catalyst attached to the propagating polymer chain remains active and continues to incorporate equivalents of monomer added sequentially to the reaction mixture (Figure 2-9). Precipitation of the resulting polymers in MeOH affords *poly*-**2a** in greater than 90% isolated yield. GPC analysis for various monomer/catalyst loadings at 90 °C in toluene shows a PDI of ~1.02, the lowest value ever reported for ROAMP (Figure 2-10, Table 2-2). Extended reaction times do not lead to a deterioration of the PDI. The molecular weights of *poly*-**2a** determined by GPC, calibrated to polystyrene standards, scale linearly with the conversion of monomer (Figure 2-9), are proportional to the initial [**2a**]/[**1**] loading, and show a unimodal distribution (Figure 2-10). No evidence for branching or the formation of cyclic polymers could be observed by $^1$H NMR analysis and mass spectrometry (Figure 2-11). $^1$H NMR end-group analysis of the tolyl group reveals that GPC overestimates the $M_n$ of *poly*-**2a**. A correction factor ~0.7–1.0 correlates well with the degree of polymerization determined by NMR analysis and the expected molecular weight based on the [**2a**]/[**1**] loading.

**Table 2-2.** Molecular weight analysis of *poly*-**2a**. [a] calibrated to narrow polydispersity polystyrene standards; b degree of polymerization determined by $^1$H NMR end-group analysis.

| [**5a**]/[**1**] | T (°C) | $M_n$ theo | $M_n$ GPC[a] | $M_w$ GPC[a] | $X_n$[b] | PDI GPC |
|---|---|---|---|---|---|---|

|       |    | r y        |            |            |     | [a]      |
|-------|----|------------|------------|------------|-----|----------|
| 10/1  | 60 | 4,000      | 7,200      | 7,700      | -   | 1.07     |
| 10/1  | 70 | 4,000      | 7,300      | 7,800      | -   | 1.07     |
| 10/1  | 80 | 4,000      | 9,100      | 9,500      | -   | 1.04     |
| 10/1  | 90 | 4,000      | 6,100      | 6,600      | 11  | 1.08     |
| 20/1  | 90 | 8,100      | 11,400     | 11,800     | 23  | 1.03     |
| 50/1  | 90 | 20,200     | 21,500     | 22,100     | 47  | 1.02     |
| 100/1 | 90 | 40,400     | 40,600     | 41,500     | 99  | 1.02     |
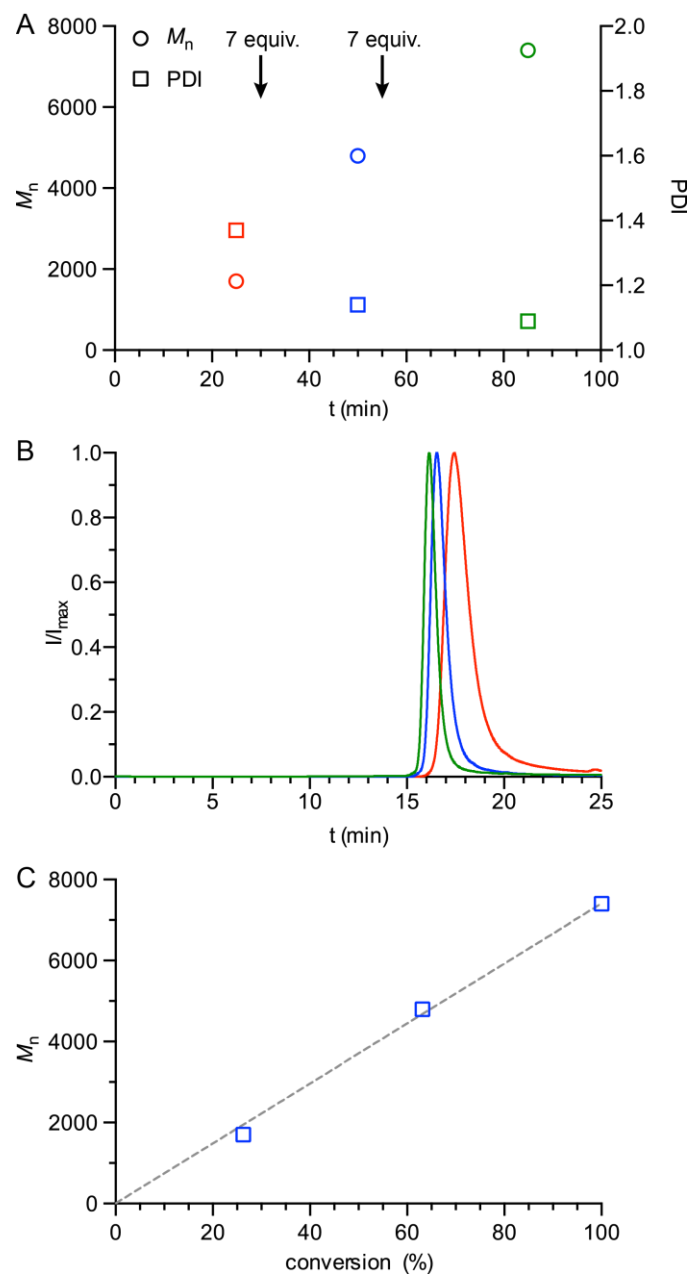
**Figure 2-9.** A) Sequential addition of equivalents of monomer **2a** after consumption of initial monomer loading at 90 °C in Tol-$d_8$. Complete consumption of monomer was confirmed by ^{1}H NMR. B) GPC traces for living polymer samples taken at 25 min (red), 50 min (blue), and 80 min (green). C) Linear correlation between $M_n$ and % conversion.
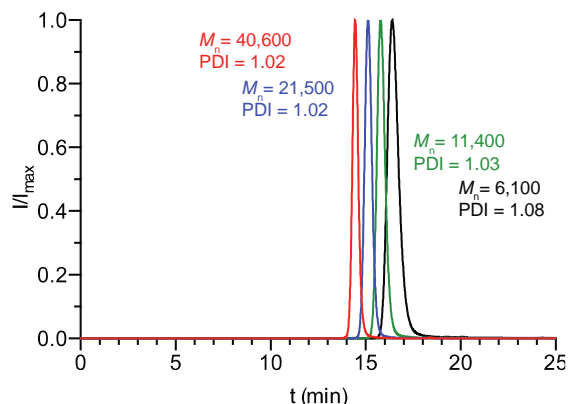
**Figure 2-10.** GPC traces for *poly*-**2a** produced through ROAMP of **2a** with catalyst **1** at variable loadings of [**2a**]/[**1**] = 100 (red), 50 (blue), 20 (green), 10 (black) (T = 90°); calibrated to polystyrene standards.
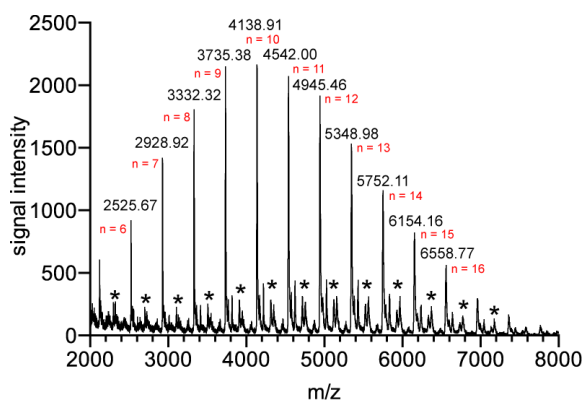


**Figure 2-11.** MALDI of *poly*-**2a** ($M_n$ = 6,100 as determined by GPC). The main family of peaks is separated by a mass of 404 Da (the mass of the monomer **2a**) and corresponds to molecular ions of [*poly*-**2a**]. The two minor families of peaks marked with * are separated by 404 Da and corresponds to molecular ions of [*poly*-**2a**+226]$^+$, an adduct between *poly*-**2a** and the matrix dithranol, and ions of [*poly*-**2a**+487]$^+$, an adduct between *poly*-**2a** and the ONO pincer ligand **9**.

### 2.3.2 Kinetic Studies of Initiation and Propagation of ROAMP of 2a by Complex 1

The proposed kinetic scheme for the polymerization of a ring-strained monomer **5a** with catalyst **1** is depicted in Scheme 2-6. In a fast initiation reaction, 1 equiv. of **5a** reacts with **2** to form the initiated complex **7** (n = 1). Binding of KOR to **7** stabilizes the initiated complex and reversibly blocks the active site. Dissociation of KOR from **6** regenerates the active propagating species that undergoes linear chain-growth polymerization with further equivalents of **5a** to form extended living polymer chains.

**Initiation Reaction**

$$\text{Ar–[Mo]·KOR} \underset{k_{-1}}{\overset{k_1}{\rightleftharpoons}} \text{Ar–[Mo]} + \text{KOR}$$

**1**          **10**

$$\text{Ar–[Mo]} + \text{2a} \overset{k_i}{\longrightarrow} \text{P}_n\text{–[Mo]}$$

**10**    **2a**      **11**

**Propagation Reaction**

$$\text{P}_n\text{–[Mo]·KOR} \underset{k_{-2}}{\overset{k_2}{\rightleftharpoons}} \text{P}_n\text{–[Mo]} + \text{KOR}$$

**12**          **11**

$$\text{P}_n\text{–[Mo]} + \text{2a} \overset{k_p}{\longrightarrow} \text{P}_{n+1}\text{–[Mo]}$$

**11**    **2a**      **11**

**Scheme 2-6**. Proposed kinetic scheme for the ROAMP of **2a** by **1**.

To meet the stringent criteria for a living polymerization the initiation of the catalyst must be fast and quantitative ($k_i > k_p$), the concentration of propagating species has to remain constant throughout the reaction, all propagating chains have to grow at the same rate, and irreversible termination and chain-transfer processes should be absent.[39] The rate laws for both the initiation and the propagation reaction are derived employing the following assumptions: i) The release of ring-strain stored in the cyclic monomer **2a** makes the initiation and the propagation irreversible. ii) The rate of propagation $k_p$ is comparable for all propagating species irrespective of the degree of polymerization. iii) The dissociation equilibria are faster than the rate of initiation/propagation. iv) Catalyst **1** initiates quantitatively. It is thus reasonable to assume that, during the polymerization, the concentration of **11** reaches steady state. The rate law of the propagation is derived, assuming that the rate constant of polymerization is $k_p$, the catalyst concentration is $[C_p]$, and the concentration of monomer is $[M]$. This gives a rate of propagation

$$-\frac{d[M]}{dt} = k_p[C_p][M] \tag{E1}$$

If all metal centers have been initiated and react at comparable rates then $[C_p]$ can be expressed as

$$[C]_0 = [C_p] + [C_p \bullet KOR] \qquad \text{(E2)}$$

or

$$K_{diss,p} = \frac{k_2}{k_{-2}} = \frac{[C_p][KOR]}{[C_p \bullet KOR]} \qquad \text{(E3)}$$

Solving (E3) for $[C_p \bullet KOR]$ gives:

$$[C_p \bullet KOR] = \frac{[C_p][KOR]}{K_{diss,p}} \qquad \text{(E4)}$$

Substituting (E4) in (E2) and solving for $[C_p]$ gives:

$$[C_p] = \frac{[C]_0}{\left( \dfrac{[KOR]}{K_{diss,p}} + 1 \right)} \qquad \text{(E5)}$$

Substituting (E5) in (E1) gives:

$$-\frac{d[M]}{dt} = \frac{k_p[C]_0[M]}{\left( \dfrac{[KOR]}{K_{diss,p}} + 1 \right)} \qquad \text{(E6)}$$

where $[M]$ is the concentration of monomer **2a**, $[C]_0$ is the starting concentration of **1**, and $K_{diss,p}$ is the dissociation constant of **11**. In the derived rate law, the rate of polymerization is proportional to the concentration of catalyst in solution, and first order in the concentration of monomer. It is no surprise that large concentrations of alkoxide result in smaller rates of polymerization, since the free alkoxide effectively blocks active sites.

Since the rate of initiation of complex **10** is very fast at the temperatures used throughout the polymerization, we herein rely on an approximation based on initial rates of reaction

$$\frac{d[C_i]}{dt} = \frac{k_i[C]_0[M]}{\left( \dfrac{[KOR]}{K_{diss}} + 1 \right)} = k_{i,obs}[C]_0[M] \qquad \text{(E7)}$$

where $[C_i]$ is the concentration of all initiated species **11/12**, and $K_{diss}$ is the dissociation constant of **1**.

Experimental data are consistent with the proposed rate laws. Plots of $\ln([M]/[M]_0)$ over time (Figure 2-12) are linear throughout the entire polymerization and fit a rate law

first order in monomer. The concentration of propagating species is constant throughout the reaction and irreversible termination processes are absent. The observed rate of propagation shows a linear dependence on the catalyst loading (Figure 2-13).
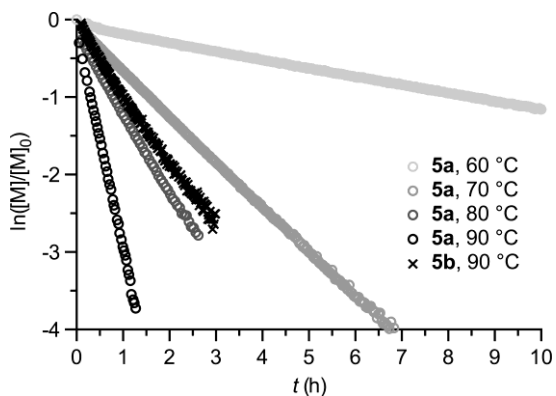


**Figure 2-12**. Kinetic studies of the rate of polymerization of **5a** and **5b** by **1** at various temperatures.
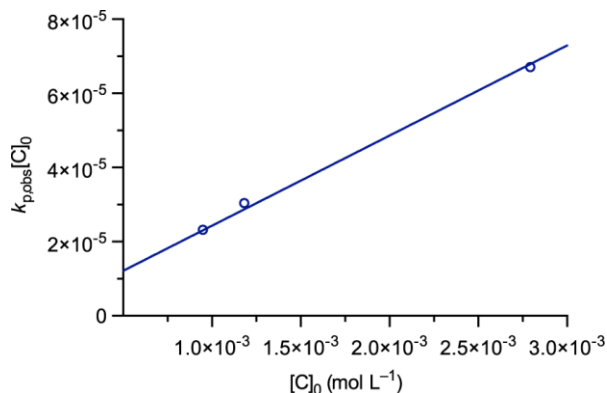


**Figure 2-13.** Observed rate of propagation $k_{p,obs}$ [C]$_0$ at different loadings of ROAMP catalyst **1** (T = 60 °C). $R^2$ = 0.997
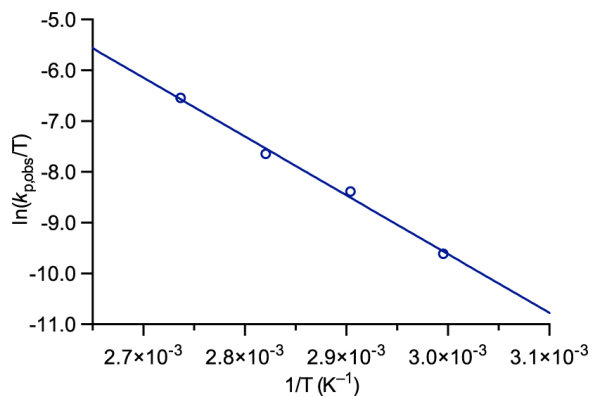


**Figure 2-14.** Eyring plot of the observed rate of propagation $k_{p,obs}$ at different temperatures. $R^2$ = 0.995.

Similarly, the rate of initiation shows a linear dependence on the concentration of monomer [M] and catalyst $[C]_0$. The observed rate constants $k_{i,obs}$ and $k_{p,obs}$ at various temperatures are summarized in Table 2-3. The standard activation enthalpy for the initiation ($\Delta H^{\ddagger} = 20.7 \pm 1.2$ kcal mol$^{-1}$) and for the propagation reaction ($\Delta H^{\ddagger} = 23.0 \pm 1.2$ kcal mol$^{-1}$) can be derived from Eyring analysis (Figures 2-14 and 2-15).
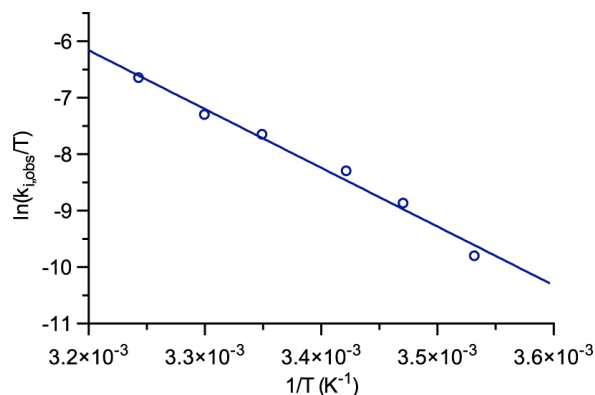


**Figure 2-15.** Eyring plot of the observed rate of initiation $k_{i,obs}$ at different temperatures. $R^2 = 0.986$.

**Table 2-3.** Observed rates of initiation $k_{obs,i}$ and rates of propagation $k_{obs,p}$ at different temperatures. [a] The rate of initiation at T > 40 °C is too fast to be monitored by $^{19}$F NMR.

| T(°C) | $k_{i,obs}$ (M$^{-1}$s$^{-1}$)[a] | T(°C) | $k_{p,obs}$ (M$^{-1}$s$^{-1}$) |
|-------|-------------------|-------|-------------------|
| 10 | 0.0158 | 60 | 0.0227 |
| 15 | 0.0407 | 70 | 0.0787 |
| 20 | 0.1210 | 80 | 0.1642 |
| 25 | 0.2197 | 90 | 0.5271 |
| 30 | 0.4066 | | |
| 35 | 0.8650 | | |

### 2.3.3 Mechanistic Investigation of the Role of Alkoxide on Catalytic Reactivity

We studied the role of the weakly coordinating alkoxide ligand during the initiation and the polymerization reaction. At elevated temperatures (T > 60 °C) a rapid equilibrium is established between the -ate complexes **1** and **12**, and the dissociated complexes **10** and **11**, respectively (Figure 2-4). The dissociation constants of the initiated catalyst **12** ($K_{p,diss}$) at selected temperatures are summarized in Table 2-4. Van't Hoff analysis reveals that the change in standard free enthalpy ($\Delta H° = 7.1 \pm 0.2$ kcal mol$^{-1}$) and entropy ($\Delta S° = 13.8 \pm 0.6$ eu) associated with the dissociation of KOR from **12** is smaller than the respective changes observed for the dissociation of **1** ($\Delta H° = 9.5 \pm 0.5$

51

kcal mol$^{-1}$, $\Delta S^\circ$ = 16.8 ± 2.1 eu) (Figures 2-6 and 2-16). The rates of dissociations of **12** ($k_2$) at various temperatures were measured by Selective Inversion Recovery (SIR) $^{19}$F NMR experiments (Table 2-4, Figure 2-17).[40,41] The standard activation enthalpies for the dissociation of **1** ($\Delta H^\ddagger$ = 10.4 ± 0.6 kcal mol$^{-1}$) and **12** ($\Delta H^\ddagger$ = 12.8 ± 0.4 kcal mol$^{-1}$) were derived from Eyring plots (Figures 2-8 and 2-16).

**Table 2-4.** Dissociation constants ($K_{diss}$, $K_{p,diss}$) and selected rate constants ($k_1$, $k_2$) for **1** and **6** at different  temperatures. [a] The resonance signals in the $^{19}$F NMR are broadened and could not be inverted for SIR experiments.

| T (°C) | $K_{p,diss}$ (M) | $k_2$ (s$^{-1}$) |
|---|---|---|
| 10.0 | 3.70 10$^{-3}$ | 1.2 |
| 15.0 | 4.26 10$^{-3}$ | 1.9 |
| 20.0 | 5.98 10$^{-3}$ | 2.9 |
| 25.0 | 6.62 10$^{-3}$ | 4.3 |
| 27.5 | 7.13 10$^{-3}$ | 4.9 |
| 30.0 | 8.07 10$^{-3}$ | 6.4 |
| 32.5 | 9.00 10$^{-3}$ | 7.1 |
| 35.0 | 9.94 10$^{-3}$ | 8.2 |
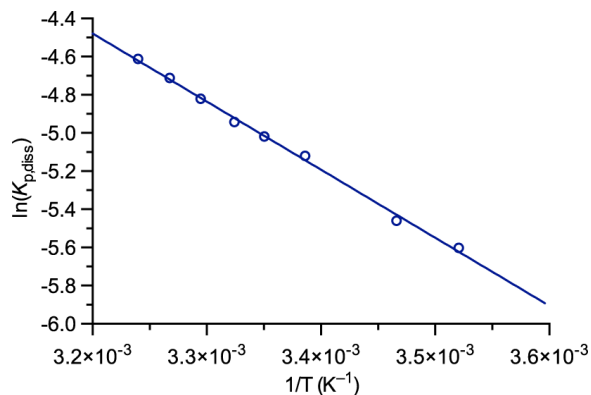


**Figure 2-16.** Van't Hoff plot of $K_{p,diss}$ of **12** between 10 °C and 35 °C. $R^2$ = 0.998.
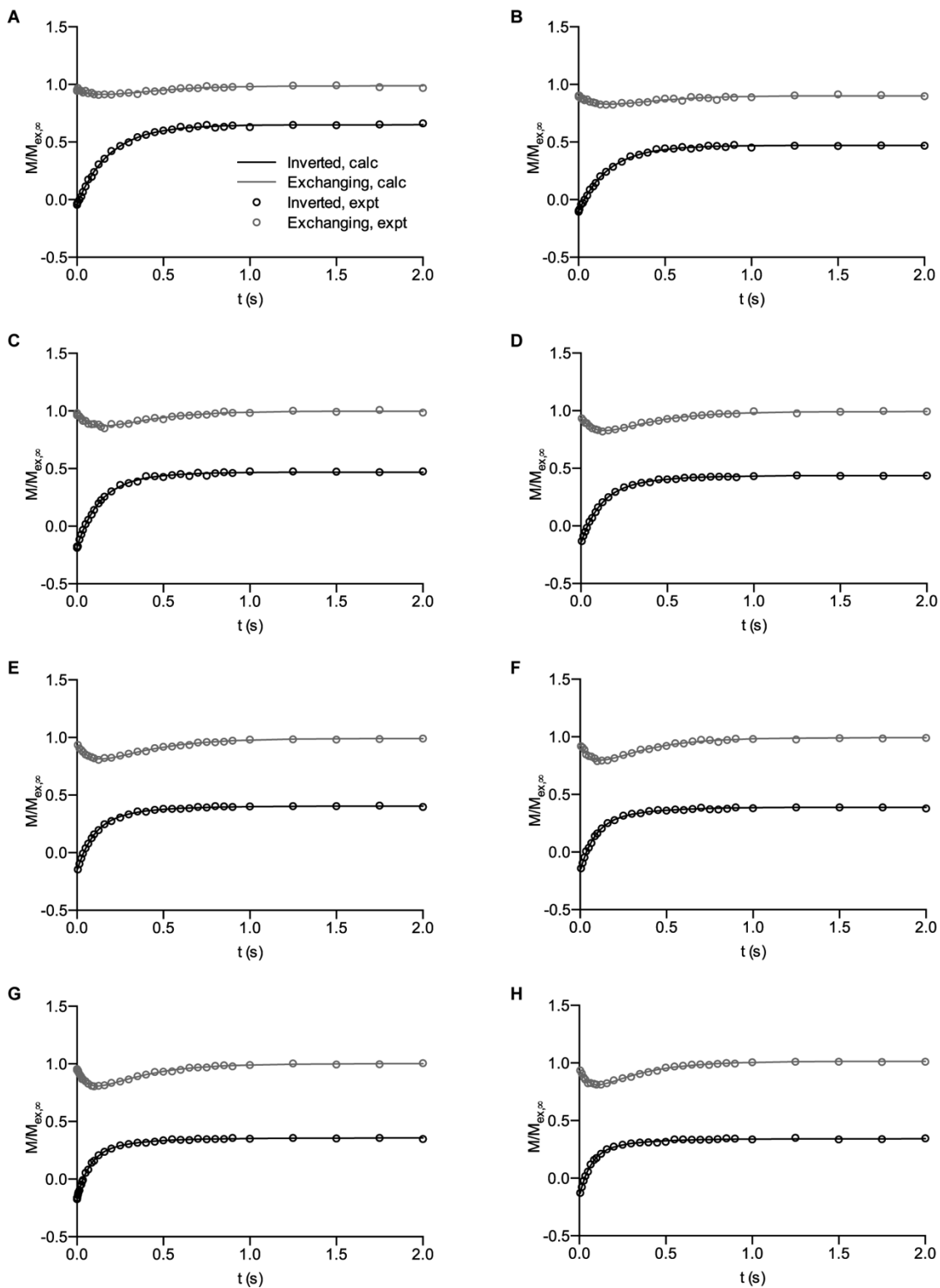
**Figure 2-17.** SIR experiments of the dissociation of **12** at (A) 10.0 °C, (B) 15.0 °C, (C) 20.0 °C, (D) 25.0 °C, (E) 27.5 °C, (F) 30.0 °C, (G) 32.5 °C, and (H) 35.0 °C.
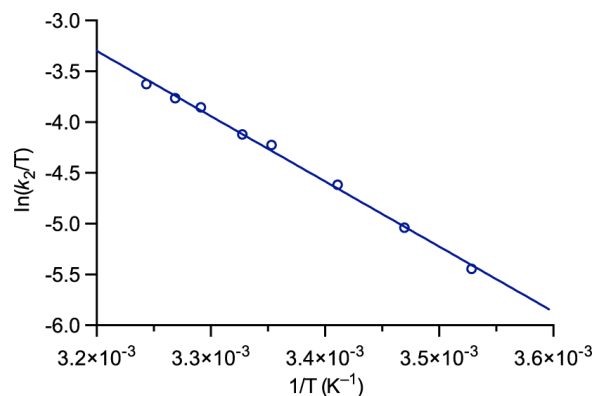
**Figure 2-18.** Eyring plot for the rate of dissociation ($k_2$) of **12**. ($R^2 = 0.997$).

To highlight the importance of the KOR dissociation equilibrium for the performance of ROAMP catalyst **1**, we polymerized **2a** in the presence of varying amounts of a Lewis acid. Addition of 2 equiv. of BPh$_3$ to a solution of **1** in toluene efficiently shifts the dissociation equilibrium towards the pentacoordinate complex **10** (2 equiv. of a Lewis acid are required to trap the labile hexafluoro-*tert*-butoxide and the isopropyl ether found in the crystal unit cell of **1**). Polymers formed in the absence of free hexafluoro-*tert*-butoxide feature broad weight distributions (PDI > 1.3) and $M_n$ that do not reflect the initial [**2a**]/[**1**] loading (Figure 2-19). BPh$_3$ traps free KOCCH$_3$(CF$_3$)$_2$ in solution and shifts the dissociation equilibrium of **1** toward the pentacoordinate complex **10**. The GPC of the resulting polymers reveal that in the absence of a stabilizing alkoxide ligand (KOCCH$_3$(CF$_3$)$_2$) the polymerization is uncontrolled and leads to polymers with broad PDIs and unpredictable $M_n$.
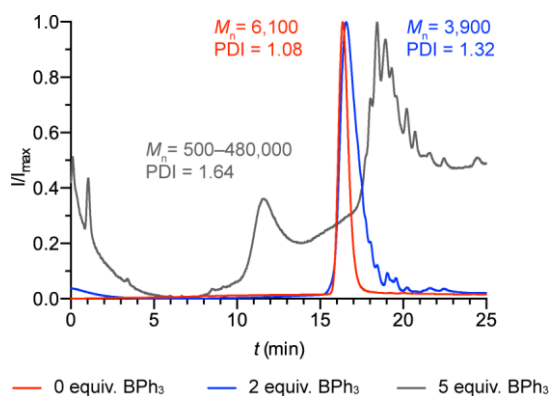


**Figure 2-19.** Polymerization of **2a** by **1** in the absence (red), and in the presence of 2 equiv. (blue) (2 equiv. of a Lewis acid are required to trap the labile hexafluoro-*tert*-butoxide and the isopropyl ether found in the crystal unit cell of 1) and 5 equiv. (gray) of a Lewis acid.

As mentioned earlier, the rate law of the propagation is

$$-\frac{d[M]}{dt} = \frac{k_p[C]_0[M]}{\left(\dfrac{[KOR]}{K_{diss,p}} + 1\right)}$$

(E6)

In order to confirm the rate law and the role of the weakly bound alkoxyde, we studied the relationship between the rate contact $k_{p,obs}$ and [KOR]. A plot of $1/([KOR]/K_{diss,p}+1)$ versus $k_{p,obs}$ at 90 °C shows a linear correlation between the rate of propagation and the inverse of the concentration of KOR (Figure S5). Excess KOR added to the reaction mixture slows the rate of initiation.
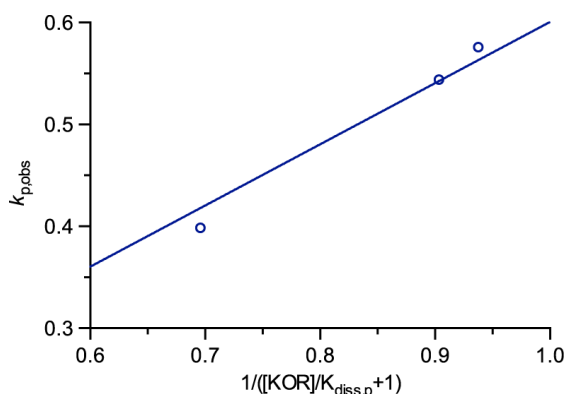


**Figure 2-20.** Observed rate of propagation $k_{p,obs}$ at different concentrations of [KOR] (T = 90 °C). $R^2 =$ 0.970

With these studies in mind, we see that the rate constant is dependent on the concentration of alkoxide, while also affecting the PDI. Therefore, we may conclude that the alkoxide seems to act as a stabilizing donor for the catalyst **1** and the propagation species **12**. This ligand effectively blocks the active side and prevents termination reactions such as chain transfer and chain backbiting.

### 2.3.4 Insights into the Mechanism of ROAMP by Complex *1*

Figure 2-21 summarizes the experimentally determined kinetic and thermodynamic parameters for the initiation and the propagation reaction at standard conditions. The association of KOR is a fast pre-equilibrium to the rate-determining step. The rate of initiation is faster than the rate of propagation even though the equilibrium concentration of the alkoxide free uninitiated species **10** is lower than the concentration of the dissociated propagating species **11**. The rate-determining transition state for the propagation is 3.6 kcal mol$^{-1}$ higher than the transition state for the initiation reaction. This subtle difference satisfies one of the main criteria for living polymerization: a rate of

initiation that is much faster than the corresponding rate of propagation. The observed difference in metathesis activity between **10** and **11** can be rationalized by a combination of electronic and steric effects imposed by the growing polymer chain. The steric bulk associated with the *ortho*-substituted polymer backbone increases the barrier for the incorporation of the next ring-strained monomer. The initiated catalyst **11** features an electron donating hexyloxy substituent on the benzylidyne that further stabilizes the Mo(VI) complex as compared to the CH$_3$ group in **10** (Scheme 2-5).
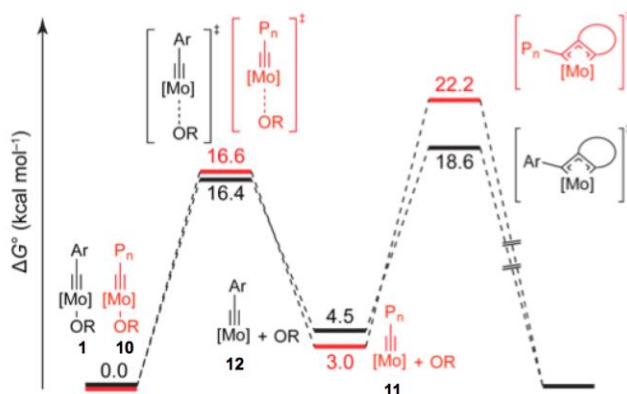


**Figure 2-21.** Reaction coordinate diagram for the initiation (black) and the propagation reaction (red) at 25 °C.

## 2.4 Block Copolymers via Ring-Opening Alkyne Metathesis Reactivity of Complex **1**

### 2.4.1 Ring-Opening Alkyne Metathesis Polymerization by Complex **1** of PEG-Monomer **2b**

To expand the substrate scope of ROAMP with catalyst **1** we synthesized ring-strained monomer **2b** (Scheme 2-5) featuring solubilizing triethylene glylcol chains. Even though the ether oxygen atoms in the side chains compete with the free alkoxide and the ring strained monomer for binding to the propagating molybdenum species **11**, the $M_n$ and the PDIs for polymers obtained from the ring opening of **2b** are comparable those obtained with **2a** and are summarized in Table 2-5. The observed rate constant for the ROAMP of **2b** at 90 °C is slower ($k_{p,obs} = 0.144$ M$^{-1}$ s$^{-1}$) than for **2a** ($0.5271$ M$^{-1}$ s$^{-1}$) resulting in a $t_{1/2} \sim 38$ min ($t_{1/2} \sim 10$ min for **2a**) (Figure 2-12).

**Table 2-5.** Molecular weight analysis of *poly*-**2b** and block copolymers *poly*-**2a**-block-*poly*-**2b**. [a] calibrated to narrow polydispersity polystyrene standards; [b] degree of polymerization determined by $^1$H NMR end-group analysis; [c] sample taken from the reaction mixture after t = 30 min.

| [**5a**]/[**5b**]/[**1**] | T (°C) | $M_n$ theory | $M_n$ GPC[a] | $M_w$ GPC[a] | $X_{n[5a]}$/$X_{n[5b]}$[b] | PDI GPC[a] |
|---|---|---|---|---|---|---|
| 0/10/ | 90 | 5,40 | 5,70 | 6,10 | 0/9 | 1.0 |

| | | | | | | |
|---|---|---|---|---|---|---|
| 1 | | 0 | 0 | 0 | | 8 |
| 10/0/1 [c] | 90 | 4,000 | 3,300 | 3,800 | 10/0 | 1.15 |
| 10/10/1 | 90 | 8,300 | 11,000 | 11,800 | 11/12 | 1.07 |
| 20/0/1 [c] | 90 | 8,100 | 14,400 | 15,000 | 20/0 | 1.04 |
| 20/20/1 | 90 | 13,400 | 25,400 | 27,200 | 20/20 | 1.07 |

*2.4.2 Ring-Opening Alkyne Metathesis Polymerization by Complex 1 of Monomers 2a and 2b*

    With two chemically distinct monomers at hand we studied the performance of ROAMP catalyst **1** in the synthesis of amphiphilic block-copolymers. At 90 °C, 10 (20) equiv. of **2a** were reacted with **1** for 30 min. Prior to the addition of 10 (20) equiv. of **2b**, an aliquot was removed from the reaction mixture and analyzed by GPC. After the consumption of all monomers, as judged by $^1$H NMR spectroscopy, the reaction was quenched with MeOH. Unlike *poly*-**2a**, low molecular weight ($M_n$ = 8000) *poly*-**2a**-block-*poly*-**2b** is soluble in MeOH and only precipitates from concentrated solutions as a pale orange solid in >90% yield. GPC analysis reveals an increase in $M_n$ upon addition of **2b** to the living chains of *poly*-**2a** (Figure 2-22). The PDI of *poly*-**2a**-block-*poly*-**2b** is exceptionally low (1.08) and matches the catalyst performance achieved for the respective homopolymers. End-group analysis reveals that the ratio of monomers in *poly*-**2a**-block-*poly*-**2b** scales linearly with the monomer loading.
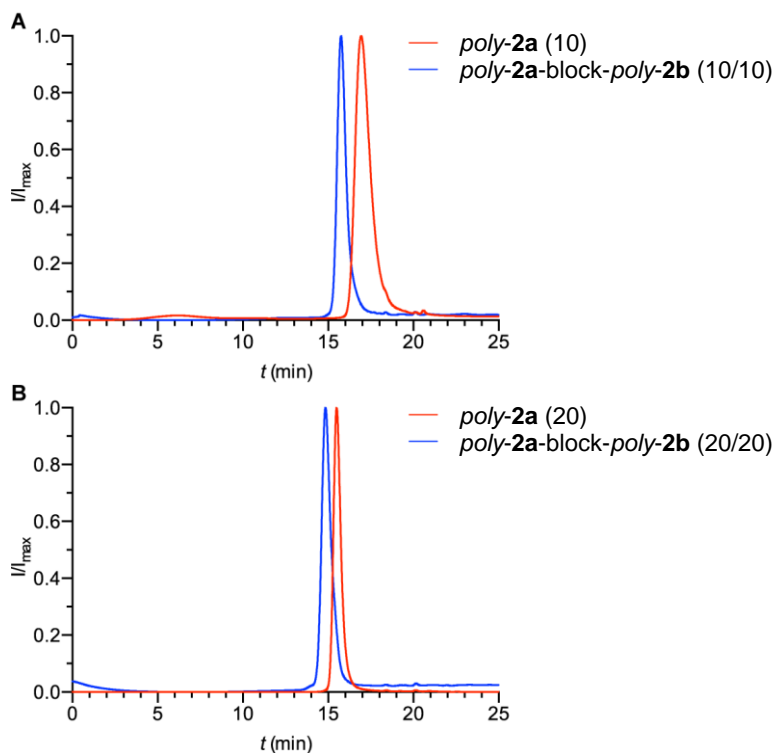
**Figure 2-22.** A) GPC traces for *poly*-**2a** (red) and *poly*-**2a**-block-*poly*-**2b** (blue) at a monomer loading of **2a**:**2b** = 10:10. B) GPC traces for *poly*-**2a** (red) and *poly*-**2a**-block-*poly*-**2b** (blue) at a monomer loading of **2a**:**2b** = 20:20.

## 2.5 Ring-Opening Alkyne Metathesis Reactivity of Other Catalysts

The performance of a series of other catalysts in the ROAMP of cyclic alkyne 3,8-dihexyloxy-5,6-dihydro-11,12-didehydrodibenzo[a,e]-[8]annulene **2a** that have been tested are summarized in Figure 2-23
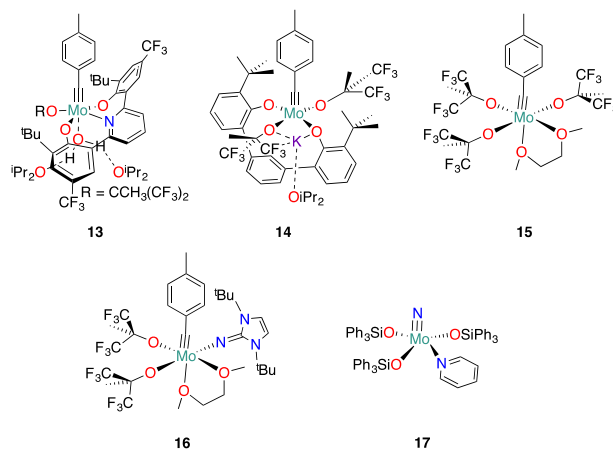


**Figure 2-23.** Benzylidyne complexes attempted for the ROAMP of **2a**.

In an attempt to lower the activation barrier for ROAMP we synthesized a catalyst featuring electron withdrawing substituents. Pincer complexes **13** and **14** are structurally related to catalyst **1**. The main difference between complex **13** and **1** is the presence of trifluoromethyl groups *para* to the phenolate oxygen (Figure 2-24). **13** crystalized with trace amount of water bound *trans* to the carbyne. Water in this case is analogous to the alkoxide studied earlier, but less stable, such that it is less sigma donating and may potentially serve as a source of protons during the reaction. Addition of **13** to the monomer **2a** results in an uncontrolled ROAMP at 24 °C. Although ROAMP product is observed, the reaction is instantaneous and high molecular weight polymers precipitate from solution. Only a small fraction of **13** initiates, and consumes the ring-strained monomer leading to polymers featuring >1000 times the theoretically expected molecular weight.
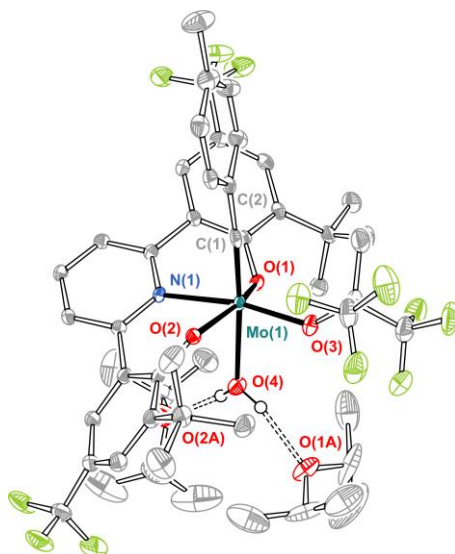


**Figure 2-24.** ORTEP representation of the X-ray crystal structure of **13**. Thermal ellipsoids are drawn at the 50% probability level. Color coding: C (gray), O (red), N (blue) F (green), Mo (turquoise). Hydrogen atoms are omitted for clarity except those in water.

Catalyst **14** features a phenyl ring rather than a pyridine in the pincer ligand. In the X-ray structure, the pincer complex adopts a *trans* conformation with respect to the carbyne. In the absence of a competent sigma donor ligand, the *trans* effect of the carbyne dominates the coordination sphere (Figure 2-25). Whereas the pyridine serves as a σ donor, and thus considered labile due to the *trans* effect of the carbyne, it also serves as a π acceptor, interacting with a frontier *d* orbital. However, in the case of **14**, the weakly bound alkoxide is *cis* to the carbyne, and the phenyl group in the pincer ligand blocks the site *trans* to the carbyne. This provides an active site that is readily available cis to the carbyne, which leads to alkyne polymerization. ROAMP of **2a** with **14** results in the formation of polymers but no sign of strain release is observed by monitoring the shift of the bridge protons by $^1$H NMR.
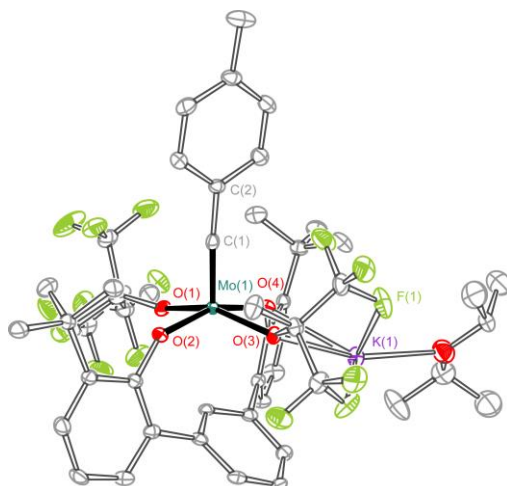
**Figure 2-25.** ORTEP representation of the X-ray crystal structure of **14**. Thermal ellipsoids are drawn at the 50% probability level. Color coding: C (gray), O (red), F (green), Mo (turquoise). Hydrogen atoms are omitted for clarity except those in water.

The GPC traces of complexes **14-16** are shown in Figure 2-26. Catalysts **15** and **16** were synthesized in analogy to the method used by Tamm et al. and **17** was commercially available.[6-7] Catalyst **17** is used in literature for Ring-Closing Alkyne Metathesis (RCAM), thus it is no surprise that it gives rise to oligomers with a broad molecular weight distribution. However, an improvement is seen with catalysts **15** and **16**. A molecular weight 3-times larger than theoretically expected, and a PDI of 1.30, were found for catalyst **15**. Catalyst **16** is an active alkyne cross metathesis (ACM) catalyst. Under ROAMP conditions **16** leads to high molecular weight polymers. This may occur due to undesired terminations or incomplete initiation.
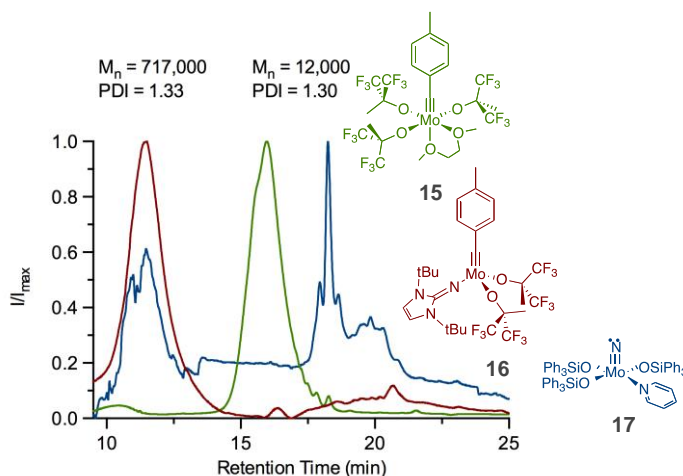


**Figure 2-26.** GPC traces of catalysts **15** (green), **16** (red), and **17** (blue).

We conclude that the presence of a pincer ligand or an electron donating ligand alone is not responsible for the living nature of the ROAMP by **1**. It is the combined presence

of a strong sigma donor, a pincer ligand, and a donating weakly coordinating alkoxide that contributes to the unique selectivity of **1** for strained over unstrained alkynes.


## 2.6 Conclusion

In summary, we have described the synthesis of the first molecularly well-defined 16-electron ROAMP catalyst based on a molybdenum benzylidyne ONO pincer complex [TolC≡Mo(ONO)(OR)]•KOR (R = CCH$_3$(CF$_3$)$_2$) **1**. The incorporation of a permanent electron donating tridentate ligand irreversibly blocks one of the catalyst's active sites, prevents undesired alkyne polymerization reactions, and significantly increases its stability towards air and moisture. The catalyst is capable of selectively ring-opening strained alkynes in a controlled polymerization to yield high molecular weight polymers with exceptionally low PDIs (1.02). Mechanistic studies reveal that the ROAMP catalyst **1** meets all the criteria for a controlled living polymerization: the initiation reaction is quantitative and ~10$^3$ timers faster than the propagation ($k_i > k_p$), the concentration of catalytically active complex is constant throughout the reaction, and all propagating chains grow at the same rate. The reversible coordination of KOR to the propagating catalyst prevents undesired chain termination and bimolecular decomposition of the catalyst. We demonstrate for the first time the synthesis of structurally well-defined block-copolymers through a controlled living ROAMP. The catalyst developed herein provides an unprecedented control and access to functionalized homo- and block-copolymers derived from ring-strained alkynes with potential applications in advanced thin-film electronics/photonics, molecular sensing, and nano-patterning.


## 2.7 Experimental

### 2.7.1. Synthetic Details

*Materials and General Methods.* Unless otherwise stated, all manipulations of air and/or moisture sensitive compounds were carried out in oven-dried glassware, under an atmosphere of Ar or N$_2$. All solvents and reagents were purchased from Alfa Aesar, Spectrum Chemicals, Acros Organics, TCI America, and Sigma-Aldrich and were used as received unless otherwise noted. Organic solvents were dried by passing through a column of alumina and were degassed by vigorous bubbling of N$_2$ or Ar through the solvent for 20 min. Flash column chromatography was performed on SiliCycle silica gel (particle size 40–63 μm). Thin layer chromatography was carried out using SiliCycle silica gel 60 Å F-254 precoated plates (0.25 mm thick) and visualized by UV absorption. All $^1$H, {$^1$H}$^{13}$C, and $^{19}$F NMR spectra were recorded on Bruker AV-600, DRX-500, AV-500, and AV-900 MHz spectrometers, and are referenced to residual solvent peaks (CDCl$_3$ $^1$H NMR $\delta$ = 7.26 ppm, $^{13}$C NMR $\delta$ = 77.16 ppm; C$_6$D$_6$ $^1$H NMR $\delta$ = 7.16 ppm, $^{13}$C NMR $\delta$ = 128.06 ppm; Tol-$d_8$ $^1$H NMR $\delta$ = 2.08 ppm; THF-$d_8$ $^1$H NMR $\delta$ = 1.78 ppm, $^{13}$C NMR $\delta$ = 67.21 ppm) or trifluorotoluene ($^{19}$F NMR $\delta$ = –63.72 ppm). The concentration of **1**, **10**, **11**, **12**, and KOCCH$_3$(CF$_3$)$_2$ were determined by $^{19}$F NMR using the ERETIC method against an external standard of 13.6 mM trifluorotoluene in Tol-d$_8$.[1] The concentration of monomer **2a** and **2b** was verified by $^1$H NMR applying the ERETIC

method against an external standard of 19.4 mM of hexamethyldisiloxane in Tol-$d_8$.[1] Selective Inversion Recovery (SIR) experiments were performed using TopSpin for data acquisition, and fitted with CIFIT.[2-4] The temperature in all VT NMR experiments is calibrated to ethylene glycol or MeOH standards. ESI mass spectrometry was performed on a Finnigan LTQFT (Thermo) spectrometer in positive ionization mode. MALDI mass spectrometry was performed on a Voyager-DE PRO (Applied Biosystems Voyager System 6322) in positive mode using a matrix of dithranol. Elemental analysis (CHN) was performed on a Perkin Elmer 2400 Series II combustion analyzer (values are given in %). Gel permeation chromatography (GPC) was carried out on a LC/MS Agilent 1260 Infinity set up with a guard and two Agilent Polypore 300 x 7.5 mm columns at 35 °C. All GPC analyses were performed on a 0.2 mg/mL solution of polymer in chloroform. An injection volume of 25 μL and a flow rate of 1 mL/min were used. Calibration was based on narrow polydispersity polystyrene standards ranging from $M_w$ = 100 to 4,068,981. X-ray crystallography was performed on APEX II QUAZAR, using a Microfocus Sealed Source (Incoatec IμS; Mo-Kα radiation), Kappa Geometry with DX (Bruker-AXS build) goniostat, a Bruker APEX II detector, QUAZAR multilayer mirrors as the radiation monochromator, and Oxford Cryostream 700 for **1**. For **2a**, X-ray crystallographic data was collected on MicroSTAR-H APEX II, with Microfocus Rotating Anode (Cu-Kα radiation) as the X-ray source, Kappa Geometry with DX (Enraf-Nonius build) goniostat, Bruker APEX II detectors, HELIOS multilayer mirrors as the radiation monochromator, and Oxford Cryostream 700. All crystallographic data was refined with SHELXL-97, solved with SIR-2007, visualized with ORTEP-32, and finalized with WinGX. **9**,[5] KOCCH3(CF3)2,[6] 4,9-dimethoxy-6,7-dihydro-1*H*-dibenzo[*a*,*e*]cyclopropa[*c*][8]annulen-1-one,[7] and KBn[8] were synthesized following literature procedures.
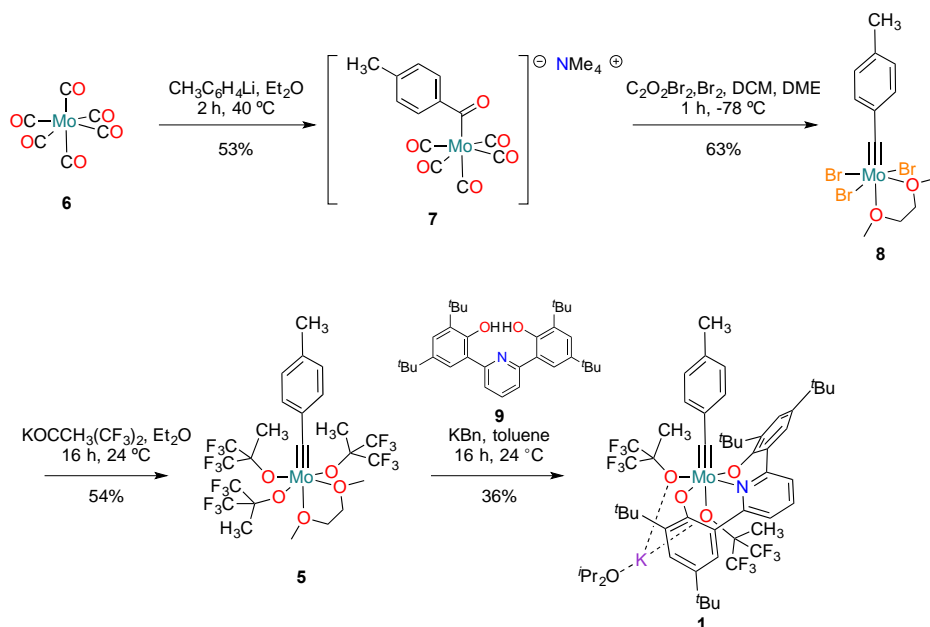


**Scheme 2-7.** Synthesis of **1**.

*[N(CH₃)₄][(CO)₅MoCOC₆H₄(CH₃)]* (**7**) A 100 mL Schlenk flask was charged with 4-iodotoluene (10 g, 46 mmol, 1.0 equiv.) in dry Et₂O (28 mL) and cooled to −78 °C. $^n$BuLi (2.5 M, 19.3 mL, 48 mmol, 1.05 equiv.) was added dropwise and the reaction mixture was stirred at −78 °C for 30 min, and then warmed to 24 °C. The reaction mixture was transferred dropwise into a refluxing solution of Mo(CO)₆ (**6**) (12.1 g, 46 mmol, 1 equiv.) in dry Et₂O (300 mL). The reaction mixture was stirred for 2 h at 40 °C and the solvent was removed under vacuum. The residue was dissolved in H₂O (10 mL) and filtered into a solution of [N(CH₃)₄]Br (10.6 g, 69 mmol, 1.5 equiv.) in H₂O (25 mL). The precipitate was collected and washed with H₂O (100 mL). The crude product was recrystallized from CH₂Cl₂/Et₂O to yield **7** (10.5 g, 53%) as orange crystals. $^1$H NMR (600 MHz, CD₂Cl₂, 22 °C) $\delta$ = 7.39 (d, $J$ = 7.9 Hz, 2H), 7.14 (d, $J$ = 7.6 Hz, 2H), 3.28 (s, 12H), 2.32 (s, 3H) ppm; {$^1$H}$^{13}$C NMR (151 MHz, CD₂Cl₂) $\delta$ = 297.8, 218.6, 213.1, 212.0, 153.5, 146.7, 138.7, 128.6, 127.4, 125.9, 56.8, 21.5 ppm; Anal. Calcd for [N(CH₃)₄][(CO)₅MoCOC₆H₄(CH₃)]: C, 47.56; H, 4.46; N, 3.26. Found: C, 47.19; H, 4.20; N, 3.44.

*[TolC≡MoBr₃(DME)]* (**8**) A 100 mL Schenk flask was charged with **7** (2.50 g, 5.84 mmol, 1.0 equiv.) in dry CH₂Cl₂ (60 mL) and cooled to −78 °C. A precooled solution of oxalyl bromide (2.92 mL, 5.84 mmol, 1.0 equiv.) in CH₂Cl₂ (5 mL) was added and the reaction mixture was stirred for 10 min at −78 °C. The cooling bath was removed and the reaction mixture was warmed until the color changed to a clear yellow. The cooling bath was immediately replaced and the reaction mixture stirred for 15 min at −78 °C. The reaction mixture was filtered through a Schlenk filter into a precooled Schlenk flask at −78 °C. Anhydrous DME (6.30 mL, 60.7 mmol, 10.4 equiv.) and Br₂ (0.3 mL, 5.84 mmol, 1.0 equiv.) in CH₂Cl₂ (5 mL) were added at −78 °C and stirred at this temperature for 45 min. The green/brown suspension was placed in a water/ice bath, and the solvent was removed under vacuum. The brown solid was dissolved in CH₂Cl₂ (10 mL), precipitated with pentane (10 mL), and cooled to −35 °C. The precipitate was collected to afford **8** (1.94 g, 63%) as a brown powder. $^1$H NMR (600 MHz, C₆D₆, 22 °C) $\delta$ = 7.50 (d, $J$ = 8.0 Hz, 2H, C₆$H$₂H₂CH₃), 6.81 (d, $J$ = 8.0 Hz, 2H, C₆H₂$H$₂CH₃), 3.54 (s, 3H, DME-C$H$₃), 3.19–3.04 (br, 5H, DME), 2.90 (br, 2H, DME-C$H$₂), 2.11 (s, 3H, C₆H₄C$H$₃) ppm; Anal. Calcd for [TolC≡MoBr₃(DME)]: C, 27.25; H, 3.24. Found: C, 26.93; H, 3.13.

*[TolC≡Mo(OC(CF₃)₂CH₃)₃(DME)]* (**5**) A 100 mL round bottom flask was charged with **8** (779 mg, 1.48 mmol) in dry Et₂O (22 mL). A solution of KOCCH₃(CF₃)₂ (1.00 g, 4.55 mmol, 3.1 equiv.) in Et₂O (18 mL) was added and the reaction mixture was stirred at 24 °C for 16 h. The resulting suspension was filtered, and extracted with Et₂O. The solvent was removed and the residue was recrystallized from $^i$Pr₂O (5 mL) at −35 °C to yield **5** (665 mg, 54%) as red solid. $^1$H NMR (500 MHz, C₆D₆, 22 °C) $\delta$ = 7.05 (d, $J$ = 8.2 Hz, 2H, C₆$H$₂H₂CH₃), 6.76 (d, $J$ = 8.2 Hz, 2H, C₆H₂$H$₂CH₃), 3.23 (s, 6H, DME-C$H$₃), 3.03 (s, 4H, DME-C$H$₂), 2.02 (s, 3H, C₆H₄C$H$₃), 1.86 (s, 9H, OCC$H$₃(CF₃)₂) ppm; {$^1$H}$^{13}$C NMR (126 MHz, C₆D₆, 22 °C) $\delta$ = 295.4, 141.7, 139.9, 130.3, 129.0, 124.8 (q), 85.0–82.7 (m), 71.6, 63.3, 21.1, 19.1 ppm; $^{19}$F NMR (470 MHz, C₆D₆, 22 °C) $\delta$ = −77.89 ppm; Anal.

Calcd for [TolC≡Mo(OC(CF₃)₂CH₃)₃(DME)]: C, 34.63; H, 3.15. Found: C, 34.25; H, 2.80.

*[TolC≡Mo(ONO)(OCCH₃(CF₃)₂)]* •KOCCH₃(CF₃)₂•*ⁱPr₂O* (**1**). A 25 mL vial was charged with **9** (88 mg, 0.18 mmol, 1.0 equiv.) in dry toluene (3 mL). A suspension of KBn (48 mg, 0.37 mmol 2.05 equiv.) in dry toluene (8 mL) was added dropwise and the reaction mixture stirred for 15 min at 24 °C. The resulting suspension was added dropwise to a solution of **5** (164 mg, 0.2 mmol, 1.1 equiv.) in toluene (7 mL). An immediate color change to dark brown was observed, and the reaction mixture was stirred for 30 h at 24 °C. The suspension was filtered and the solvent was removed under dynamic vacuum. The precipitate was dissolved in cold $CH_2Cl_2$/pentane (3:2, 4 mL) and filtered through a precooled frit. $^iPr_2O$ (1 mL) was added to the solution, the solvent was removed under vacuum. The residue was recrystallized from $^iPr_2O$ (2 mL) (–35 °C), to yield pure **1** (78 mg, 36%) as a dark brown crystalline solid. Crystals for X-ray analysis were grown from saturated $^iPr_2O$ solutions at –35 °C. In toluene, **1** is in equilibrium with the dissociated pentacoordinate complex **10** and free $KOC(CF_3)_2CH_3$. $^1H$ NMR (500 MHz, Tol-$d_8$, 22 °C) δ = 7.70 (**10**), 7.63 (s, 2H, Ar-*H*), 7.42 (s, 2H, Ar-*H*), 7.27 (**10**), 7.20 (d, $J$ = 8.0 Hz, 2H, 3,5-NC₅$H_2$H), 6.91 (t, $J$ = 8.0 Hz, 1H, 4-NC₅$H_2$*H*), 6.58 (d, $J$ = 7.6 Hz, 2H, C₆H₂ $H_2$CH₃), 6.44 (**10**), 6.30 (d, $J$ = 7.6 Hz, 2H, C₆$H_2$H₂CH₃), 6.26 (**10**), 2.01 (s, 3H, C₆H₄-C$H_3$), 1.93 (s, 3H, OC(CF₃)₂C$H_3$), 1.71 (**10**), 1.64 (s, 18H, ᵗBu-*H*), 1.46 (s, 18H, ᵗBu-*H*), 1.37 (**10**), 1.00 (s, 3H, K-OC(CF₃)₂C$H_3$) ppm; $^{19}F$ NMR (470 MHz, Tol-$d_8$, 22 °C) δ = –76.79 (**10**), –77.80, –78.26, –81.18 (dissociated KOC(C$F_3$)₂CH₃) ppm. In THF, only the dissociated species **10•THF** is observed, resulting in the presence of free $KOC(CF_3)_2CH_3$. $^1H$ NMR (500 MHz, THF-$d_8$, 22 °C) δ = 7.92 (t, $J$ = 8.0 Hz, 1H, 4-NC₅$H_2$*H*), 7.70 (d, $J$ = 8.0 Hz, 2H, 3,5-NC₅$H_2$*H*), 7.52 (d, $J$ = 2.3 Hz, 2H, Ar-*H*), 7.46 (d, $J$ = 2.3 Hz, 2H, Ar-*H*), 6.74 (d, $J$ = 7.9 Hz, 2H, C₆$H_2$ $H_2$CH₃), 6.12 (d, $J$ = 7.9 Hz, 2H, C₆$H_2$H₂CH₃), 2.20 (s, 3H, C₆H₄C$H_3$), 1.78 (s, 3H, OC(CF₃)₂C$H_3$), 1.52 (s, 18H, ᵗBu-*H*), 1.39 (s, 18H, ᵗBu-*H*) ppm; {$^1H$}$^{13}C$ NMR (126 MHz, THF-$d_8$, 22 °C) δ = 307.5, 166.2, 155.6, 141.5, 140.5, 139.1, 138.8, 137.5, 136.8, 130.3, 127.6, 126.0, 125.4, 124.9, 123.1, 84.2, 36.0, 34.8, 32.4, 30.8, 23.5, 21.6 ppm; $^{19}F$ NMR (470 MHz, THF-$d_8$, 22 °C) δ = – 76.92 ppm; FTMS (ESI-TOF) ($m/z$): [[TolC≡Mo(ONO)(OCCH₃(CF₃)₂)]+H]⁺ calcd. [$C_{45}H_{54}$ F₆MoNO₃], 868.3056; found, 868.3076; Anal. Calcd. for [[TolC≡Mo(ONO)(OCCH₃(CF₃)₂)₂]KO$^i$Pr₂]₂•□$^i$Pr₂O: C, 56.21; H, 6.26; N, 1.13. Found: C, 56.04; H, 6.40; N, 1.38; Crystal data: CCDC no., 998197; formula, $C_{60.5}H_{83}F_{12}KMoNO_{6.25}$; fw, 1297.32 g mol⁻¹; temp, 100(2) K; cryst. system, monoclinic; space group, P2(1)/n; color, black; $a$, 12.751(5) Å; $b$, 29.140(5) Å; $c$, 17.008(5) Å; $\alpha$, 90.000(5)°; $\beta$, 93.406(5)°; $\gamma$, 90.000(5)°; $V$, 6308(3) Å³; $Z$, 4; $R1$, 0.0367; $wR2$, 0.0818; GOF, 1.051.

*Poly-3,8-dihexyloxy-5,6-dihydro-11,12-didehydrodibenzo[a,e][8]annulene* (*poly-***5a**). A 10 mL resealable Schlenk tube was charged with a stock solution of **2a** (220 mM) in toluene. If required, the solution was diluted with additional dry toluene to reach a total of 0.5 mL. A stock solution of **1** (11 mM, 100 µL) in toluene was added and the reaction mixture was heated in a bath at 90 °C for 2 h. The reaction mixture was cooled and

polymers were precipitated with MeOH (2 mL). The precipitate was filtered, washed with MeOH (2 mL), and dried in vacuum to yield *poly*-**2a** (92% isolated yield) as a pale brown solid. ^{1}H NMR (600 MHz, CDCl$_3$, 22 °C) δ = 7.40 (d, *J* = 8.4 Hz, 2H, Ar-*H*), 6.77–6.52 (m, 4H, Ar-*H*), 3.67 (t, *J* = 6.5 Hz, 4H, OC*H*$_2$), 3.19 (s, 4H, C*H*$_2$), 1.69–1.58 (m, 4H, O(C*H*$_2$)$_5$CH$_3$), 1.41–1.19 (m, 12H, O(C*H*$_2$)$_5$CH$_3$), 0.87 (t, *J* = 7.0 Hz, 6H, C*H*$_3$) ppm; {^{1}H}^{13}C NMR (151 MHz, CDCl$_3$, 22 °C) δ = 159.2, 145.3, 133.5, 115.3, 114.6, 113.0, 90.5, 67.9, 36.6, 31.8, 29.4, 25.9, 22.8, 14.2 ppm.

*Poly-3,8-di(2-(2-(2-methoxyethoxy)ethoxy)ethoxy)-5,6-dihydro-11,12-didehydrodibenzo[a,e][8]annulene* (*poly*-**2b**). A 10 mL resealable Schlenk tube was charged with a stock solution of **2b** (220 mM) in toluene. If required, the solution was diluted with additional dry toluene to reach a total of 0.5 mL. A stock solution of **1** (11 mM, 100 µL) in toluene was added and the reaction mixture was heated in a bath at 90 °C for 7 h. The reaction mixture was concentrated and the solid residue suspended in cold MeOH (2 mL). The precipitate was filtered, washed with cold MeOH (2 mL), and dried in vacuum to yield *poly*-**2b** (53% isolated yield) as a pale orange solid. ^{1}H NMR (900 MHz, CDCl$_3$, 22 °C) δ = 7.38 (s, 2H, Ar-H), 6.66 (s, 4H, Ar-H), 3.91–3.24 (m, 30H), 3.17 (s, 4H, C*H*$_2$) ppm; {^{1}H}^{13}C NMR (226 MHz, CDCl$_3$, 22 °C) δ = 158.8, 145.1, 133.6, 115.7, 114.8, 113.1, 90.6, 72.0, 70.9, 70.7 (2C), 69.7, 67.4, 59.2, 36.2 ppm.

*Poly-2a-block-poly-2b*. A 10 mL resealable Schlenk tube was charged with a stock solution of **2a** (230 mM, 200 µL) in toluene. A stock solution of **1** (7.7 mM, 300 µL) in toluene was added and the reaction mixture was heated at 90 °C for 30 min. An aliquot (150 µL) was quickly removed and precipitated with MeOH (2 mL). A stock solution of **2b** (46 mM, 700 µL) in toluene was added and the reaction was heated for an additional 7 h. The reaction mixture was cooled and polymers were precipitated with MeOH (2 mL). The precipitate was filtered, washed with MeOH (2 mL), and dried in vacuum to yield *poly*-**2a**-block-*poly*-**2b** (94% isolated yield) as a pale orange solid. ^{1}H NMR (500 MHz, CDCl$_3$, 22 °C) δ = 7.40 (d, *J* = 8.4 Hz, 4H, Ar-*H*), 6.79–6.42 (m, 8H, Ar-*H*), 4.19–3.42 (m, 34H), 3.18 (s, 8H, C*H*$_2$), 1.79–1.49 (m, 4H, O(C*H*$_2$)$_5$CH$_3$), 1.40–1.16 (m, 12H, O(C*H*$_2$)$_5$CH$_3$), 0.86 (t, *J* = 6.9 Hz, 6H, C*H*$_3$) ppm; {^{1}H}^{13}C NMR (126 MHz, CDCl$_3$, 22 °C) δ = 159.2, 145.2, 133.4, 115.2, 114.5, 113.0, 90.4, 72.0, 70.9, 70.7 (2C), 69.7 (2C), 67.9, 59.2, 36.6, 31.8, 29.4, 25.9, 22.8, 14.2 ppm.
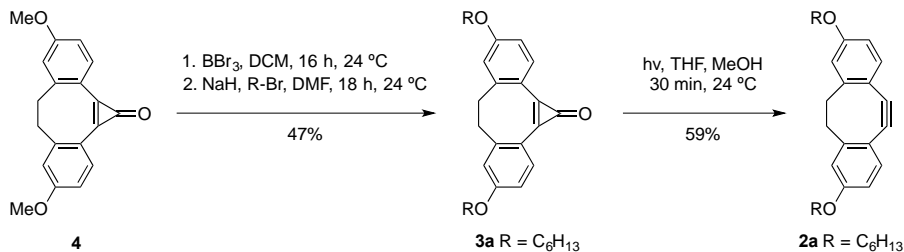
**Scheme 2-8.** Synthesis of **2a**.

*4,9-Dihexyloxy-6,7-dihydro-1H-dibenzo[a,e]cyclopropa[c][8]annulen-1-one* (**3a**) A 100 mL round bottom flask was charged under $N_2$ with 4,9-dimethoxy-6,7-dihydro-1*H*-dibenzo[*a,e*]cyclopropa[*c*][8]annulen-1-one (**4**)[15] (750 mg, 2.57 mmol) in dry $CH_2Cl_2$ (30 mL). The solution was cooled to –78 °C, and $BBr_3$ (1.5 mL, 16.0 mmol) was added dropwise. The reaction mixture was stirred for 30 min at –78 °C and for 16 h at 24 °C. The reaction mixture was cooled to –78 °C, quenched with MeOH (15 mL), and concentrated in vacuum. The residue was redissolved in dry DMF (30 mL) and 1-bromohexane (2.11 g, 12.8 mmol) was added followed by NaH (0.18 g, 7.2 mmol). The reaction mixture was stirred for 18 h at 24 °C, quenched with $H_2O$ (60 mL), and extracted with $CH_2Cl_2$ (3 x 120 mL). The combined organic layers were dried over $MgSO_4$, and concentrated on a rotary evaporator. Column chromatography ($SiO_2$; 100:1 $CH_2Cl_2$/MeOH) yielded **3a** (0.52 g, 47%) as a colorless solid. ^{1}H NMR (500 MHz, $CDCl_3$, 22 °C) $\delta$ = 7.92 (d, *J* = 8.8 Hz, 2H, Ar-*H*), 7.01-6.73 (m, 4H, Ar-*H*), 4.02 (t, *J* = 6.6 Hz, 4H, OC*H₂*), 3.32 (d, *J* = 10.8 Hz, 2H, C*H₂*), 2.62 (d, *J* = 10.5 Hz, 2H, C*H₂*), 1.86–1.74 (m, 4H, OCH₂C*H₂*(CH₂)₃CH₃), 1.58–1.29 (m, 12H, OCH₂CH₂(C*H₂*)₃CH₃), 0.91 (t, *J* = 5.3 Hz, 6H, C*H₃*) ppm; {^{1}H}^{13}C NMR (126 MHz, $CDCl_3$, 22 °C) $\delta$ = 162.2, 153.9, 147.9, 142.2, 135.9, 129.7, 116.4, 112.3, 68.4, 37.3, 31.7, 29.2, 25.8, 22.7, 14.2 ppm; FTMS (MALDI) (*m/z*): $[C_{29}H_{36}O_3+H]^+$ calcd for $[C_{29}H_{37}O_3]$, 433.27; found, 433.16.

*3,8-Dihexyloxy-5,6-dihydro-11,12-didehydrodibenzo[a,e][8]annulene* (**2a**) A 100 mL round bottom flask was charged with **3a** (0.52 g, 1.2 mmol) in 1:1 THF/MeOH (26 mL) and the reaction mixture was purged with nitrogen. The reaction mixture was stirred at 24 °C under a 500 Watt Hg lamp for 30 min. The reaction mixture was concentrated on a rotary evaporator and the residue was recrystallized from hexanes/EtOAc to yield **2a** (0.295 g, 59%) as a yellow solid. Crystals for X-ray analysis were grown from saturated hexanes/EtOAc solutions. mp: 68 °C. ^{1}H NMR (600 MHz, $CDCl_3$, 22 °C) $\delta$ = 7.19 (d, *J* = 8.4 Hz, 2H, Ar-*H*), 6.88 (d, *J* = 2.4 Hz, 2H, Ar-*H*), 6.75 (d, *J* = 8.2 Hz, 2H, Ar-*H*), 3.97 (t, *J* = 6.5 Hz, 4H, OC*H₂*), 3.19–3.18 (m, 2H, C*H₂*), 2.45–2.44 (m, 2H, C*H₂*), 1.84–1.71 (m, 4H, OCH₂C*H₂*(CH₂)₃CH₃), 1.51–1.43 (m, 4H, OCH₂CH₂C*H₂*(CH₂)₂CH₃), 1.39–1.30 (m, 8H, OCH₂CH₂CH₂(C*H₂*)₂CH₃), 0.91 (t, *J* = 6.6 Hz, 6H, C*H₃*) ppm; {^{1}H}^{13}C NMR (151 MHz, $CDCl_3$, 22 °C) $\delta$ = 158.8, 155.0, 126.8, 116.9, 116.2, 111.9, 110.6, 68.3, 36.8, 31.7, 29.4, 25.9, 22.8, 14.2 ppm. FTMS (MALDI) (*m/z*): $[C_{28}H_{36}O_2]^+$ calcd for $[C_{28}H_{36}O_2]$, 404.27; found, 404.55.



**4**      **3b** R = (CH₂CH₂O)₃CH₃      **2b** R = (CH₂CH₂O)₃CH₃
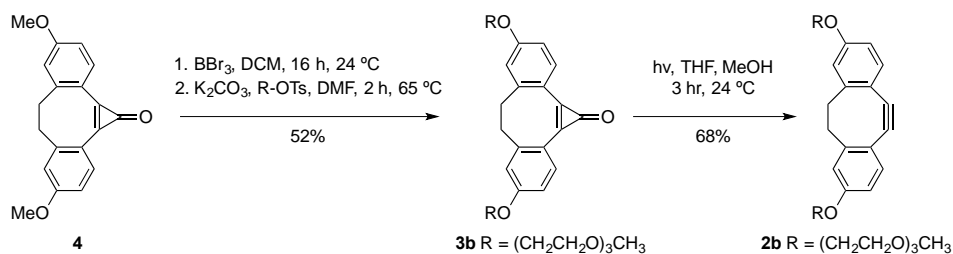
**Scheme 2-9.** Synthesis of **2b**.

*4,9-Di-(2-(2-(2-methoxyethoxy)ethoxy)ethoxy)-6,7-dihydro-1H-dibenzo[a,e]cyclopropa[c][8]annulen-1-one* (**3b**) A 100 mL round bottom flask was charged under N$_2$ with 4,9-dimethoxy-6,7-dihydro-1*H*-dibenzo[a,e]cyclopropa[c][8]annulen-1-one (**4**) (1 g, 3.43 mmol) in dry CH$_2$Cl$_2$ (40 mL) and cooled to −78 °C. Boron tribromide (2 mL, 21.33 mmol) was added dropwise. The reaction mixture was stirred for 30 min at −78 °C and for 3 h at 24 °C. The reaction mixture was cooled to −78 °C, quenched with MeOH (15 mL), and concentrated in vacuum. The resulting solid was redissolved in DMF (30 mL) and TsO(CH$_2$CH$_2$O)$_3$Me (1.81 g, 5.64 mmol, 3 eq.) was added followed by K$_2$CO$_3$ (1.56 g, 11.28 mmol). The reaction mixture was stirred for 2 h at 65 °C, filtered over a short SiO$_2$ plug, and eluted with 200 mL of 1:10 MeOH/EtOAc. The combined organic layers were dried over MgSO$_4$, and concentrated on a rotary evaporator. Column chromatography (SiO$_2$; 10:90 MeOH/EtOAc) yielded **3b** (1.10 g, 52%) as a yellow oil. $^1$H NMR (600 MHz, CDCl$_3$, 22 °C) $\delta$ = 7.94 (d, *J* = 8.8 Hz, 2H, Ar-*H*), 6.93–6.90 (m, 4H, Ar-*H*), 4.22 (t, *J* = 4.8 Hz, 4H, OC*H*$_2$), 3.90 (t, *J* = 4.3 Hz, 4H, OC*H*$_2$), 3.76 (t, *J* = 2.2 Hz, 4H, OC*H*$_2$), 3.70 (t, *J* =4.4 Hz, 4H, OC*H*$_2$), 3.67 (t, *J* = 5.1 Hz, 4H, OC*H*$_2$), 3.56 (t, *J* = 4.4 Hz, 4H, OC*H*$_2$), 3.40 (s, 6H, OC*H*$_3$), 3.34 (d, *J* = 10.8 Hz, 2H, C*H*$_2$), 2.64 (d, *J* = 10.5 Hz, 2H, C*H*$_2$) ppm; {$^1$H}$^{13}$C NMR (126 MHz, CDCl$_3$, 22 °C) $\delta$ = 161.7, 153.8, 147.9, 142.4, 135.8, 116.6, 116.4, 112.5, 72.0, 71.0, 70.7, 70.7, 69.6, 67.7, 59.2, 37.2 ppm; FTMS (MALDI) (*m/z*): [C$_{31}$H$_{41}$O$_9$+H]$^+$ calcd [C$_{31}$H$_{41}$O$_9$], 556.65; found, 556.92.

*3,8-Di-(2-(2-(2-methoxyethoxy)ethoxy)ethoxy)-5,6-dihydro-11,12-didehydrodibenzo[a,e][8]annulene* (**2b**) A 100 mL round bottom flask was charged with **3b** (0.50 g, 0.90 mmol) in 1:1 THF/MeOH (20 mL) and the reaction mixture was purged with nitrogen. The reaction mixture was stirred at 24 °C under a 500 Watt Hg lamp for 3 h. The reaction mixture was concentrated on a rotary evaporator. Column chromatography (SiO$_2$; 10:90 MeOH/EtOAc) yielded **2b** as a colorless oil (0.32 g, 68%). $^1$H NMR (600 MHz, CDCl$_3$, 22 °C) $\delta$ = 7.20 (d, *J* = 8.3 Hz, 2H, Ar-*H*), 6.91 (d, *J* = 2.5 Hz, 2H, Ar-*H*), 6.78 (dd, *J* = 8.3, 2.4 Hz, 2H, Ar-*H*), 4.16 (t, *J* = 4.8 Hz, 4H, OC*H*$_2$), 3.88 (t, *J* = 4.3 Hz, 4H, OC*H*$_2$), 3.75 (t, *J* = 2.2 Hz, 4H, OC*H*$_2$), 3.69 (t, *J* = 4.4 Hz, 4H, OC*H*$_2$), 3.66 (t, *J* = 5.1 Hz, 4H, OC*H*$_2$), 3.56 (t, *J* = 4.4 Hz, 4H, OC*H*$_2$), 3.38 (s, 6H, OC*H*$_3$), 3.20–3.18 (m, 2H, C*H*$_2$), 2.46–2.43 (m, 2H, C*H*$_2$) ppm; {$^1$H}$^{13}$C NMR (151 MHz, CDCl$_3$) $\delta$ = 158.4, 155.0, 126.8, 117.0, 116.6, 112.1, 110.5, 72.1, 71.0, 70.8, 70.7, 69.8, 67.7, 59.2, 36.8 ppm; FTMS (MALDI) (*m/z*): [C$_{30}$H$_{40}$O$_8$]$^+$ calcd for [C$_{30}$H$_{40}$O$_8$], 528.64; found, 528.19.

*2.7.2. Kinetic Experiments Set-Up*

Polymerization:

A typical kinetic polymerization experiment of 5a consisted of the following:

- stock solution of **2a** (22 mM) in Tol-$d_8$

- stock solution of **1** (11 mM) in Tol-$d_8$

A J. Young NMR tube was charged with 500 µL aliquot of monomer **2a** and 100 µL aliquot of catalyst **1**. The tube was kept at −196 °C prior to inserting the probe into the NMR. The $^1$H NMR spectra were recorded at a calibrated temperature during regular intervals. The disappearance of the resonance for the ethylene bridge in the ring-strained monomer **2a** at 3.18 ppm was monitored and integrated with respect to an external ERETIC standard. If required, excess $KOC(CF_3)_2(CH_3)$ or $BPh_3$ was added to the solution of 5a before addition of the catalyst.

The data was analyzed by fitting a line to $\ln([M]/[M]_0)$ vs. $t$. Dividing the slope by $[C]_0$, as determined by ERETIC, provides $k_p$.

A typical kinetic polymerization experiment of **2b** consisted of the following:

stock solution of **2b** (54 mM) in Tol-$d_8$ stored over molecular sieves

- stock solution of **1** (2.7 mM) in Tol-$d_8$

A J. Young NMR tube was charged with 200 µL aliquot of monomer **2b** and 400 µL aliquot of catalyst **1**. The tube was kept at −196 °C prior to inserting the probe into the NMR. The $^1$H NMR spectra were recorded at a calibrated temperature during regular intervals. The disappearance of the resonance for the ethylene bridge in the ring-strained monomer **2b** at 3.76–3.59 ppm was monitored and integrated with respect to an external ERETIC standard.

The data was analyzed by fitting a line to $\ln([M]/[M]0)$ vs. $t$. Dividing the slope by $[C]_0$, as determined by ERETIC, provides $k_p$.

Initiation:

A typical kinetic initiation experiment consisted of the following:

- cold stock solution of **2a** (22 mM) and $KOC(CF_3)_2(CH_3)$ (4 mM) in Tol-$d_8$ containing 30 mM of trifluorotoluene, as a standard

- cold stock solution of **1** (2 mM) in Tol-$d_8$

A J. Young NMR tube was charged at −35 °C with 200 µL aliquot of 1, and 200 µL aliquot of **2a**. The tube was kept at −196 °C prior to inserting the probe into the NMR. The $^{19}$F NMR spectra were recorded at a calibrated temperature during regular intervals. The appearance of the resonance corresponding to the free propagating species, **11**, at −73.62 ppm was monitored and integrated with respect to an external ERETIC standard.

*Ligand Dissociation Studies*

Equilibrium and SIR studies of **1**:

A stock solution of **1** (4 mM) and trifluorotoluene (28 mM) in Tol-$d_8$ was prepared. All peaks of interest were monitored using ERETIC at the calibrated temperatures.

The same sample was used for subsequent SIR experiments by inverting the $^{19}$F resonance of the *cis* alkoxide on **1** while monitoring the resonances of **10**, at −77.8 ppm and −76.8 ppm respectively.

Equilibrium and SIR studies of **12**:

A stock solution of **12** (2 mM) was prepared by addition of 4 equiv. of **2a** to 1 equiv. of **1**, and trifluorotoluene (2 mM) in Tol-$d_8$. The sample was heated to 90 °C for 90 min. All peaks of interest were monitored using ERETIC at the calibrated temperatures.

The same sample was used for subsequent SIR experiments by inverting the $^{19}$F resonance of the *cis* alkoxide on **12** while monitoring the resonances of **11**, at −77.6 ppm and −76.9 ppm respectively.

*Rate of Initiation:*

$$-\frac{d[C]}{dt} = \frac{d[C_i]}{dt} = k_i[C][M] \tag{E8}$$

The total concentration of metal centers $[C]_0$ can be expressed as:

$$[C]_0 = [C \bullet KOR] + [C] + [C_i] \tag{E9}$$

where $[C_i] = [C_p] + [C_p \bullet KOR]$. For t = 0, $[C_i]$ approaches 0.

The dissociation constant of $[C \bullet KOR]$ is

$$K_{diss} = \frac{k_1}{k_{-1}} = \frac{[C][KOR]}{[C \bullet KOR]} \tag{E10}$$

Solving (E10) for $[C \bullet KOR]$ gives:

$$[C \bullet KOR] = \frac{[C][KOR]}{K_{diss}} \tag{E11}$$

Substituting (E11) in (E9) and solving for [C] gives:

$$[C] = \frac{[C]_0}{\left( \dfrac{[KOR]}{K_{diss}} + 1 \right)} \tag{E12}$$

Substituting (E12) in (E8) gives:

$$\frac{d[C_i]}{dt} = \frac{k_i[C]_0[M]}{\left(\frac{[KOR]}{K_{diss}} + 1\right)}$$

(E7)

## 2.8 References

(1)   *Handbook of Metathesis*, Vol 1-3 (R. H. Grubbs, Ed.), WILEY-VCH, Weinheim, **2003**.

(2)   Schrock, R. R. *Angew. Chem. Int. Ed. Engl.* **2006**, *45*, 3748–3759.

(3)   Fürstner, A. *Angew. Chem. Int. Ed. Engl.* **2013**, *52*, 2794–2819.

(4)   Schrock, R. R. *Chem. Commun*. **2013**, *49*, 5529–5531.

(5)   Jyothish, K.; Zhang, W. *Angew. Chem. Int. Ed. Engl.* **2011**, *50*, 8628–8630.

(6)   Wu, X.; Tamm, M. *Beilstein J. Org. Chem.* **2011**, *7*, 82–93.

(7)   Tamm, M. *Chim. Oggi* **2010**, 28, 60–63.

(8)   Zhang, W.; Moore, J. S. *Adv. Synth. Catal*. **2007**, *349*, 93–120.

(9)   Fürstner, A.; Davies, P. W. *Chem. Commun.* **2005**, 2307–2320.

(10)   Schrock, R. R. *Chem. Rev*. **2002**, *102*, 145–179.

(11)   a) Poloukhtine, A. A.; Mbua, N. E.; Wolfert, M. A.; Boons, G.; Popik, V. V. *J. Am. Chem. Soc.* **2009**, *131*, 15769–15776; b) Jewett, J. C.; Sletten, E. M.; Bertozzi, C. R. *J. Am. Chem. Soc.* **2010**, *132*, 3688–3690; c) Friscount, F.; Ledin, P. A.;  Mbua, N. E.; Flanagan-Steet. H. R.; Wolfert, M. A.; Steet, R.; Boons, G. *J. Am. Chem. Soc.* **2012**, *134*, 5381–5389; d) Arumugam, S. A.; Popik, V. V. J. *Org. Chem.* **2014**, *79*, 2702–2708.

(12)   Paley, D. W.; Sedbrook, D. F.; Decatur, J.; Fischer, F. R.; Steigerwald, M. L.; Nuckolls, C. *Angew. Chem. Int. Ed.* **2013**, *52*, 4591–4594.

(13)   Sedbrook, D. F.; Paley, D. W.; Steigerwald, M. L.; Nuckolls, C.; Fischer, F. R. *Macromolecules* **2012**, *45*, 5040–5044.

(14)   Lysenko, S.; Haberlag, B.; Wu, X.; Tamm, M. *Macromol. Symp*. **2010**, *293*, 20–23.

(15)   Fischer, F. R.; Nuckolls, C. *Angew. Chem. Int. Ed.* **2010**, *49*, 7257–7260.

(16)   Zhang, X. P.; Bazan, G. C. *Macromolecules* **1994**, *27*, 4627–4628.

(17)   Krouse, S.; Schrock, R.; Cohen, R. *Macromolecules* **1987**, *20*, 903–904.

(18)   Bunz, U. H. F. *Acc. Chem. Res.* **2001**, *34*, 998–1010.

(19)   McQuade, D. T., Pullen, A. E., Swager, T. M. *Chem. Rev.* **2000**, *100*, 2537.

(20)   Voskerician, G., Weder, C. *Adv. Polym. Sci.* **2005**, *177*, 209-248.

(21)    Zhang, W.; Moore, J. S. *Macromolecules* **2004**, *37*, 3973–3975.

(22)    Blankenburg, L.; Bunz, U. H. F.; Klemm, E.; Moore, J. S.; Pautzsch, T.; Ray, C. R.; Swager, T. M.; Voskerician, G.; Weder, C.; Yamaguchi, I.; Yamamoto, T.; Yasuda, T.; Zheng, J., Poly(arylene ethynylene)s: From Synthesis to Application; Weder, C. (Eds.); Springer: Berlin, **2005**.

(23)    Krouse, S.; Schrock, R. *Macromolecules* **1989**, *22*, 2569–2576.

(24)    Fu, R.; Bercaw, J. E.; Labinger, J. A. *Organometallics*. **2011**, *30*, 6751–6765.

(25)    Fischer, E. O.; Massböl, A. *Chem. Ber.* **1967**, *100*, 2445–2456.

(26)    Fischer, E. O.; Kreis, G.; Kreiter, C. G.; Müller, J.; Huttner, G.; Lorenz, H. *Angew. Chem. Int. Ed. Engl.* **1973**, *12*, 564–565.

(27)    Haberlag, B.; Wu, X.; Brandhorst, K.; Grunenberg, J.; Daniliuc, C. G.; Jones, P. G.; Tamm, M. *Chem. Eur. J.* **2010**, *16*, 8868–8877.

(28)    Freudenberger, J. H.; Schrock, R. R.; Churchill, M. R.; Rheingold, A. L.; Ziller, J. W. *Organometallics* **1984**, *3*, 1563–1573.

(29)    McCullough, L. G.; Schrock, R. R. *J. Am. Chem. Soc.* **1984**, *106*, 4067–4068.

(30)    McCullough, L. G.; Schrock, R. R.; Dewan, J. C. *J. Am Chem. Soc.* **1985**, *107*, 5987–5998.

(31)    Beer, S.; Hrib, C. G.; Jones, P. G.; Brandhorst, K.; Grunenberg, J.; Tamm, M. *Angew. Chem. Int. Ed. Engl*. **2007**, *46*, 8890–8894.

(32)    Beer, S.; Brandhorst, K.; Hrib, C. G.; Wu, X.; Haberlag, B.; Grunenberg, J.; Jones, P. G.; Tamm, M. *Organometallics* **2009**, *28*, 1534–1545.

(33)    Wu, X.; Daniliuc, C. G.; Hrib, C. G.; Tamm, M. *J. Organoment. Chem.* **2011**, *696*, 4147–4151.

(34)    Haberlag, B.; Freytag, M.; Daniliuc, C. G.; Jones, P. G.; Tamm, M. *Angew. Chem. Int. Ed.* **2012**, *51*, 13019–13022.

(35)    Lysenko, S.; Daniliuc, C. G.; Jones, P. G.; Tamm, M. *J. Organomet. Chem.* **2013**, *744*, 7–14.

(36)    a) O' Reilly, M. E.; Veige, A. S. *Chem. Soc. Rev.* **2014**, *43*, 6325–6369; b) O' Reilly, M. E.; Nadif, S. S.; Ghiviriga, I.; Abboud, K. A.; Veige, A. S. *Organometallics* **2014**, *33*, 836–839; c) O' Reilly, M. E.; Ghiviriga, I.; Abboud, K. A.; Veige, A. S. *Dalton Trans.* **2013**, *42*, 3326–3336; d) McGowan K. P.; O' Reilly, M. E.; Ghiviriga, I.; Abboud, K. A.; Veige, A. S. *Chem. Sci.* **2013**, *4*, 1145–1155; e) O' Reilly, M. E.; Ghiviriga, I.; Abboud, K. A.; Veige, A. S. *J. Am. Chem. Soc.* **2012**, *134*, 11185–11195; f) Sakar, S.; McGowan, K. P.; Kuppuswamy, S.; Ghiviriga, I.; Abboud, K. A.; Veige, A. S. *J. Am. Chem. Soc.* **2012**, *134*, 4509–4512.

(37)    Wu, Z.; Wheeler, D. R.; Grubbs, R. H. *J. Am. Chem. Soc.* **1992**, *114*, 146–151.

(38)    Bielawski, C. W.; Grubbs, R. H. *Prog. Polym. Sci.* **2007**, *32*, 1–29.

(39)    a) Matyjaszewski, K. *J. Phys. Org. Chem.* **1995**, *8*, 197–207; b) Flory, P. J. *J. Am. Chem. Soc*. **1940**, *62*, 1561.

(40)    Bain, A. D.; Cramer, J. A. *J.  Magn. Reson., Series A* **1996**, *118*, 21–27.

(41)    Bain, A. D. Prog. Nucl. Magn. Reson. Spectrosc. **2003**, 43, 63–103.

(42)    Akoka, S., Barantin, L., Trierweiler, M. *Anal. Chem.* **1999**, *71*, 2554-2557.

(43)    Schlosser, M.; Hartman, R. *Angew. Chem. Int. Ed.* **1973**, *12*, 508–509.

# 3 Chapter Synthesis of Poly-(o-Phenylene Ethynylene)s by Ring-Opening Alkyne Metathesis Polymerization

## 3.1 Introduction: Alkyne Metathesis Chemistry and Poly(phenylene ethynylene)s

Semiconducting π-conjugated polymers have been widely explored as functional materials in advanced electronic devices. They combine the superior processability and mechanical performance of polymers with readily tunable optical, electrical, and magnetic properties of small molecules.[1] Applications for these polymers include electronic devices such as organic photovoltaics (OPVs),[2,3] organic light-emitting diodes (OLEDs),[4,5] organic field-effect transistors (OFETs),[6,7] photorefractive devices,[8] and environmental sensors.[9–13] Among these materials, *poly*-(phenylene ethynylenes) (PPE), a class of conjugated polymers featuring a pattern of alternating aromatic rings and triple bonds, have stood out for their stability, moderate fluorescence quantum yields,[14,15] and readily tunable band gap.[16,17] The macromolecular assembly of PPEs in solution and thin films can be tuned from densely packed linear organizations to well defined helical coiled or zig-zag structures[18] by varying the substitution pattern (*para-*, *meta-*, *ortho-*) of the aromatic rings along the backbone of the polymer chain. The classical syntheses of PPEs rely on step-growth polymerizations based on either transition metal catalyzed cross-coupling reactions or alkyne cross-metathesis (ACM).[19,20] While ACM and cyclodepolymerization of linear polymers have previously been used to access cyclic topologies, the thermodynamic products of these reactions are usually small cylic oligomers comprised of not more than 3–6 alkynes.[21–24] Transition-metal catalyzed cross-

coupling polymerizations of aryl halides with aromatic alkynes, instead, suffer from undesired termination reactions, e.g. dehalogenation, and structural defects along the polymer backbone such as butadiyne groups emerging from oxidative coupling of terminal alkynes. While these strategies benefit from readily accessible monomers, they lack the precise control over degree of polymerization, molecular weight, end-group functionality, and polydispersity unique to a controlled ring-opening alkyne metathesis polymerization (ROAMP) mechanism.[25–27]

In this chapter we report a novel route towards fully conjugated PPE based on ROAMP. Catalysts [MesC≡Mo(OC(CH$_3$) (CF$_3$)$_2$)$_3$] **1** and [EtC≡Mo(OC(CH$_3$)(CF$_3$)$_2$)$_3$(DME)] (DME = 1,2-dimethoxyethane) **2** (Scheme 3-1) selectively yield PPE featuring either linear or cyclic polymer topology (catalyst **2** was synthesized and studied by Stephen von Kugelgen). Both catalysts rapidly initiate the polymerization of ring-strained monomer 5,6,11,12-tetradehydrobenzo[*a*,*e*][8]annulene (**3**) to form *poly*-(*ortho*-phenylene ethynylene) (P*o*PE) featuring a mesityl or an ethyl end-group, respectively. Time-resolved NMR spectroscopy reveals that the active chain ends of the polymers featuring a mesityl end-group are stable under the reaction conditions. In the absence of monomer, living polymers formed from **2** instead undergo highly regioselective backbiting into the least sterically hindered alkyne (EtC≡C) at the end-group to give cyclic P*o*PE with n > 5 and the starting catalyst **2**. We herein demonstrate an unprecedented structural control over polymer topology by taking advantage of the unique selectivities of two ROAMP catalysts to form either linear or cyclic fully conjugated polymers derived from ring-strained monomers. Both catalysts will be described here with data collected by other authors. We believe that including the data from catalysts **1** and **2** provides a comprehensive story.
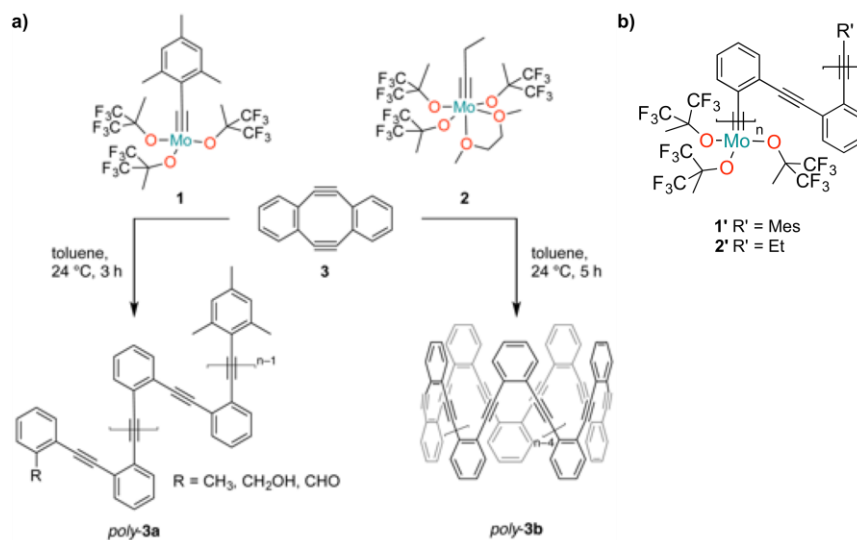


**Scheme 3-1. a)** Synthesis of linear *poly*-**3a** and cylic *poly*-**3b** from ring strained monomer **3** using ROAMP catalyst **1** and **2**. **b)** Living catalyst remains attached to polymer chain.

## 3.2 Initiator Control of Polymer Topology

### 3.2.1. Design and Synthesis of [MesC≡Mo(OC(CH₃) (CF₃)₂)₃] and [EtC≡Mo(OC(CH₃)(CF₃)₂)₃(DME)] (DME = 1,2-dimethoxyethane)

In order to control the topology of the resulting polymers, we syntehsized two catalysts that transfer their respective carbyne susbtituent to the end-group of the polymer chain. We hypothesized that the steric demand of the polymer end group directly affects the rate and the selectivity of intramolecular backbiting and intermolecular chain transfer reactions. Catalyst **1** was synthesized from Mo(CO)₆ and MesLi following a procedure described by Tamm.[28] The DME adduct of catalyst **2** was obtained through cross-metathesis of the nitrido-complex [N≡Mo(OC(CH₃)(CF₃)₂)₃] with hex-3-yne as described by Johnson.[29] Orange prisms of **2** suitable for X-ray crystallography were obtained from a saturated toluene solution at –35 °C. The geometry at the Mo center is pseudo-octahedral. In solution the octahedral complex **2** is in dynamic equilibrium with the pentacoordinate monodentate DME complex and the fully DME dissociated tetracoordinate complex.[30] At 24 °C in benzene, the equilibrium lies on the side of the associated complexes **2** ($K_d = 6.2 \times 10^{-5}$ mol L$^{-1}$) (Experiments and calculations carried out by Stephen von Kugelgen). Variable temperature NMR reveals that the exchange is fast suggesting that an open coordination site is readily available to bind the alkyne substrate.

### 3.2.2. Ring-Opening Alkyne Metathesis Polymerization by [MesC≡Mo(OC(CH₃) (CF₃)₂)₃] and [EtC≡Mo(OC(CH₃)(CF₃)₂)₃(DME)] (DME = 1,2-dimethoxyethane)

We studied the ROAMP of 5,6,11,12-tetradehydrobenzo[*a*,*e*][8]annulene (**3**) with **1** and **2** (Scheme 3-1a), synthesized by Dr. Ryan Cloke.[31] Addition of **1** to a solution of **3** (50 mM) in toluene ([**3**]/[**1**] = 10) at 24 °C leads to the precipitation of polymers within 1 h. ¹H and ¹⁹F NMR indicate that **1** quantitatively initiates with a half-life of $t_{1/2} \ll 1$ min to form the propagating species. Monomer **3** is consumed in less than 1 h at 24 °C. The active ROAMP catalyst remains attached to the growing polymer chain, **1'** (Scheme 3-1b). The molecular weight of the resulting polymers scales linearly with monomer conversion (Figure 3-1).
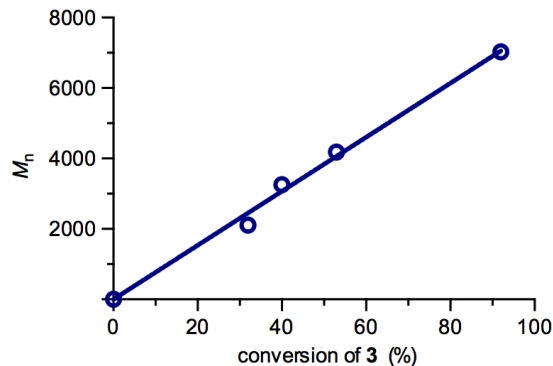
**Figure 3-1.** GPC analysis of samples taken at different time points from a polymerization reaction of **3** with catalyst **1**. $M_n$ increases linearly with the conversion of **3**.

Precipitation of the resulting polymer with MeOH affords *poly*-**3a** in 82% isolated yield. Gel permeation chromatography (GPC) analysis for various [**3**]/[**1**] loadings at 24 °C in toluene shows a PDI of 1.3–1.7 (Table 3-1). The molecular weights of *poly*-**3a** determined by GPC, calibrated to polystyrene standards, scale with the conversion of monomer, are proportional to the initial [**3**]/[**1**] loading and show a unimodal distribution (Figure 3-2a). Extended reaction times do not lead to a broadening of the PDI. Mass spectrometry of polymers that have been quenched with MeOH is consistent with the characteristic signature for one mesityl end-group and a statistical mixture of $CH_3$, $CH_2OH$, or CHO end-groups resulting from the cleavage of the propagating molybdenum carbyne species (Figure 3-3). While the $^1H$ NMR of *poly*-**3a** features two distinct resonance signals in the aromatic region, the $^{13}C$ NMR reveals a characteristic upfield shift for the alkyne carbon resonances (109.5 ppm in **3** to 92.6 ppm in *poly*-**3a**) associated with the release of the ring-strain stored in **3**. No evidence for branching or the formation of cyclic polymers could be observed by $^1H$ NMR analysis and mass spectrometry. End-group analysis of the mesityl group resonance signals ($^1H$ NMR) indicates that GPC overestimates the $M_n$ of *poly*-**3a**. A correction factor of 1.1–1.2 correlates well with the degree of polymerization ($X_n$) determined by NMR analysis and the expected molecular weight based on the initial [**3**]/[**1**] loading.

**Table 3-1.** Molecular weight analysis of *poly*-**3a**. [a] [3]/[1] loadings > 30 lead to precipitation of insoluble polymers before all monomer is consumed; [b] calibrated to narrow polydispersity polystyrene standards; [c] degree of polymerization determined by $^1H$ NMR end-group analysis.

| [**3**]/[**1**] | $M_n$ theory | $M_n$ GPC[b] | $M_w$ GPC[b] | $X_n$[c] | PDI GPC[a] |
|---|---|---|---|---|---|
| 10/1 | 2134 | 1700 | 3000 | 11 | 1.7 |
| 20/1 | 4134 | 4800 | 6400 | 21 | 1.3 |

| | 30/1[a] | 6134 | 6600 | 9400 | 29 | 1.4 |

If the polymerization of **3** is initiated with the molybdenum propylidyne complex **2** ([**3**]/[**2**] = 10) at 24 °C in toluene no precipitation of polymers can be observed. Catalyst **2** quantitatively reacts with **3** to form a propagating molybdenum complex ($t_{1/2} \ll 1$ min) as indicated by $^1$H and $^{19}$F NMR. Addition of MeOH to the homogeneous reaction mixture leads to the precipitation of *poly*-**3b**. GPC analysis of samples prepared from various [**3**]/[**2**] loadings at 24 °C in toluene indicates the formation of discrete cyclic oligomers (*poly*-**3b**) and some higher molecular weight linear polymers ($M_n$ = 5,000–10,000) resulting from intermolecular cross-metathesis of living polymer chains. The ratio of products emerging from an intra- *vs.* intermolecular chain transfer is concentration dependent ranging from 93% cyclic polymers at [**2**] = 1 mM to 86% at [**2**] = 10 mM as determined by $^1$H NMR. The linear polymers can be removed by Soxhlet extraction or fractional precipitation to give pure cyclic *poly*-**3b** in > 60% isolated yield (Figure 3-2a). Mass spectrometry of *poly*-**3b** shows evenly spaced peaks corresponding to integer multiples of **3** ($m/z$ = [n × 200] g mol$^{-1}$, n = 5, 6, 7, …, 20; Figure 3-2b). The absence of end-groups in *poly*-**3b** is further corroborated by $^1$H and $^{13}$C NMR spectroscopy and highlights the unusual selectivity of catalyst **2** for the formation cyclic *poly*-**3b** over linear *poly*-**3a**.
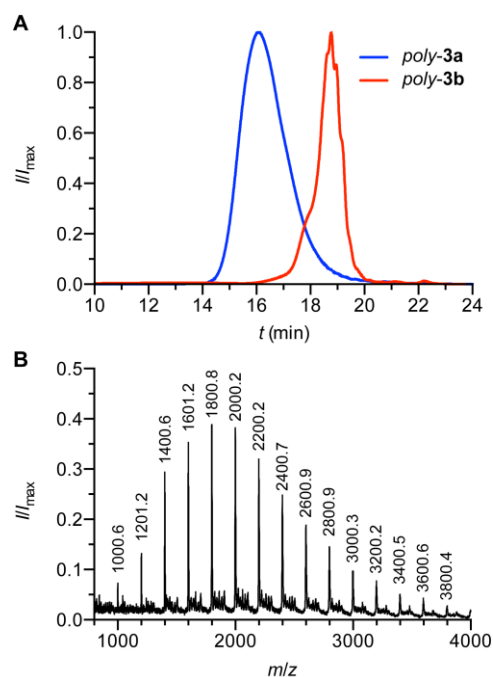


**Figure 3-2.** A) GPC traces for linear *poly*-**3a** and purified cyclic *poly*-**3b** obtained through ROAMP of **3** with catalyst **1** and **2** respectively; calibrated to polystyrene standards. B) MALDI mass spectrum of cyclic *poly*-**3b** showing integer multiples of the mass of monomer **3** ($M_W$ = 200 g mol$^{-1}$) and the absence of end-groups.
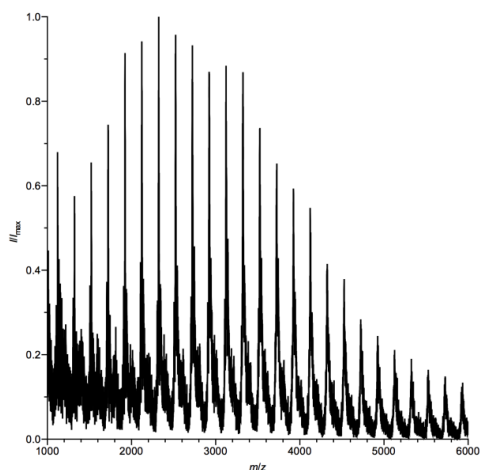
**Figure 3-3.** MALDI mass spectrum of linear *poly*-**3a** showing peaks separated by integer multiples of the mass of monomer **3**.

### 3.2.2. Mechanistic Studies on the Ring-Opening Alkyne Metathesis Polymerization by [MesC≡Mo(OC(CH₃) (CF₃)₂)₃] and [EtC≡Mo(OC(CH₃)(CF₃)₂)₃(DME)] (DME = 1,2-dimethoxyethane)

To gain insight into the reaction mechanism we studied the ROAMP of $^{13}$C-labeled **3\*** with **1**. In the presence of monomer the resting state of the catalyst observed by $^{13}$C NMR is the interconverting metallacyclobutadienes **1a** and **1b** (Figure 3-4a, Figure 3-5, Figure 3-6) characterized by two broad sets of $^{1}$H and $^{19}$F resonances for the alkoxides (axial and equatorial) and two sets of $^{13}$C resonances for the metallacyclobutadiene carbons (one β carbon and two α carbons).[30,32] If the metallacyclobutadienes were resonance structures of each other, one would expect to see one peak as α and α'. Instead, two peaks corresponding to two inequivalent α carbons are observed. Following the consumption of **3\*** the metallacyclobutadiene **1b** undergoes a final cycloreversion to give the labeled, ring-opened molybdenum benzylidyne complex **1c**. In the absence of monomer, **1c** is stable for > 10 h and remains attached to one end of the polymer chain pending MeOH solvolysis. If the same polymerization is performed with **2**, the dominant molybdenum species observed in $^{13}$C NMR are the interconverting metallacyclobutadienes **2a** and **2b**.

78
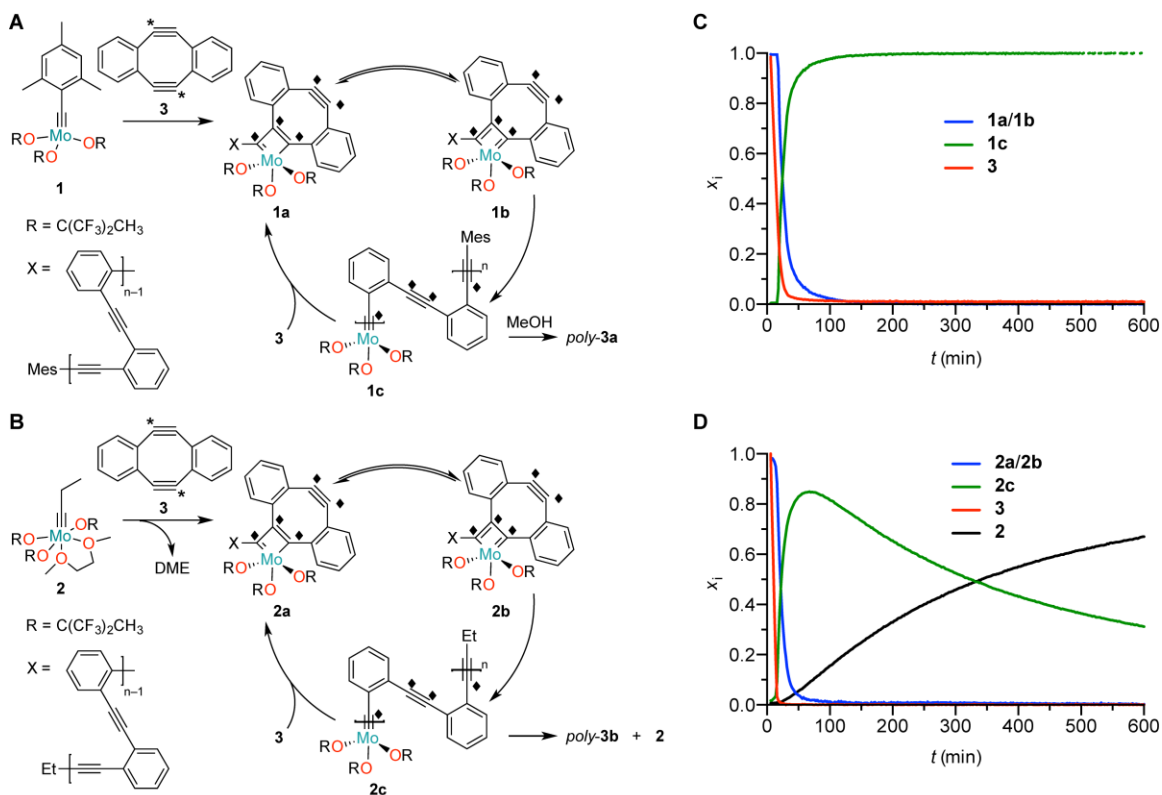
**Figure 3-4.** ROAMP of isotopically labeled **3\*** with catalyst **1** (A) and **2** (B) followed by time resolved $^{1}$H, $^{19}$F, and $^{13}$C NMR spectroscopy. Mole fraction of transient intermediates during the reaction of **1** (C) and **2** (D) with **3** derived from $^{1}$H NMR. Isotopic labeling: \* 99.5% $^{13}$C, □ 50% $^{13}$C.

Following the consumption of monomer, **2b** undergoes a final cycloreversion to give the ring-opened molybdenum benzylidyne complex **2c**. While **1c** is stable in the reaction mixture, **2c** undergoes highly regioselective backbiting into the butynyl end-group to give cyclic *poly*-**3b** and the original unlabeled molybdenum propylidyne complex **2**. The outstanding selectivity of this backbiting reaction is reflected in the absence of half-integer multiples of the monomer ($m/z = [n \times 200 + 100]$ g mol$^{-1}$) in the mass spectrum of *poly*-**3b** (Figure 3-4b). The increased steric demand of internal alkynes lining the backbone of the growing polymer chain (**2c**) prevents a stochastic backbiting process and directs the reaction exclusively towards the unhindered butynyl end-group.
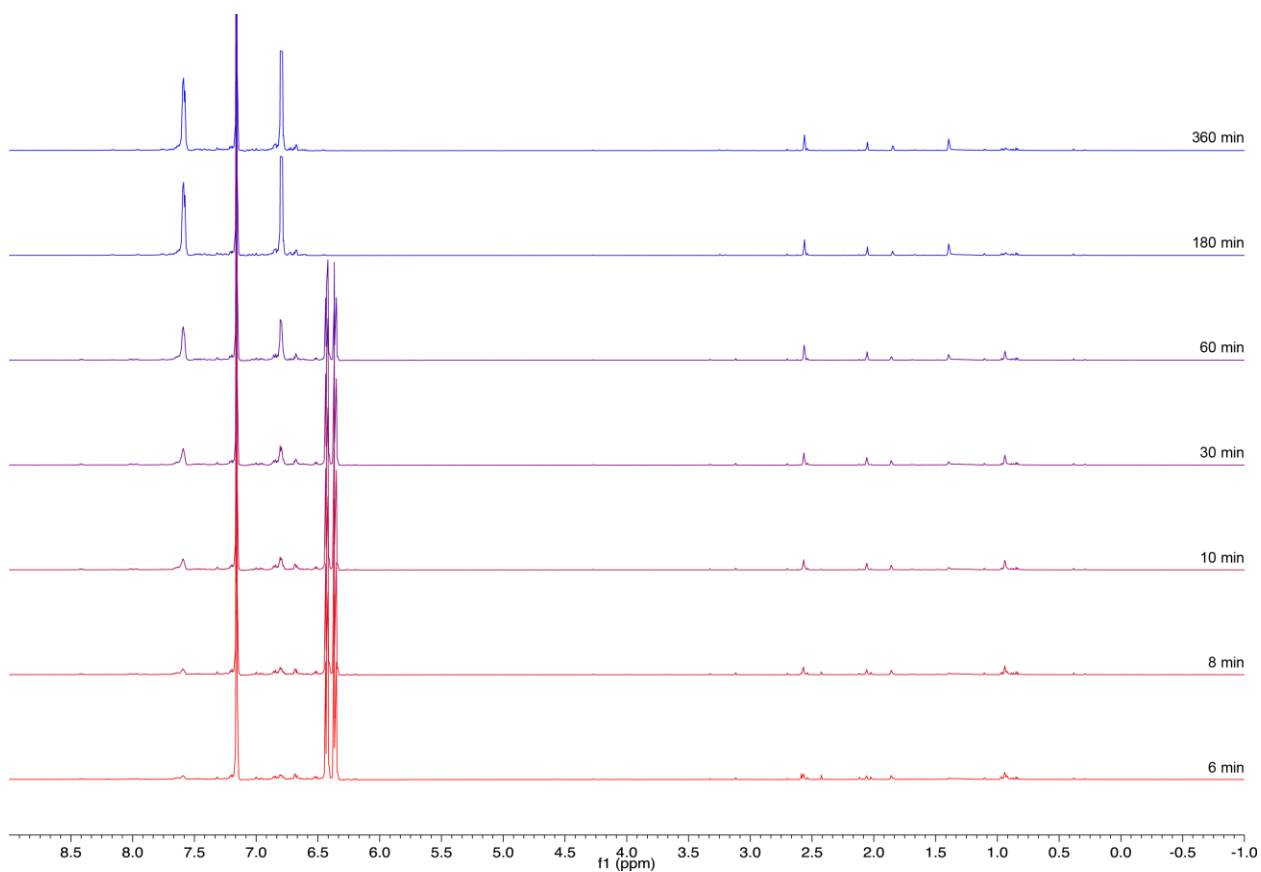
**Figure 3-5.** Transient ^{1}H NMR spectra of the polymerization of **3\*** with **1**.
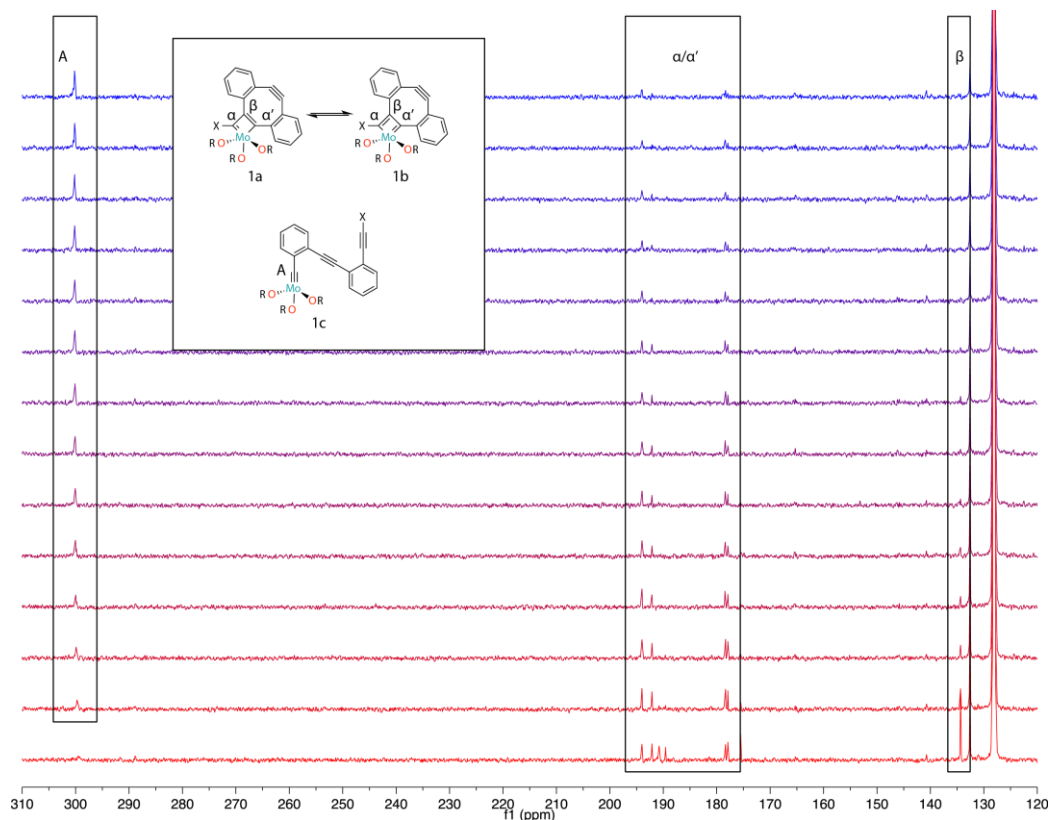
**Figure 3-6.** Transient $^{13}C$ NMR spectra of the polymerization of **3\*** with **1**. Each spectrum is the sum of 7.5 min of acquisition. The resonances due to the molybdacyclobutadiene intermediate (α/α' and β) decay and the polymer-bound carbyne complex **1c** (A) grows in following the final cycloreversion after **3\*** is consumed.

### 3.2.3. Kinetic Studies Using Model System [TolC≡Mo(OC(CH₃)(CF₃)₂)₃(DME)] (DME = 1,2-dimethoxyethane)

Catalyst [TolC≡Mo(OC(CH₃)(CF₃)₂)₃(DME)] (**4**) featuring a benzylidyne  substituent was chosen as a model complex for the propagating species **2c**. X-ray crystallography of **4** (Figure 3-7) confirms the presence of a C(1)≡Mo(1) triple bond with a bond length of 1.755 Å. Three hexafluoro-*tert*-butoxide ligands adopt a meridional conformation featuring typical Mo(1)–O(1), Mo(1)–O(2), and Mo(1)–O(3) distances of 1.955 Å, 1.924 Å and, 1.965 Å. In the crystal structure one equivalent of DME is coordinated to the Mo complex. The bond distances are 2.228 Å and 2.427 Å for the Mo(1)–O(4) *cis* and Mo(1)–O(5) *trans* to the carbyne, respectively.

We studied the rate of reaction of **4** with internal alkynes. Kinetic studies show that the rate of cross-metathesis with the sterically less demanding 1-(but-1-yn-1-yl)-2-methylbenzene (**5a**) is ~200 times faster ($k = 1.3 \times 10^{-1}$ M$^{-1}$s$^{-1}$) than with 1,2-bis(*o*-tolyl)acetylene (**5b**) ($k = 7.1 \times 10^{-4}$ M$^{-1}$s$^{-1}$) (Figure 3-8 and Figure 3-9). The subtle kinetic selectivity that directs the intramolecular cross-metathesis of **2c** toward the sterically less hindered butynyl end-group has previously been observed for acyclic diyne metathesis (ADMET).[21]

**Figure 3-7.** ORTEP representation of the X-ray crystal structure of **4**. Thermal ellipsoids are drawn at the 50% probability level. Color coding: C (gray), O (red), F (green), Mo (turquoise). Hydrogen atoms are omitted for clarity.
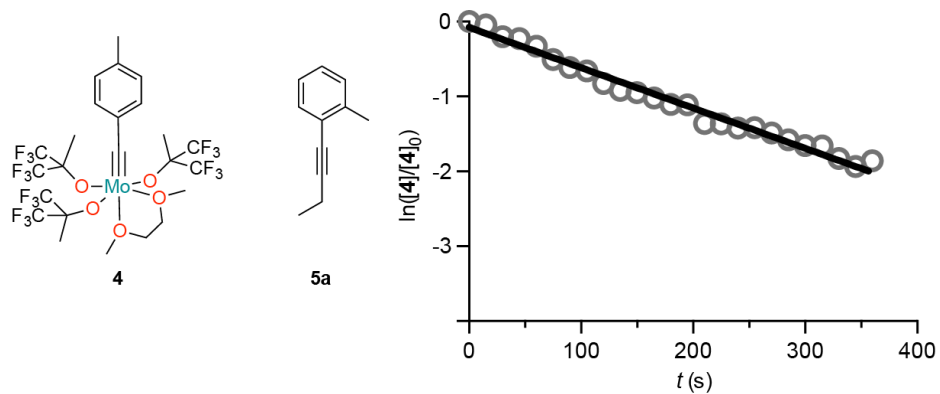


**Figure 3-8.** Pseudo-first order reaction of **4** with **5a**. [**5a**] = 41 mM, [**4**]$_0$ = 1.9 mM, $R^2$ = 0.963.
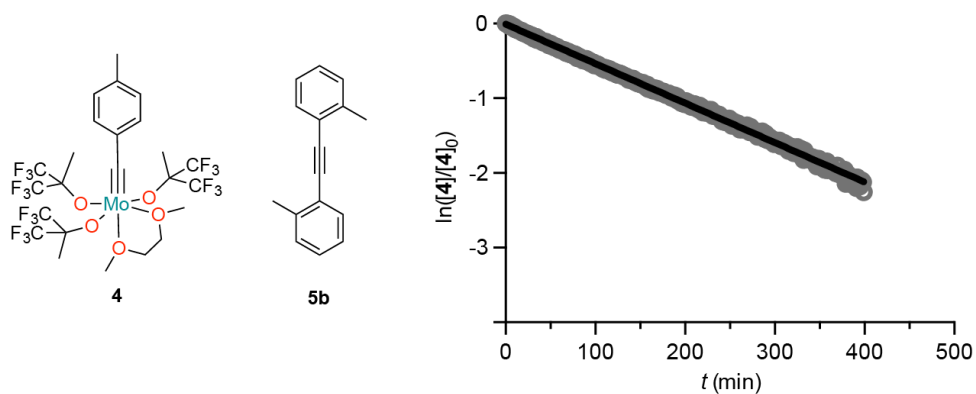


**Figure 3-9.** Pseudo-first order reaction of **4** with **5b**. [**5b**] = 124 mM, [**4**]$_0$ = 1.9 mM, $R^2$ = 0.998.

*3.2.4. Differences Between Linear Polymers Poly-3a and Cylic Polymers Poly-3b*

The topological difference of linear and cyclic polymers, *poly*-**3a** and *poly*-**3b**, is reflected in their photophysical properties. Although the UV-Vis absorption spectra of *poly*-**3a** and *poly*-**3b** appear similar (Figure 3-10), cyclic *poly*-**3b** exhibits a higher fluorescence quantum yield upon excitation at 300 nm ($\Phi_F$ = 8.4% and 18.6% for *poly*-**3a** and *poly*-**3b**, respectively). As the emission spectrum does not shift to longer wavelengths, the observed enhancement can not be explained by the formation of excimer complexes between adjacent monomer units as has been observed for e.g. cyclic polystyrene.[33] Instead, the enhanced quantum yield can be attributed to the reduced conformational entropy of cyclic *poly*-**3b**. Cyclic *poly*-**3b** experiences less nonradiative relaxation than linear *poly*-**3a** due to the restricted intramolecular rotation about the polymer backbone.[34,35] The unique control over polymer topology enables tuning the mechanical and photophysical properties of P*o*PEs with minimal effect on their electronic structure.
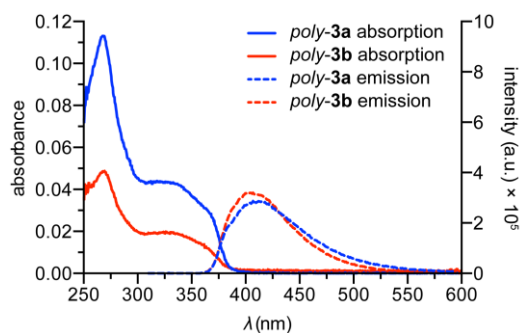


**Figure 3-10.** UV/Vis absorption and fluorescence emission ($\lambda_{ex}$ = 300 nm) of linear *poly*-**3a** and cyclic *poly*-**3b** in chloroform solution (1.6 and 0.6 µg mL$^{-1}$ *poly*-**3a** and *poly*-**3b**, respectively).

Another method of identifying the differences between linear *poly*-**3a** and cyclic *poly*-**3b** is by Atomic-Force Microscopy (AFM) (Dr. Ryan Cloke). The polymers obtained by ROAMP of **3** by **4** (*poly*-**3c**) were studied by AFM. Linear *poly*-**3c** exhibits a fibrous topology, suggesting a helical primary structure induced by π-π stacking (Figure 3-11). In contrast, the AFM of cyclic *poly*-**3b** exhibits spherical topologies (Figure 3-12).
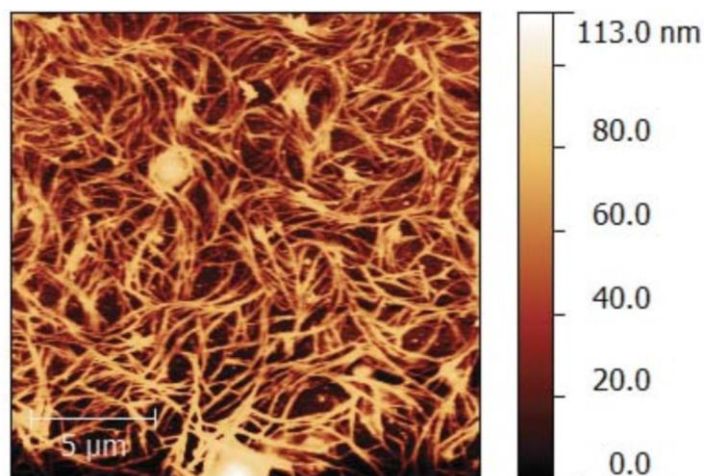
**Figure 3-11.** AFM of linear *poly*-**3c**.
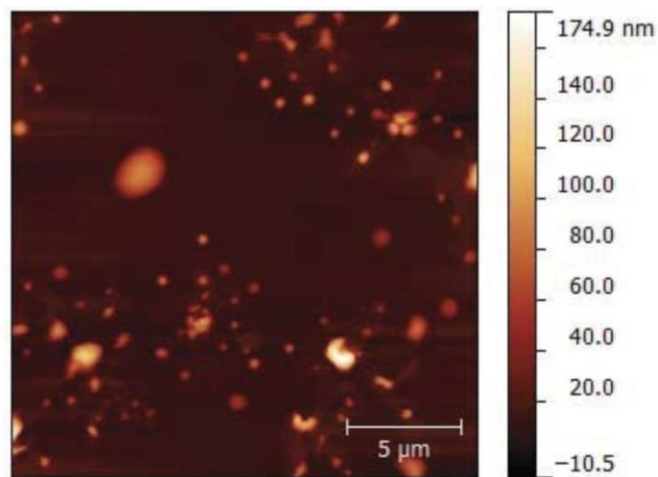


**Figure 3-12.** AFM of cyclic *poly*-**3b**.

## 3.3 Other Studies of Ring-Opening Alkyne Metathesis Polymerization Reactions

### 3.3.1. ROAMP of 3 by Catalyst [TolC≡Mo(OC(CH₃)(CF₃)₂)₃(DME)] (4)

In an effort to further elucidate the steric effect of carbyne substituents on the topology of the resulting polymers, we synthesized **4** according to Bellone et al. and as described in Chapter II.[31] The reaction of catalyst **4** and monomer **3** was monitored by $^1$H NMR (Figure 3-13). Upon addition of the monomer, we observed the formation of two distinctive metallacyclobutadienes. one which is instantaneously formed and decays with time (blue) and one which reaches a maximum during the reaction (green) with $^1$H NMR peaks at 0.95 and 0.92 ppm, respectively. We hypothesize that the initial metallacyclobutadiene, which appears at 0.95 ppm by $^1$H NMR, corresponds to a stoichiometric complex formed by the reaction of **4** with one equivalent of **3**. This

metallacyclobutadiene contains features a tolyl substituent (**4a'**) in one of the alpha positions and decays the fastest. On the other hand, the metallacycle formed by the association of the diyne to a growing polymer chain is observed at 0.92 ppm and reaches a maximum in concentration (**4a**). Similar to catalyst **2**, the amount of polymer bound catalyst decreased, and the amount of initial catalyst increased. This suggests the formation of cyclic polymers by chain back-biting. Therefore, the polymeric product obtained constitutes of a mixture of linear and cyclic polymers. This places the reactivity of catalyst **4** between that of catalysts **1** and **2**. Although cyclic polymers are formed, these are not formed as fast as with complex **2**.
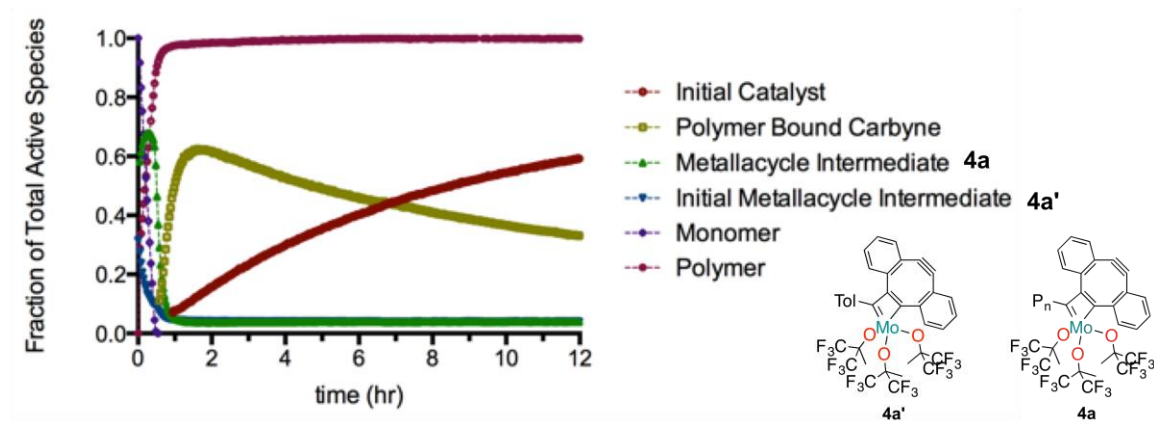


**Figure 3-13.** Relative species concentration during the reaction of **4** with **3**.

In an effort to gain further mechanistic insight into the ring-opening of **3** with catalyst **4**, we monitored the change in molecular weight and PDI over time (Figure 3-14). Even after all monomer is consumed (5 h, $^1$H NMR) the number average molecular weight of polymer chains continues to increase while the PDI broadens. This observation suggests that although the catalyst remains attached to one end of the growing polymer chain backbiting and chain-transfer processes continue to be effective even after all the monomer is consumed.
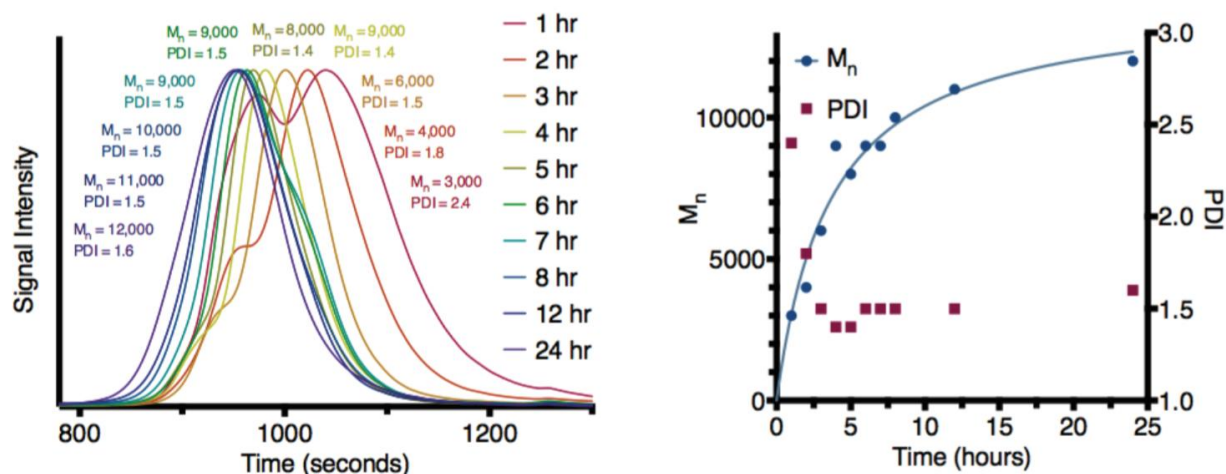
**Figure 3-14.** GPC trace of aliquots from the reaction of **3** with **4**.

Moreover, we explore whether sequential addition of monomer to a growing polymer chain would result in an increase in molecular weight. Aliquots were taken from the initial reaction of 20 equiv. of **3** with **4** and analyzed by GPC (Figure 3-15). An additional 20 equiv. of **3** were added to the reaction mixture and after 5 h the resulting polymers were analyzed with GPC. Figure 3-15 shows only a small increase in the molecular weight. This suggests that the active sites in growing polymer chains have undergone irreversible termination or backbiting to form cyclic polymers and the original catalyst **4**. The additional 20 equiv. of monomer are not incorporated into the growing polymer chains.
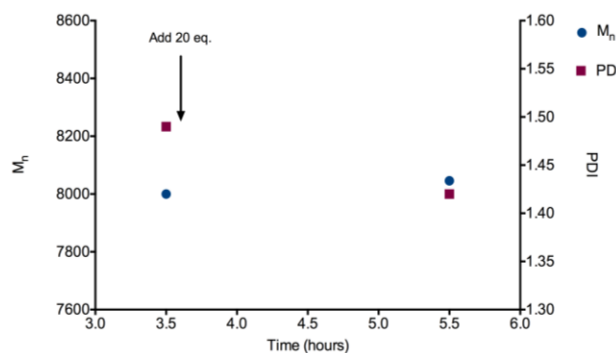


**Figure 3-15.** Molecular weight and PDI data of a reaction where and additional 20 equiv. of monomer were added.

### 3.3.2. ROAMP of Functionalized Monomers by Catalyst [TolC≡Mo(OC(CH₃)(CF₃)₂)₃(DME)] (4)

$3.3.2.$ *ROAMP of Functionalized Monomers by Catalyst* $[TolC{\equiv}Mo(OC(CH_3)(CF_3)_2)_3(DME)]$ *(4)*

One of the limitations of the ROAMP of **3** with **4** is the low solubility that prevents the formation of high molecular weight polymers. In an effort to increase the solubility of *poly*-(*o*-phenylene ethynylenes) we synthesized diynes **5** and **6** featuring solubilizing

octyloxy and 2-ethyl-1-hexyloxy groups, respectively (Dr. Ryan Cloke). ROAMP of diynes **5** and **6** was carried out under the conditions analogous to those described for **3** (Scheme 3-2).
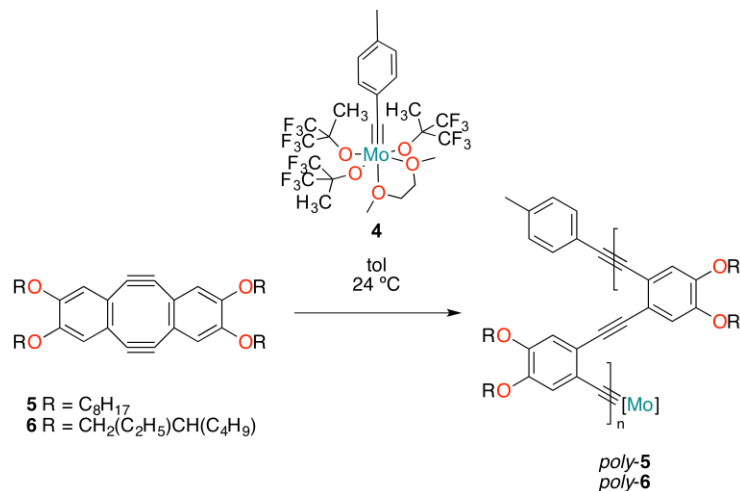


**Scheme 3-2.** ROAMP of functionalized diynes **5** and **6** by catalyst **4**.

Aliquots taken from the reaction mixture at various time points were analyzed by GPC. The reaction of 5 equiv. of **5** with **4** is faster than that of monomer **3**. GPC traces reveal that the molecular weight increases and the PDI broadens over time as seen by the increase of polymers with retention time at $t = 500$ s (Figure 3-16). The increase in the high molecular weight peak at $t = 500$ s suggests intermolecular chain transfer processes leading to higher molecular weight polymers. The overall higher reactivity of the electron rich alkoxy substituted strained monomer **5** results in a in a less controlled reaction. The degree of polymerization ($X_n = M_{w,polymer}/M_{w,monomer}$) is 6, suggesting a complete initiation of all catalyst centers. Similar results have been obtained for the ROAMP of **6** (Figure 3-17).
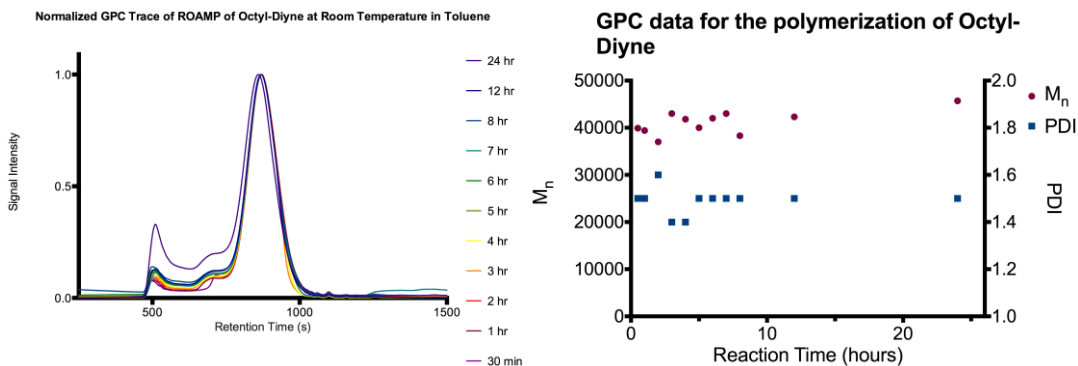


**Figure 3-16.** GPC trace of aliquots from the reaction of **5** with **4**.
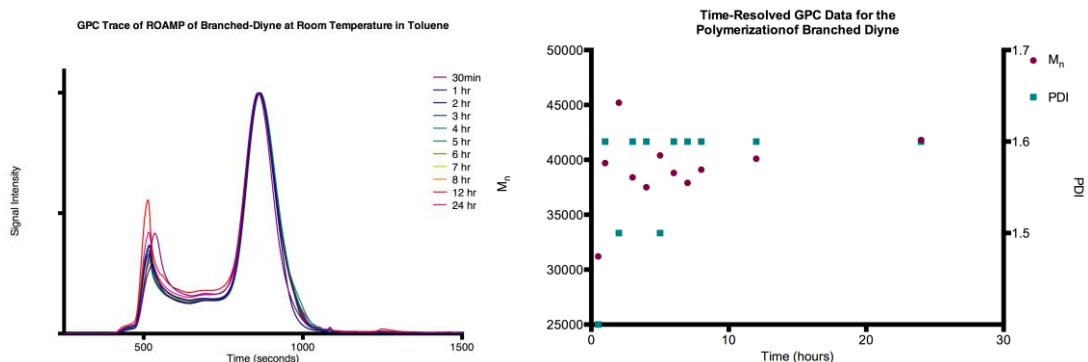
**Figure 3-17.** GPC trace of aliquots from the reaction of **6** with **4**.

### 3.3.3. ROAMP of 3 by Other Catalysts

A key intermediate in the ROAMP with **1** is the metallacyclobutadienes **1a** and **1b** (Figure 3-4). The presence of such a long-lived intermediate may lead to undesired ring expansion and alkyne polymerization. We sought to decrease the stability of the metallacyclobutadiene intermediate by developing a catalyst featuring sterically demanding alkoxide substituents. We synthesized catalyst [MesC≡Mo(OCPh(CF$_3$)$_2$)$_3$] (**7**) and [TolC≡Mo(OCPh(CF$_3$)$_2$)$_3$] (**8**) in a procedure analogous to the one described for **1**. X-ray quality crystals of **7** were grown from a pentane solution at −35 ℃ (Figure 3-18). X-ray crystallography of **7** (Figure 3-18) confirms the presence of a C(1)≡Mo(1) triple bond with a bond length of 1.755 Å. Three hexafluoro-*tert*-butoxide ligands exhibit typical Mo(1)–O(1), Mo(1)–O(2), and Mo(1)–O(3) distances of 1.881 Å, 1.939 Å and, 1.899 Å. The steric bulk induced by the phenyl substituent leads to slightly longer Mo≡C and Mo–O bonds when compared to **1** (C(1)≡Mo(1), Mo(1)–O(1), Mo(1)–O(2), and Mo(1)–O(3) 1.7438 Å, 1.8946 Å, 1.9243 Å, and 1.8963 Å, respectively).[28] ROAMP of **7** and **8** with **3** leads to polymers featuring a broad PDI when compared to **1** (Figure 3-19).
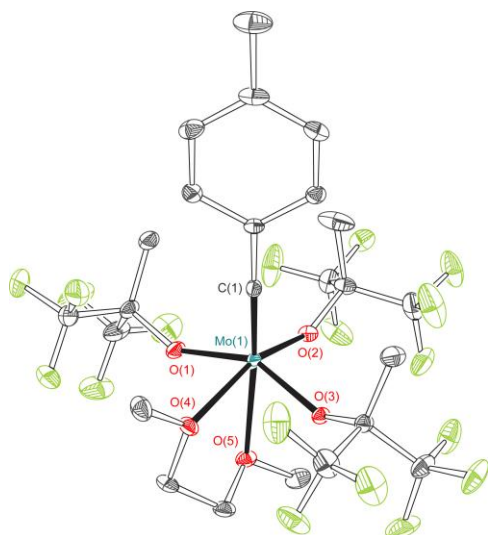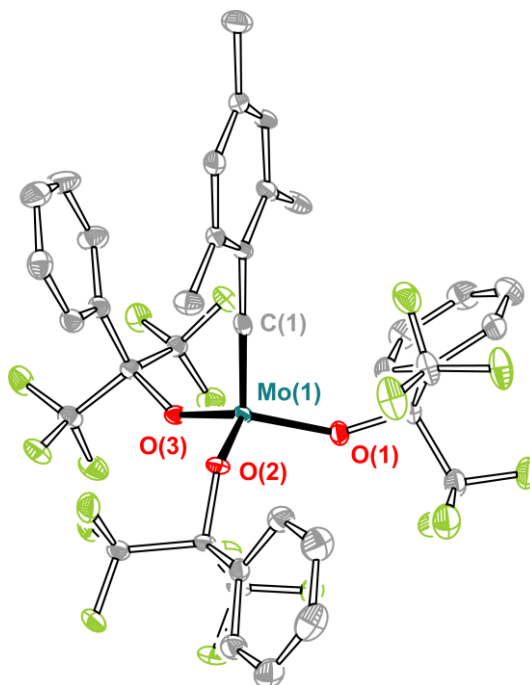
**Figure 3-18.** ORTEP representation of the X-ray crystal structure of **7**. Thermal ellipsoids are drawn at the 50% probability level. Color coding: C (gray), O (red), F (green), Mo (turquoise). Hydrogen atoms are omitted for clarity.
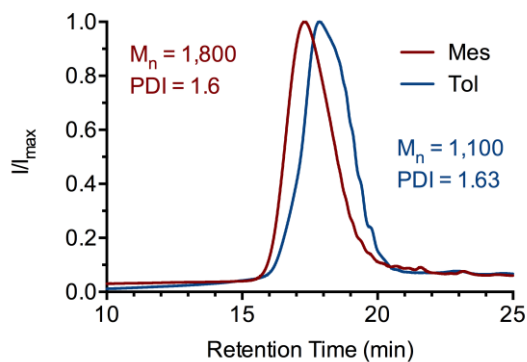


**Figure 3-19.** GPC trace of the polymers obtained by reacting monomer **3** with catalysts **7** (Tol, blue) and **8** (Mes, red).

Finally, we tested the ROAMP of **3** with the living catalyst **9** described in Chapter 2 (Scheme 3-2). Upon addition of the monomer to the catalyst, we observe immediate color change. $^1$H NMR and $^{19}$F NMR (Figure 3-20) reveal the consumption of **9**, yet no polymers could be isolated from the reaction mixture.
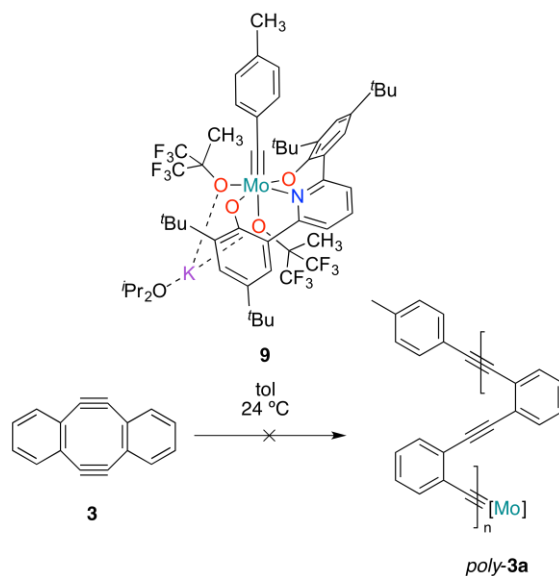
**Scheme 3-2.** Attempted ROAMP of **3** with catalyst **9**.

By $^1$H NMR, broadening of the catalyst peaks, but no appearance of polymers is observed. $^{19}$F NMR reveals the dissociation of the weakly bound axial alkoxide. These preliminary experiments suggest the irreversible coordination of one equivalent of monomer, but no ring-opening event.
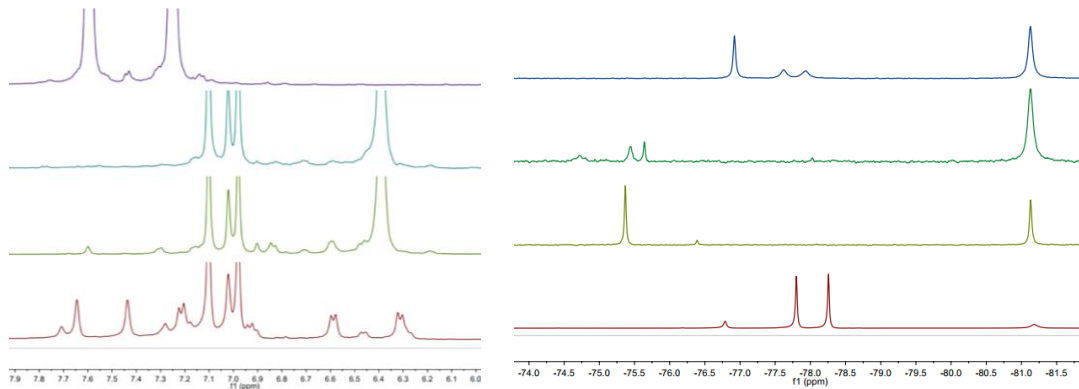


**Figure 3-20.** $^1$H NMR and $^{19}$F NMR of the reaction mixture in tol-d$_8$. (Left) From bottom to top, we see the $^1$H NMR of catalyst, reaction at RT 1h, reaction at 95 °C 2h, and the expected polymer. (Right) From bottom to top, we see the $^1$H NMR of catalyst, reaction at RT 1h, reaction at 95 °C 2h, and the initiated catalyst with another monomer as described in Chapter 2.

## 3.4 Conclusion

We describe the synthesis of a fully conjugated *poly*(*o*-phenylene ethynylene) using living ring-opening alkyne metathesis polymerization. Tuning the steric demand of the molybdenum carbyne initiator directs the synthesis of either linear or cyclic polymers with high selectivity. The polymerization mechanism and catalyst resting states were investigated through multinuclear NMR kinetic and $^{13}$C labeling studies. The catalyst

system described herein represents an extraordinary access to the field of conjugated organic materials, simultaneously enabling exceptional control over polymer structure, sequence and topology. Tuning the steric demand of both the carbyne and the alkoxide ligand did not lead to an improvement in the PDI of the resulting polymers. Although not reported here, attempts to synthesize block-copolymers with catalyst **4** and diyne **3** were unsuccessful.

Furthermore, we hope to make working organic light-emitting diodes (OLEDs) with *poly*-**3a**. We built OLEDs with the architecture as ITO/PEDOT:PSS/*poly*-**3a**/Ca/Al. Although diode behavior was observed with such a device, no light emission was observed at voltages of up to 30 V and currents of 30 mA in the 350–800 nm range.

## 3.5 Experimental

### 3.5.1. Synthetic Details

*Materials and General Methods.* Unless otherwise stated, all manipulations of air and/or moisture sensitive compounds were carried out in oven-dried glassware, under an atmosphere of Ar or $N_2$. All solvents and reagents were purchased from Alfa Aesar, Spectrum Chemicals, Acros Organics, TCI America, and Sigma-Aldrich and were used as received unless otherwise noted. Organic solvents were dried by passing through a column of alumina and were degassed by vigorous bubbling of $N_2$ or Ar through the solvent for 20 min. Flash column chromatography was performed on SiliCycle silica gel (particle size 40–63 μm). Thin layer chromatography was carried out using SiliCycle silica gel 60 Å F-254 precoated plates (0.25 mm thick) and visualized by UV absorption. All $^1$H, {$^1$H}$^{13}$C, and $^{19}$F NMR spectra were recorded on Bruker AV-600, DRX-500, and AV-500 spectrometers, and are referenced to residual solvent peaks (CDCl$_3$ $^1$H NMR $\delta$ = 7.26 ppm, $^{13}$C NMR $\delta$ = 77.16 ppm; C$_6$D$_6$ $^1$H NMR $\delta$ = 7.16 ppm, $^{13}$C NMR $\delta$ = 128.06 ppm; Tol-$d_8$ $^1$H NMR $\delta$ = 2.08 ppm; THF-$d_8$ $^1$H NMR $\delta$ = 1.78 ppm, $^{13}$C NMR $\delta$ = 67.21 ppm) or hexafluorobenzene ($^{19}$F NMR $\delta$ = −162.90 ppm). The concentrations of **4**, **5a**, and **5b** were determined by $^1$H and $^{19}$F NMR using the ERETIC method[36] against an external standard of 18.2 mM 1,3,5-tris(trifluoromethyl)benzene in C$_6$D$_6$. ESI mass spectrometry was performed on a Finnigan LTQFT (Thermo) spectrometer in positive ionization mode. MALDI mass spectrometry was performed on a Voyager-DE PRO (Applied Biosystems Voyager System 6322) in positive mode using a matrix of dithranol. Elemental analysis (CHN) was performed on a Perkin Elmer 2400 Series II combustion analyzer (values are given in %). Gel permeation chromatography (GPC) was carried out on a LC/MS Agilent 1260 Infinity set up with a guard and two Agilent Polypore 300 x 7.5 mm columns at 35 °C. All GPC analyses were performed on a 0.2 mg/mL solution of polymer in chloroform. An injection volume of 25 μL and a flow rate of 1 mL/min were used. Calibration was based on narrow polydispersity polystyrene standards ranging from $M_w$ = 100 to 4,068,981. X-ray crystallography was performed on APEX II QUAZAR, using a Microfocus Sealed Source (Incoatec IμS; Mo-Kα radiation), Kappa Geometry with DX (Bruker-AXS build) goniostat, a Bruker APEX II detector, QUAZAR multilayer mirrors as the radiation monochromator, and Oxford Cryostream 700 for **2**. Crystallographic data was refined with SHELXL-97, solved with SIR-2007, visualized

with ORTEP-32, and finalized with WinGX. UV-Vis absorption spectra were acquired in chloroform solution on a Varian Cary 50 spectrophotometer (Agilent, USA). Fluorescence emissions spectra were acquired at an excitation wavelength of 300 nm on a Fluoromax-4 spectrofluorometer equipped with automatic polarizers,1.0 nm slit widths for excitation/emission and a 0.5 s integration time. Quantum yields were calibrated to 1,4-bis(5-phenyloxazol-2-yl) benzene (POPOP) in cyclohexane ($\Phi_F$ = 0.97).[37] **1**,[28] **3**,[38] **4**,[31] and **5b**[39] were synthesized following literature procedures.

*Preparation of linear poly-(o-phenylene ethynylene)* (*poly-***3a**). A 5 mL vial was charged under $N_2$ with **3** (0.02 g, 0.10 mmol) in toluene (1.50 mL). **1** (3.8 mg, 5.0 µmol) in toluene (0.60 mL) was added at 24 °C and the mixture was stirred for 3 h. The reaction mixture was quenched with MeOH (10 mL). The solid precipitate was isolated by filtration and washed with MeOH (30 mL) to yield *poly-***3a** (0.02 g, 82%) as a brown solid. ^{1}H NMR (500 MHz, CDCl$_3$, 22 °C) $\delta$ = 7.56–7.45 (br, 56H), 7.20–7.09 (br, 56H), 6.81 (s, 2H), 2.46 (s, 6H), 2.24 (s, 3H) ppm; ^{13}C NMR (126 MHz, CDCl$_3$, 22 °C) $\delta$ = 132.3, 128.1, 125.8, 92.6, 21.3 ppm.

*Preparation of cyclic poly-(o-phenylene ethynylene)* (*poly-***3b**). A 20 mL vial was charged under $N_2$ with **3** (0.06 g, 0.30 mmol) in toluene (1.50 mL). **2** (43.4 mg, 55.0 µmol) in toluene (0.50 mL) was added at 24 °C and the mixture was stirred for 24 h. The reaction mixture was quenched with MeOH (10 mL). The solid precipitate was isolated by filtration and washed with MeOH (30 mL). Soxhlet extraction (hexane) of the crude mixture yielded *poly-***3b** (0.01 g, 18%) as a brown solid. The polymer remaining in the extraction thimble (30 mg) was dissolved in chloroform (15 mL) and precipitated with pentane (60 mL). After filtering off the precipitate, the filtrate was evaporated to yield additional pure *poly-***3b** (0.02 g, total yield 50%). ^{1}H NMR (600 MHz, CDCl$_3$, 22 °C) $\delta$ = 7.48–7.44 (m, 2H), 7.13–7.09 (m, 2H) ppm; ^{13}C NMR (126 MHz, CDCl$_3$, 22 °C) $\delta$ = 132.2, 128.1, 125.7, 92.5 ppm.

### 3.5.2. Loading Experiments

The monomer loading experiment of the polymerization of **3** with **1** consisted of the following

- Stock solution of monomer **3** (100 mM) in $C_6D_6$

- Stock solution of the catalyst **1** (6.67 mM) in $C_6D_6$

A *J. Young* NMR tube was charged with $C_6D_6$ (0, 150, or 200 µL), followed by an aliquot of catalyst **1** stock solution (300, 150, or 100 µL, respectively), and monomer **3** stock solution (200 µL). ^{1}H NMR were recorded at 22 °C. After consumption of the monomer, the polymer was precipitated with MeOH (500 µL), filtered, and the solid residue dried under vacuum overnight. The polymers were characterized by size exclusion GPC and ^{1}H and ^{13}C NMR. The degree of polymerization was determined by integrating the peak ($C_{(Ar)}$–H) of the polymer at 7.50 ppm to the peak ($C_{(Ar)}$–H) of the mesityl end-group at 6.81 ppm.

### 3.5.3. Monomer Conversion vs. $M_n$

Monomer **3** (12 mg) was dissolved in of $C_6D_6$ (600 µL), and catalyst **1** (2 mg) was dissolved in $C_6D_6$ (500 µL). HMDSO (6 µL) was added to the solution of monomer **1**. An aliquot of the monomer solution (100 µL) was diluted with $C_6D_6$ (300 µL), to obtain the initial $^1H$ NMR integration ratio of the monomer multiplet at 6.45 ppm to the HMDSO singlet at 0.12 ppm. The solution of catalyst was added to the remaining 500 µL solution of monomer. At different time-points, 200 µL aliquots of the reaction were diluted with $C_6D_6$ (200 µL) and quenched with $CD_3OD$ (60 µL). After obtaining a $^1H$ NMR, the polymer was precipitated with MeOH (500 µL), filtered, and dried under vacuum overnight. The polymers were characterized by size exclusion GPC.

### 3.5.4. Concentration dependence of cyclic polymer selectivity of catalyst **2**

A stock solution of monomer **3** (200 µL at 125 mM, 0.025 mmol) in toluene was diluted with an appropriate volume of toluene (600 µL, 1.6 mL, 3.6 mL, 7.6 mL) to give the desired monomer concentration. To each was added 200 µL of a 25 mM solution of **2** in toluene at room temperature with stirring. The polymerizations were stirred for 16 hours and then the catalyst deactivated by the addition of methanol (3x the solution volume). The crude polymers were concentrated by rotary evaporation to a tan solid and dried in vacuum overnight. The solids were dissolved in chloroform and the percent linear polymer ($^1H$ NMR) and MW (GPC) were determined.

### 3.5.5. In-situ NMR studies of the polymerization of **3**

A typical experiment consists of the following. To a solution of **3** (5 mg, 0.025 mmol) in $C_6D_6$ (0.3 mL) in an $N_2$ glovebox was added a solution of the appropriate amount of **1** or **2** in $C_6D_6$ (0.2 mL). The mixture was immediately transferred to a J. Young tube and frozen. The reaction mixture was thawed and the reaction followed by NMR spectroscopy. The concentrations of the different catalyst species were determined by integrating the methyl ($^1H$) or trifluoromethyl ($^{19}F$) resonances corresponding to the $OC(CH_3)(CF_3)_2$ ligands.

### 3.5.6. Cross metathesis rate studies with model complex **4**:

A stock solution of **4** (20 mM) in $C_6D_6$ was prepared.

With **5a**: For the reaction with **5a**, 50 µL of the stock solution of **4** was diluted with 450 µL $C_6D_6$ in a septum-capped NMR tube under $N_2$. The tube was placed in the NMR spectrometer and allowed to reach temperature equilibrium at 298 K, then neat **5a** (20 equiv) was injected and the reaction monitored by NMR. The concentration of **5a** was verified by ERETIC. The disappearance of **4** was fit to a pseudo-first order decay over the first 2.5 half-lives (<5% change in [**5a**]) by fitting a line to $\ln([4]/[4]_0)$ vs. $t$. Dividing the slope by [**5a**]$_0$, as determined by ERETIC, provides $k$.

With **5b**: A J. Young tube was charged with 50 µL of stock solution of **4** and 65 equiv **5b** in $C_6D_6$ (450 µL). The tube was placed in the NMR spectrometer and allowed to reach temperature equilibrium, at which point [**4**] and [**5b**] were determined by ERETIC. The disappearance of **4** was fit to a pseudo-first order decay over the first three half-lives (<2% change in [**5b**]) by fitting a line to $\ln([\mathbf{4}]/[\mathbf{4}]_0)$ vs. $t$. Dividing the slope by $[\mathbf{5b}]_0$, as determined by ERETIC, provides $k$.

## 3.6 References

(1)     Scherf, U.; List, E. j. w. *Adv. Mater.* **2002**, *14* (7), 477–487.

(2)     Cheng, Y.-J.; Yang, S.-H.; Hsu, C.-S. *Chem. Rev.* **2009**, *109* (11), 5868–5923.

(3)     Weber, J.; Thomas, A. *J. Am. Chem. Soc.* **2008**, *130* (20), 6334–6335.

(4)     Friend, R. H.; Gymer, R. W.; Holmes, A. B.; Burroughes, J. H.; Marks, R. N.; Taliani, C.; Bradley, D. D. C.; Santos, D. A. D.; Brédas, J. L.; Lögdlund, M.; Salaneck, W. R. *Nature* **1999**, *397* (6715), 121–128.

(5)     Reineke, S.; Lindner, F.; Schwartz, G.; Seidler, N.; Walzer, K.; Lüssem, B.; Leo, K. *Nature* **2009**, *459* (7244), 234–238.

(6)     Kanimozhi, C.; Yaacobi-Gross, N.; Chou, K. W.; Amassian, A.; Anthopoulos, T. D.; Patil, S. *J. Am. Chem. Soc.* **2012**, *134* (40), 16532–16535.

(7)     Knopfmacher, O.; Hammock, M. L.; Appleton, A. L.; Schwartz, G.; Mei, J.; Lei, T.; Pei, J.; Bao, Z. *Nat. Commun.* **2014**, *5*, 2954.

(8)     Fuller, M. J.; Walsh, C. J.; Zhao, Y.; Wasielewski, M. R. *Chem. Mater.* **2002**, *14* (3), 952–953.

(9)     Yang, J.-S.; Swager, T. M. *J. Am. Chem. Soc.* **1998**, *120* (46), 11864–11873.

(10)    Smith, R. C.; Tennyson, A. G.; Lim, M. H.; Lippard, S. J. *Org. Lett.* **2005**, *7* (16), 3573–3575.

(11)    Wosnick, J. H.; Mello, C. M.; Swager, T. M. *J. Am. Chem. Soc.* **2005**, *127* (10), 3400–3405.

(12)    Hussain, S.; De, S.; Iyer, P. K. *ACS Appl. Mater. Interfaces* **2013**, *5* (6), 2234–2240.

(13)    Ryu, S.; Yoo, I.; Song, S.; Yoon, B.; Kim, J.-M. *J. Am. Chem. Soc.* **2009**, *131* (11), 3800–3801.

(14)    Intemann, J. J.; Hellerich, E. S.; Tlach, B. C.; Ewan, M. D.; Barnes, C. A.; Bhuwalka, A.; Cai, M.; Shinar, J.; Shinar, R.; Jeffries-EL, M. *Macromolecules* **2012**, *45* (17), 6888–6897.

(15)    Jagtap, S. P.; Mukhopadhyay, S.; Coropceanu, V.; Brizius, G. L.; Brédas, J.-L.; Collard, D. M. *J. Am. Chem. Soc.* **2012**, *134* (16), 7176–7185.

(16)    Zhao, X.; Pinto, M. R.; Hardison, L. M.; Mwaura, J.; Müller, J.; Jiang, H.; Witker, D.; Kleiman, V. D.; Reynolds, J. R.; Schanze, K. S. *Macromolecules* **2006**, *39* (19), 6355–6366.

(17)    Guo, X.; Watson, M. D. *Macromolecules* **2011**, *44* (17), 6711–6716.

(18)    Kübel, C.; Mio, M. J.; Moore, J. S.; Martin, D. C. *J. Am. Chem. Soc.* **2002**, *124* (29), 8605–8610.

(19)    Bunz, U. H. F. *Macromol. Rapid Commun.* **2009**, *30* (9-10), 772–805.

(20)    Yang, H.; Jin, Y.; Du, Y.; Zhang, W. *J. Mater. Chem. A* **2014**, *2* (17), 5986–5993.

(21)    Zhang, W.; Moore, J. S. *J. Am. Chem. Soc.* **2005**, *127* (33), 11863–11870.

(22)    Zhang, W.; Brombosz, S. M.; Mendoza, J. L.; Moore, J. S. *J. Org. Chem.* **2005**, *70* (24), 10198–10201.

(23)    Gross, D. E.; Moore, J. S. *Macromolecules* **2011**, *44* (10), 3685–3687.

(24)    Yang, H.; Liu, Z.; Zhang, W. *Adv. Synth. Catal.* **2013**, *355* (5), 885–890.

(25)    Zhang, W.; Moore, J. S. *Adv. Synth. Catal.* **2007**, *349* (1–2), 93–120.

(26)    Jyothish, K.; Zhang, W. *Angew. Chem. Int. Ed.* **2011**, *50* (37), 8478–8480.

(27)    Fürstner, A. *Angew. Chem. Int. Ed.* **2013**, *52* (10), 2794–2819.

(28)    Haberlag, B.; Freytag, M.; Daniliuc, C. G.; Jones, P. G.; Tamm, M. *Angew. Chem. Int. Ed.* **2012**, *51* (52), 13019–13022.

(29)    Gdula, R. L.; Johnson, M. J. A. *J. Am. Chem. Soc.* **2006**, *128* (30), 9614–9615.

(30)    Freudenberger, J. H.; Schrock, R. R.; Churchill, M. R.; Rheingold, A. L.; Ziller, J. W. *Organometallics* **1984**, *3* (10), 1563–1573.

(31)    Bellone, D. E.; Bours, J.; Menke, E. H.; Fischer, F. R. *J. Am. Chem. Soc.* **2015**, *137* (2), 850–856. Strained 5,6,11,12-tetradehydrobenzo[*a*,*e*][8]annulene (**3**) decomposes rapidly at $T > 40\ °C$ and was thus incompatible with the ROAMP catalyst reported in reference 31.

(32)    O'Reilly, M. E.; Ghiviriga, I.; Abboud, K. A.; Veige, A. S. *Dalton Trans.* **2013**, *42* (10), 3326–3336.

(33)    Gan, Y.; Dong, D.; Carlotti, S.; Hogen-Esch, T. E. *J. Am. Chem. Soc.* **2000**, *122* (9), 2130–2131.

(34)    Hong, Y.; Lam, J. W. Y.; Tang, B. Z. *Chem. Commun.* **2009**, No. 29, 4332–4353.

(35)    Zhu, X.; Zhou, N.; Zhang, Z.; Sun, B.; Yang, Y.; Zhu, J.; Zhu, X. *Angew. Chem. Int. Ed.* **2011**, *50* (29), 6615–6618.

(36)    Akoka, S.; Barantin, L.; Trierweiler, M. *Anal. Chem.* **1999**, *71* (13), 2554–2557.

(37)    Lakowicz, J. R. *Principles of Fluorescence Spectroscopy (2nd) Second Edition*, First Printing edition.; Kluwer Acacemic Publishers, 1999.

(38)    Orita, A.; Hasegawa, D.; Nakano, T.; Otera, J. *Chem. – Eur. J.* **2002**, *8* (9), 2000–2004.

(39)    Chuentragool, P.; Vongnam, K.; Rashatasakhon, P.; Sukwattanasinitt, M.; Wacharasindhu, S. *Tetrahedron* **2011**, *67* (42), 8177–8182.

# 4 Termination of Ring-Opening Alkyne Metathesis Polymerization

## 4.1 Introduction: Termination of Polymerizations

As the field of ring-opening alkyne metathesis polymerization continues to grow, the focus of interest has shifted from the initiation and propagation towards new strategies to control the termination step. A variety of reactions that lead to premature termination of ROAMP have been reported including deprotonation of intermediate metallacyclobutadienes formed by terminal alkynes, intra and intermolecular chain transfer steps, and the protonation of the alkylidyne to yield a carbene complex.[1-5] Current strategies used to quench the active ROAMP catalyst attached to the end of the growing polymer chain rely on hydrolysis with MeOH and lead to a mixture of end groups ranging from aldehydes, alcohols, acetals, and even methyl groups.[3,6] Addition of water to the alkylidyne may also lead to the formation of radical polymer intermediates that can recombine under dimerization resulting in a broadening of the PDI.[3]

The unique advantage of controlling the termination step of a polymerization reaction extends beyond maintaining a low PDI. During the termination a functional end-group can be incorporated that significantly expands the structural diversity and with it the potential applications of block copolymers. Once all monomer is consumed in a ROAMP, the active species of the catalyst remains attached to one end of the polymer chain (Figure 4-1a). Alkyne cross metathesis with a chain terminating reagent leads to the selective incorporation of a functional end group (Figure 4-1b). This new functional group may for example serve as an initiator for an orthogonal polymerization yielding block copolymers (Figure 4-1c), or as a functional monomer for the synthesis of graft polymers (Figure 4-1e). Alternatively, the end group could undergo a reaction with the other end of the same polymer chain leading to a cyclic topology (Figure 4-1d). These manipulations have previously been demonstrated for ROMP and have found applications in biomedical labeling, nanoparticle formation, and polymeric functional materials.[7-9]
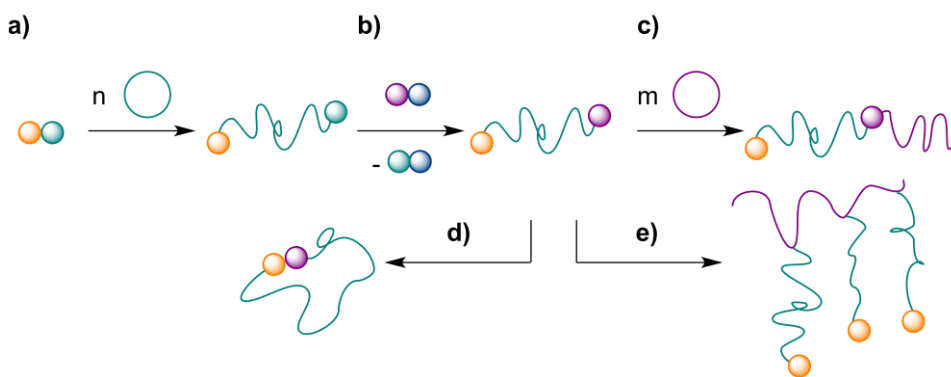


**Figure 4-1.** Manipulation the end-group of polymers for materials applications.

A competent terminating agent has to meet a series of stringent design criteria. It has to react quantitatively and regioselectively with all active polymer chain ends while sufficiently deactivating the cleaved ROAMP catalyst to prevent any chain transfer or backbiting reactions. In ROMP this goal has been accomplished by taking advantage of

the subtle differences in the reactivity of ROMP catalysts. Schrock's molybdenum and tungsten alkylidene catalysts, for example, can be quenched through a cross metathesis with aldehyde C=O groups. The thermodynamic driving force for the reaction is associated with the high oxophilicity of the metal centers (Scheme 4-1a). Ruthenium catalysts on the other hand are more selective for olefins. A competent terminating agent has to be derived from an alkene (Scheme 4-1a). Addition of vinyl ethers to an active ruthenium ROMP catalyst leads to effective termination by forming the more stable Fischer-type carbene. Inspired by these strategies we sought to adapt the latter to the design of a terminating reagent for ROAMP catalysts. Metathesis of a ROAMP catalyst with a highly polarized alkyne such as an ynamine should preferably lead to a deactivated Fischer-type carbyne complex (Scheme 4-1b).
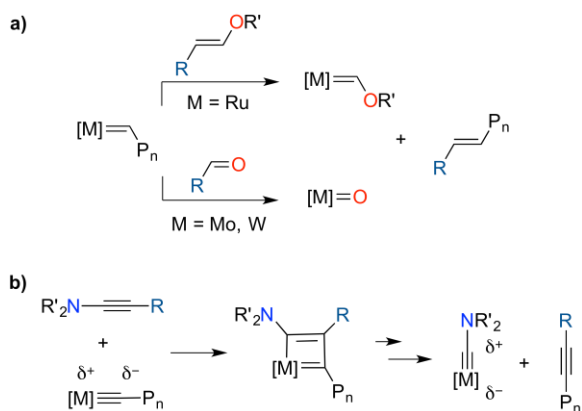


**Scheme 4-1.** a) Terminating agents used in alkene ROMP. b) Design of termination for ROAMP.

## 4.2 Uncontrolled Terminations

### 4.2.1. Quenching ROAMP Catalysts with Methanol

Levy et al. reported that the reaction of Schrock's tungsten alkylidyne catalyst [Me$_3$C≡W(OCMe$_3$)$_3$] (**1**) with water leads to a variety of products that were be characterized by gas chromatography/mass spectrometry (GCMS).[3] Upon addition of water, free carbynes with a quartet spin state are released into solution, leading to the formation of alkynes, alkenes, alkanes, alcohols, and aldehydes. We have observed similar reactivity when quenching the ROAMP catalyst **1** (Scheme 4-2) with wet methanol.
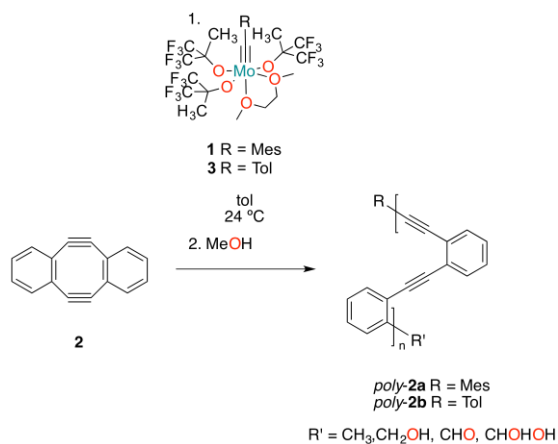
**Scheme 4-2.** Quenching **1** with methanol leads to various end-groups.

Matrix-assisted laser desorption/ionization (MALDI) spectrometry of isolated *poly*-**2a** shows broad peaks associated with polymers featuring a variety of functional end groups (Figure 4-2).
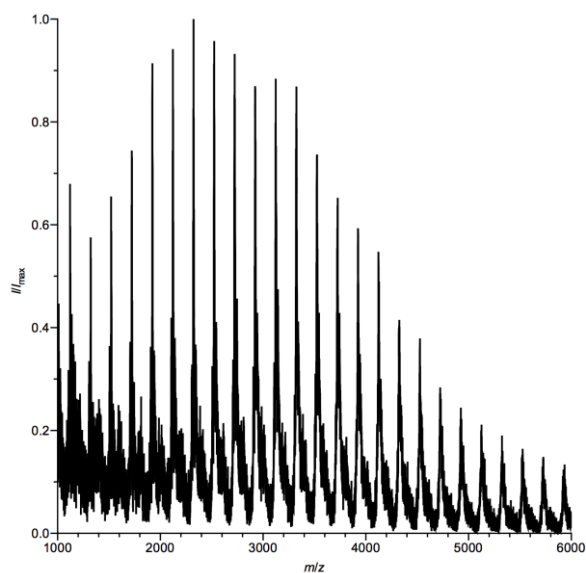


**Figure 4-2.** MALDI of *poly*-**2a**.

We studied the mechanism of termination by quenching the catalyst with methanol-$d_4$ (Scheme 4-3a). The resulting reaction mixture was analyzed by GCMS. By $^2$H NMR the –CD$_3$ group appears as a peak at 2.16 ppm. $^2$H NMR revealed the presence of *p*-xylene-$d_3$ (**5**) among other deuterated products. GCMS indicated the formation of unlabeled *p*-xylene, *p*-xylene-$d_2$ and *p*-xylene-$d_1$, (**4**) resulting from residual HOCD$_3$ in methanol-$d_4$.

A proposed mechanism for this reaction is depicted in Scheme 4-2b. Sequential coordination of methanol to the Mo complex, followed by protonation of alkylidyne leads to the formation of a Mo(VI) alkylidene. Successive additions of methanol form xylene and complex **6**.
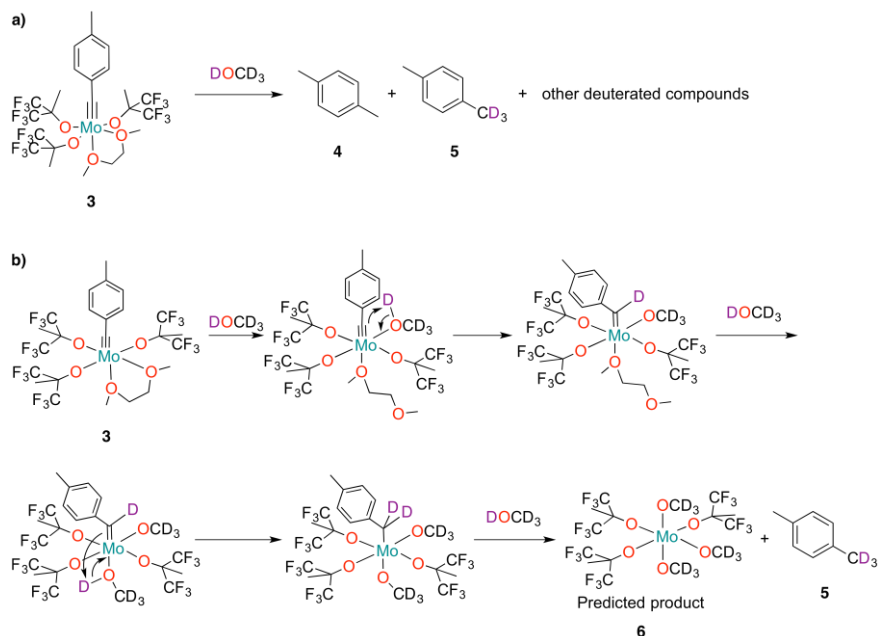


**Scheme 4-2.** a) Addition of methanol-$d_4$ leads to xylene and deuterated products. b) Proposed mechanism for quenching of alkylidyne catalysts with methanol.

### 4.2.2. Addition of Water to Active Catalysts

In analogy to the reaction with methanol, we expect that the first step in the reaction of alkylidyne catalysts with water is the association of water. The postulated intermediate complex **7** featuring a coordinated water in the axial position has been isolated from a wet solution of pentane at −35 °C (Figure 4-3).
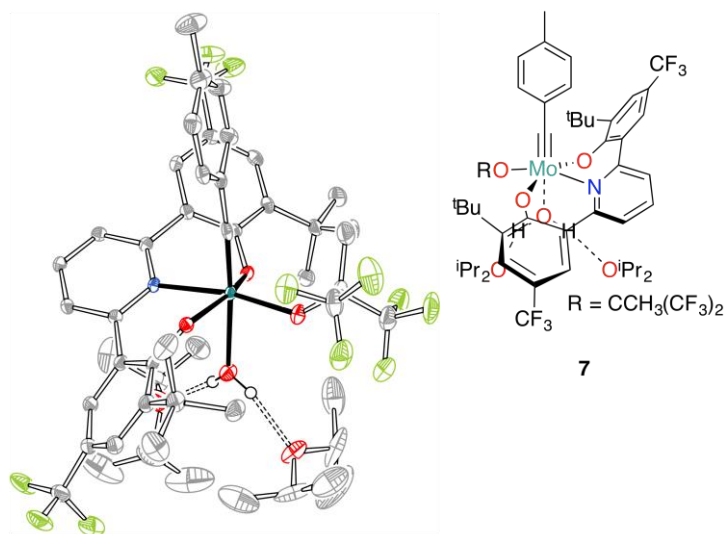
**Figure 4-7.** ORTEP representation of the X-ray crystal structure of **7**. Thermal ellipsoids are drawn at the 50% probability level. Color coding: C (gray), O (red), F (green), Mo (turquoise), N (blue). Hydrogen atoms are omitted for clarity.

The product of the reaction of catalyst **3** with water has been isolated from a wet solution of diisopropyl ether at −35 °C (Figure 4-4). The molybdenum oxo complex **8** is structurally unrelated to the proposed intermediate **7** and product **6** illustrated in the mechanism of quenching by methanol. The oxidation state of **8** is Mo(V), while the starting complex **3** is Mo(VI). X-ray crystallography of **8** supports the presence of a O(1)≡Mo(1) triple bond character, with a bond length of 1.656 Å, however this will be depicted as O=Mo in schemes.[16] Three hexafluoro-*tert*-butoxide ligands adopt a meridional conformation. In the crystal structure one equivalent of DME is coordinated to the Mo complex. The bond distances are 2.224 Å and 2.324 Å for the Mo(1)−O(3) *cis* and Mo(1)−O(6) *trans* to the carbyne, respectively.
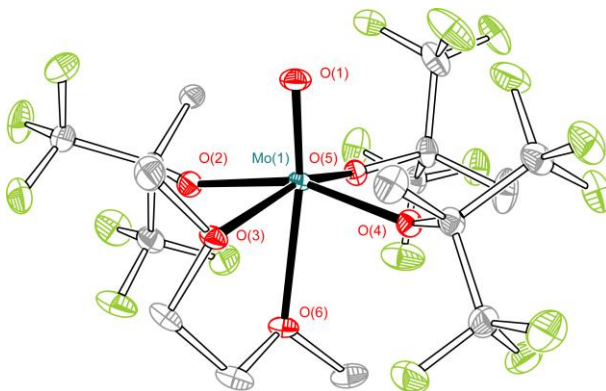


**Figure 4-8.** ORTEP representation of the X-ray crystal structure of **8**. Thermal ellipsoids are drawn at the 50% probability level. Color coding: C (gray), O (red), F (green), Mo (turquoise). Hydrogen atoms are omitted for clarity.
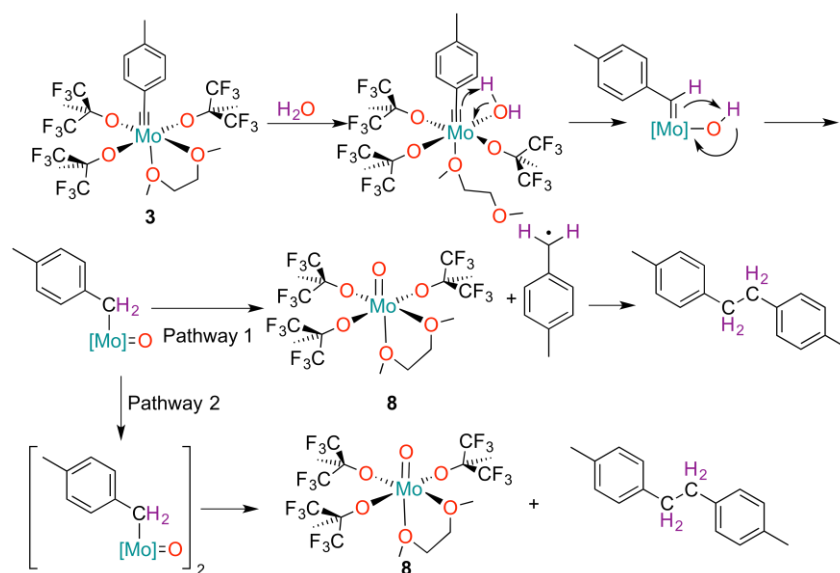
**Scheme 4-3.** Proposed mechanism for quenching of alkylidyne catalysts with water.

The reactivity that leads to the change in oxidation state is not unprecedented. Tungsten alkylidyne catalysts, for example, have been shown to form radical species upon reaction with water.[3] We studied the reaction of catalyst **3** with deuterated water in toluene. As expected, we observed *p*-xylene **4**, as well as dimerized products **9** and **10** by GCMS (Scheme 4-4). This suggests a mechanism similar to that proposed for the reaction with methanol, while the presence of **9** supports the mechanisms described in Scheme 4-3. Product **10** was confirmed by $^2$H NMR spectroscopy, as a peak at 2.61 ppm, and **11** by $^1$H NMR spectroscopy. We also observe less than 1% of aldehyde **11** in the reaction mixture.

In order to differentiate between the pathways 1 and 2 as described in Scheme 4-3, we performed the reaction in toluene-$d_8$. The C–H bond dissociation energy (BDE) of the $CH_3$ group in toluene is smaller (85.1 kcal/mol) than the O–H BDE in water (119.2 kcal/mol). If pathway 1 is predominant we would only observed dimers of toluene-$d_8$.[10] Indeed, we only detect product **13** by $^2$H NMR spectroscopy, and products **12** and **13** by GCMS. This observation supports the presence of a free radical intermediate in solution that can abstract a deuterium atom from the solvent. It is unclear whether product **4** and **14** are nondeuterated, as these were detected by GCMS. However, the presence of nondeuterated toluene and water, as shown in Scheme 4-4, may be the reason. The GCMS used in this investigation does not have the resolution to confirm full or partial deuteration. The ROAMP reactions carried out in toluene would lead to radical formation, dimerization of polymer chains, and side products. Therefore, is pertinent to find a way to control the termination of ROAMP.
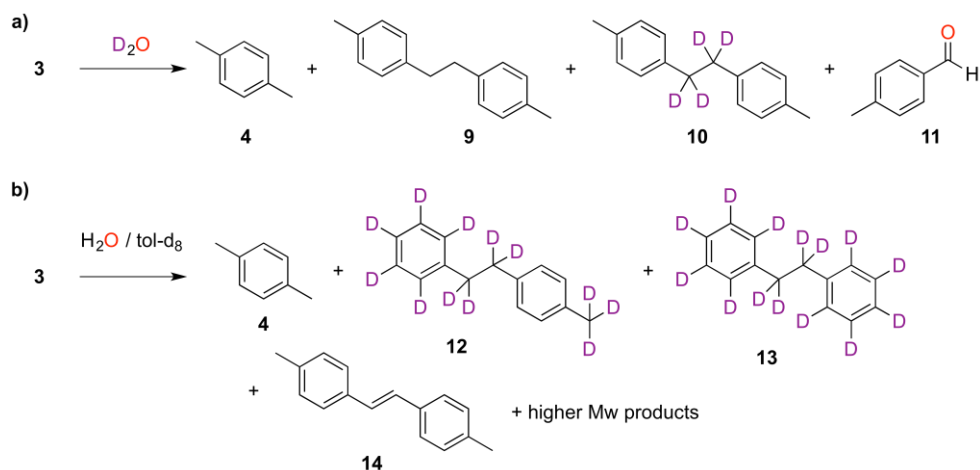
**Scheme 4-4.** Products observed when quenched with a) water-$d_2$ in toluene and b) water in toluene-$d_8$.

## 4.3 Controlled Terminations

### 4.3.1. Synthesis of Ynamines

As described earlier, we sought to develop functional terminating agents for ROAMP derived from ynamines. The ynamines were synthesized as described in the literature.[11-14] Ethynyl benzene was deprotonated with *n*-butyllithium followed by reaction of the terminal alkyne anion with with *N*-chlorosuccinimide to form **15** in 44% yield. Addition of lithium dimethylamide to **15** gave **16** in 20% yield. Synthesis of the terminal alkyne **21** was accomplished by Corey-Fuchs or Sonogoshira reactions. Chlorination of the terminal alkyne and formation of the ynamine **23** were achieved with 67% and 54% yield, respectively. Addition of lithium amides to iodo- and bromo-ethynyl arylenes did not result in the formation of the desired ynamines. The challenges pertaining to the synthesis of ynamines are the low yields, the reactivity of the final product with water, and the isolation of the ynamines.
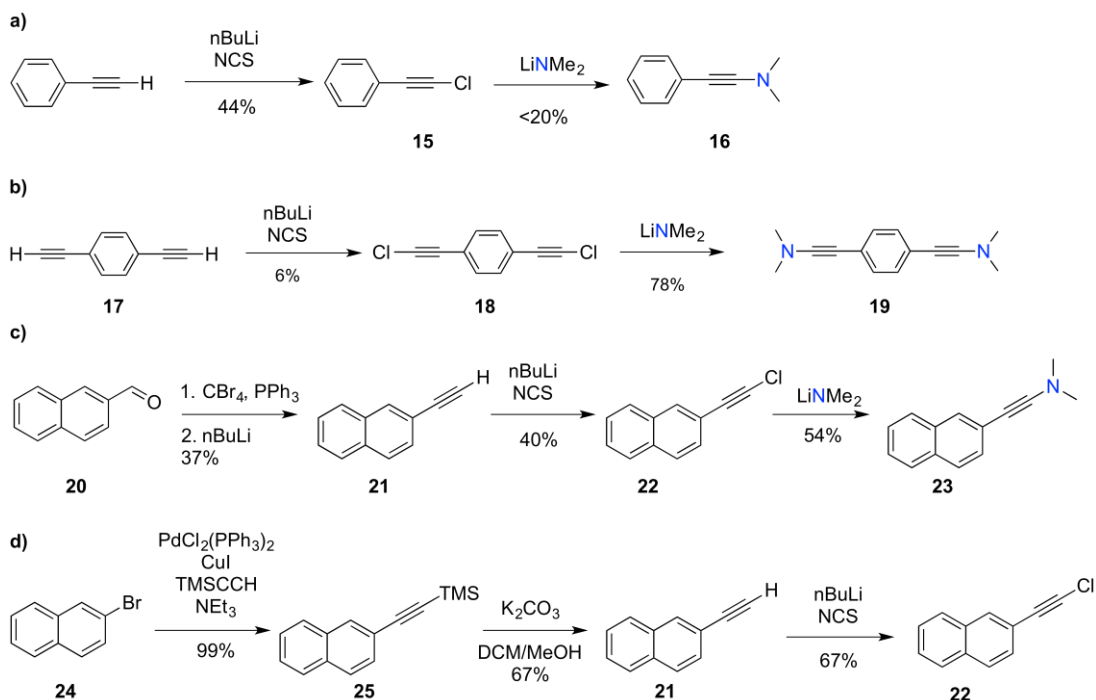
**Scheme 4-5.** Synthesis of the ynamines reported in this chapter.

### 4.3.2. Reactivity of Ynamines With ROAMP Catalysts 3 and 1

We tested the termination of catalyst **3** with ynamines as shown in Scheme 4-6. Upon addition of excess ynamine **19** to catalyst **3** in benzene-$d_6$, full termination of the catalyst was observed by $^1$H NMR spectroscopy and GCMS. Similarly, addition of ynamine **16** resulted in the desired product. The absence of tolane or 1,2-di-*p*-tolylethyne, which could emerge through cross metathesis reactions indicate that the resulting molybdenum complex is not an active alkyne metathesis catalyst. The absence of scrambled ynamines support a regioselective approach where the aryl ring of the ynamine is transferred to the polymer chain and the ethynamine is transferred to the molybdenum complex.
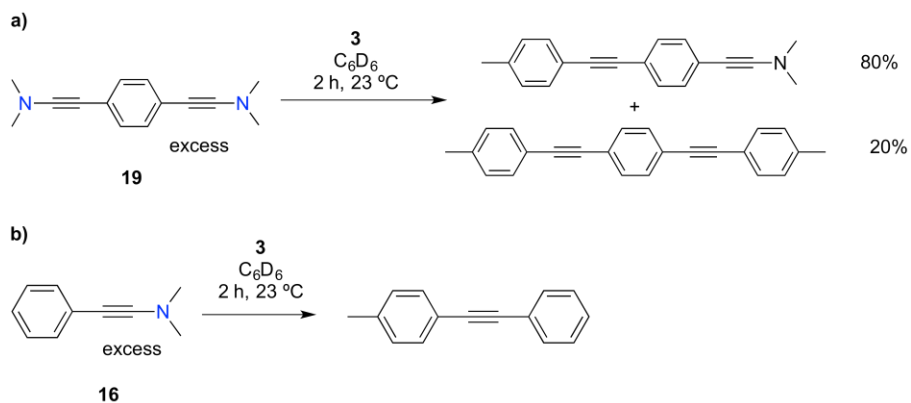


**Scheme 4-6.** Ynamine termination of catalyst **3**.

We attempted the termination of a growing polymer chain formed from **1** and monomer **26** as described in Chapter 3. Addition of **23** to the reaction mixture of **26** and catalyst **1** did not result in a broadening of the polymer molecular weight distribution. However, further analysis is required to confirm the full termination of the catalyst, such as X-ray crystallography of the terminated complex, MALDI of the polymers, and $^1$H and $^{13}$C NMR spectroscopies.
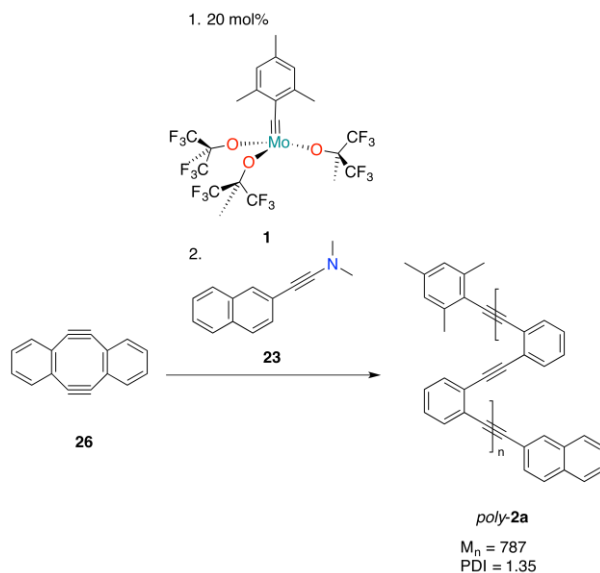


**Scheme 4-7.** Ynamine termination of initiated catalyst **1**.

The addition of a 100-fold excess of the ynamine **23** (labeled as TA in Figure 4-9) to the polymerization of **26** by **1** results in secondary polymers (Figure 4-9). We hypothesize that these polymers emerge from alkyne polymerization of the excess ynamine through a ring-expansion mechanism.
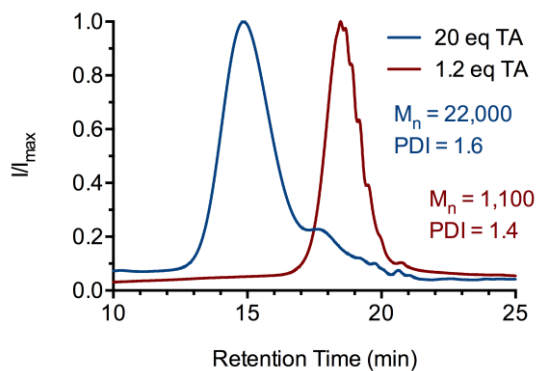


**Figure 4-9.** GPC trace of *poly*-**2a** terminated with ynamine **23**.

### 4.3.3. Reactivity of Ynamines With Living ROAMP Catalyst

In a last step we tested the termination of the **27** featuring the stabilizing ONO pincer complex described in chapter 2. Stoichiometric reaction of the uninitiated catalyst **27** with the ynamine **23** yields the expected product **28** in quantitative yield by $^1$H NMR spectroscopy (Scheme 4-8). Analogous to the reaction with catalysts **1** and **3**, the product is formed through a highly regioselective cross metathesis with **27**.
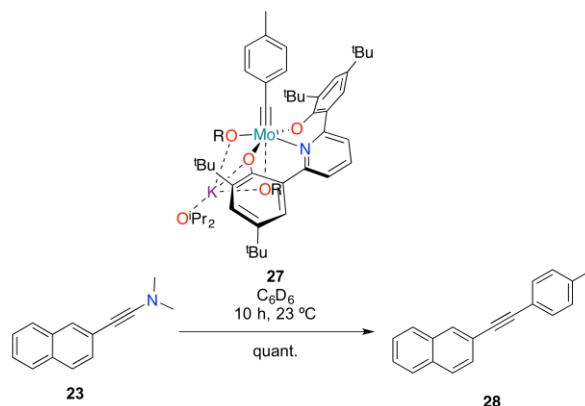


**Scheme 4-7.** Ynamine termination of uninititated catalyst **27**.

Key to a successful termination of living polymers is a highly reactive terminating agent that ensure the quantitative termination of the growing polymer chain attached to **27**. As reported in Chapter 2, the initiation reaction of **27** is significantly faster than the propagation. We tested the reaction of ynamine **23** with an initiated catalyst as shown in Scheme 4-8. The ratio of the reaction was 1:1:1 catalyst/monomer/terminating agent. As expected we obtained diyne **30**, as characterized by MALDI along with small quantities of **28** resulting from residual uninitiated catalyst. Finally, we found the decomposed complexes **31** and **32** by GCMS. These complexes correspond to the terminated catalysts once exposed to water. Ynamines decompose to form amides, and this reactivity is still present when attached to the complex.
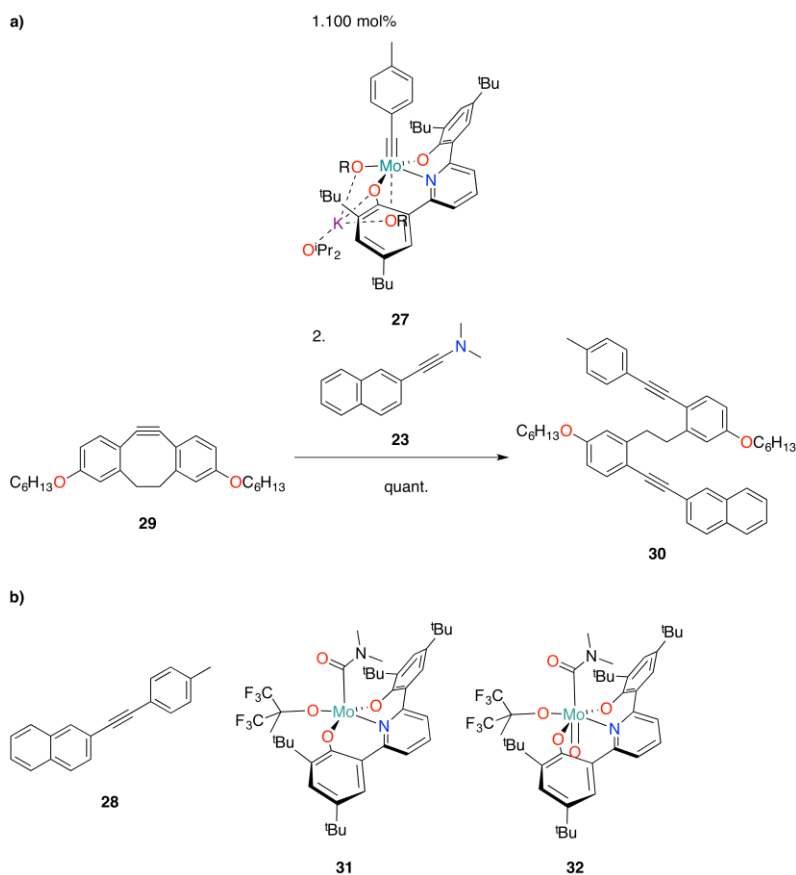
**Scheme 4-8.** Ynamine termination of inititiated ROAMP catalyst.

We tested the termination of a ROAMP of 10 equiv. of monomer **29** and catalyst **27**. Quantitative termination upon addition of **23** was confirmed by $^1$H NMR. Size exclusion GPC of the resulting polymer, *poly*-**29**, shows that low PDIs are maintained. Finally, proton NMR end group analysis of the resulting polymer confirms the identity of *poly*-**29** and shows the 1:10 ratio of naphthyl group to monomer, as expected from the loading (Figure 4-10).
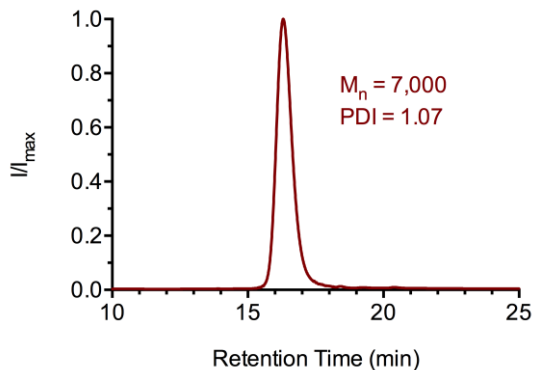


**Figure 4-9.** GPC trace of terminated *poly*-**29**.
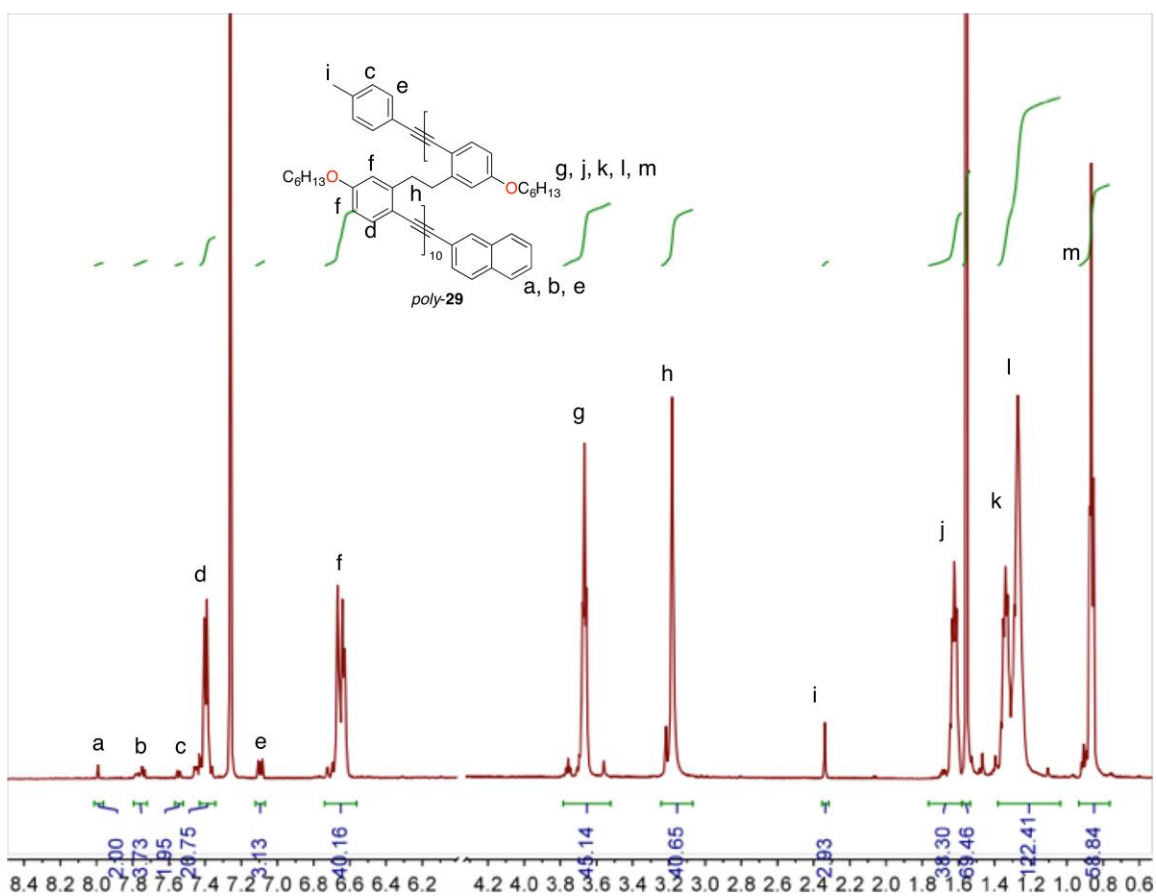
**Figure 4-10.** ^{1}H NMR of *poly*-**29** terminated by the ynamine **23**.

Crystals suitable for X-ray crystallography were obtained for the decomposed, terminated molybdenum complex. The structure of **33** features a metallacyclobutadiene which supports the hypothesis that a ring-expansion by ynamines may be possible. No electron density pertaining to a hydrogen was found bonded to the oxygen. The oxidation state of the catalyst is unknown. If the oxidation state at the metal center is Mo(VI), the Mo(1)−C(1) and Mo(1)−C(3) have a bond order of 1, as suggested by the bond lengths of 2.193 Å and 2.197 Å, respectively.[15] This indicates the presence of electrons delocalized in the metallacycle. The C(1)−C(2) and C(2)−C(3) bond lengths are 1.496 Å and 1.490 Å, which suggests a bond order of 1−1.5. The Mo(1)=O(3), Mo(1)−O(1), and Mo(1)−O(2) bond lengths are 1.694 Å, 1.998 Å, and 2.004 Å, respectively.
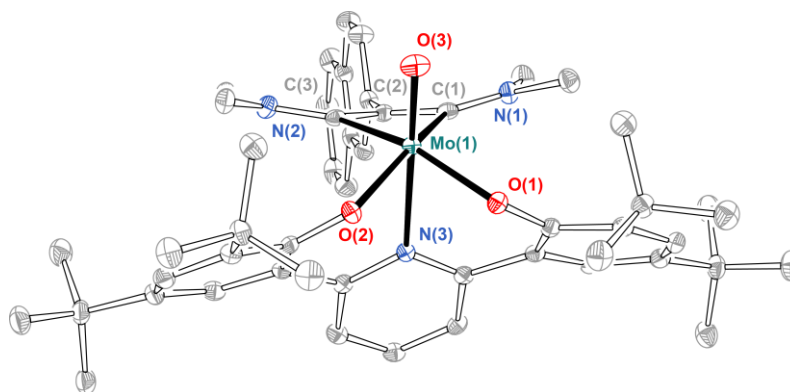
**Figure 4-11.** ORTEP representation of the X-ray crystal structure of **7**. Thermal ellipsoids are drawn at the 50% probability level. Color coding: C (gray), O (red), Mo (turquoise), N (blue). Hydrogen atoms are omitted for clarity.

## 4.4 Conclusion

We herein report the uncontrolled and controlled terminations of molybdenum ROAMP catalysts. The reliance of methanol for quenching is risky, and may lead to free carbynes, directly affecting the polydispersity of the reaction. Due to this current lack of control over the end group, and lack of polymers with terminal functionality, we studied a regioselective and quantitative method of terminating several ROAMP catalysts. Employing ynamines as the terminating agent has resulted in the desired products, and full termination of ROAMP catalysts. Control over the termination will allow the field to expand to applications in functional polymers, biomedical materials, amongst others.

## 4.5 Experimental

### 4.5.1. Synthetic Details

*Materials and General Methods.* Unless otherwise stated, all manipulations of air and/or moisture sensitive compounds were carried out in oven-dried glassware, under an atmosphere of Ar or $N_2$. All solvents and reagents were purchased from Alfa Aesar, Spectrum Chemicals, Acros Organics, TCI America, and Sigma-Aldrich and were used as received unless otherwise noted. Organic solvents were dried by passing through a column of alumina and were degassed by vigorous bubbling of $N_2$ or Ar through the solvent for 20 min. Flash column chromatography was performed on SiliCycle silica gel (particle size 40–63 μm). Thin layer chromatography was carried out using SiliCycle silica gel 60 Å F-254 precoated plates (0.25 mm thick) and visualized by UV absorption. All $^1H$ and $^2H$ NMR spectra were recorded on Bruker AV-600, DRX-500, and AV-500 spectrometers, and are referenced to residual solvent peaks (CDCl$_3$ $^1H$ NMR $\delta$ = 7.26 ppm, C$_6$D$_6$ $^1H$ NMR $\delta$ = 7.16 ppm, Tol-$d_8$ $^1H$ NMR $\delta$ = 2.08 ppm. MALDI mass spectrometry was performed on a Voyager-DE PRO (Applied Biosystems Voyager System 6322) in positive mode using a matrix of dithranol. Elemental analysis (CHN) was performed on a Perkin Elmer 2400 Series II combustion analyzer (values are given in %). Gel permeation chromatography (GPC) was carried out on a LC/MS Agilent 1260

Infinity set up with a guard and two Agilent Polypore 300 x 7.5 mm columns at 35 °C. All GPC analyses were performed on a 0.2 mg/mL solution of polymer in chloroform. An injection volume of 25 μL and a flow rate of 1 mL/min were used. Calibration was based on narrow polydispersity polystyrene standards ranging from $M_w$ = 100 to 4,068,981. X-ray crystallography was performed on APEX II QUAZAR, using a Microfocus Sealed Source (Incoatec IμS; Mo-Kα radiation), Kappa Geometry with DX (Bruker-AXS build) goniostat, a Bruker APEX II detector, QUAZAR multilayer mirrors as the radiation monochromator, and Oxford Cryostream 700 for **7**, **8**, and **33**. Crystallographic data was refined with SHELXL-97, solved with SIR-2007, visualized with ORTEP-32, and finalized with WinGX. UV-Vis absorption spectra were acquired in chloroform solution on a Varian Cary 50 spectrophotometer (Agilent, USA). Molecules **15**, **16**, **18**, **19**, **22**, **23**,[11-13, 17] and **21**, **25**[18] were synthesized following literature procedures.[12,13,17]

*(Chloroethynyl)benzene* (**15**) A 100 mL round bottom flask was charged with (ethynyl)benzene (2.86 g, 48.9 mmol) in dry THF (30 mL) and cooled to −78 °C. A solution of *n*-BuLi (12 mL, 2.5 M., 1.09 equiv.) was added dropwise over 5 min, followed by the addition of *N*-chlorosuccinimide (4.11 g, 53.5 mmol, 1.1 eq.). The reaction was stirred at this temperature for 1 h and slowly warmed up to room temperature. After 18 h, it was quenched with a saturated solution of $NH_4Cl$, extracted three times with $Et_2O$, and dried over $Na_2SO_4$. The crude was further purified in a Silica gel column using hexanes as the eluent yield **15** (1.68 g, 44%) as a clear oil. ^{1}H NMR (400 MHz, CDCl₃) $\delta$ = 7.47−7.57 (*m*, 2H), 7.40 (*m*, 3H).

*N,N-dimethyl-2-phenylethyn-1-amine* (**16**) A 35 mL vial was equipped with a stir bar and 5 mL $Et_2O$ solution of **15** (250 mg, 1.84 mmol, 1.1 equiv.) and cooled to −35 °C. A 2 mL suspension of LiNMe₂ (85 mg, 1.67 mmol) was rapidly added at −35 °C and kept at that temperature overnight. The reaction mixture was stirred at 22 °C for 2 h, and the solvent was removed. The solid was suspended in toluene, filtered through celite, and the filtrate was concentrated in vacuo to give **16** (51 mg, 20%) as a clear oil. ^{1}H NMR (600 MHz, CDCl₃) $\delta$ = 6.6-7.2 (*m*, 6H), 2.11 (*s*, 6H).

*N,N-dimethyl-2-(naphthalen-2-yl)ethyn-1-amine* (**23**) A 35 mL vial was equipped with a stir bar and 3 mL $Et_2O$ solution of **22** (159 mg, 849 mmol, 1 equiv.) and cooled to −35 °C. A 1 mL suspension of LiNMe₂ (43.4 mg, 849 mmol) was rapidly added at −35 °C and kept at that temperature overnight. The reaction mixture was stirred at 22 °C for 2 h, and the solvent was removed. The solid was suspended in toluene, filtered through celite, and the filtrate was concentrated in vacuo to give **23** (89 mg, 54%) as an orange oil. ^{1}H NMR (400 MHz, CDCl₃) $\delta$ = 7.98 (*s*, 1H), 7.81 (*s*, 1H), 7.18-7.68 (*m*, 5H), 2.53 (*s*, 6H).

### 4.5.2. Deuterium Labeling Experiments

A typical experiment consists of the following. To a solution of **3** (5 mg, 0.025 mmol) in Tol-$d_8$ or toluene (0.3 mL) in an N₂ glovebox was quenched with 0.2 mL of methanol-$d_4$, water, or D₂O. The mixture was immediately filtered through an alumina plug, and concentrated. The solids were diluted in acetone for GCMS, or in toluene for ^{2}H NMR.

## 4.6 References

(1)     Haberlag, B.; Freytag, M.; Daniliuc, C. G.; Jones, P. G.; Tamm, M. *Angew. Chem. Int. Ed.* **2012**, *51*, 1.

(2)     Jyothish, K.; Zhang, W. *Angew. Chem. Int. Ed.* **2011**, *50* (15), 3435.

(3)     Levy, O.; Musa, S.; Bino, A. *Dalton Trans.* **2013**, *42*, 12248.

(4)     Fürstner, A.; Mathes, C. *Org. Lett.* **2001**, *3* (2), 221.

(5)     Fürstner, A. *Angew. Chem. Int. Ed.* **2013**, *52* (10), 2794.

(6)     Kugelgen, von, S.; Bellone, D. E.; Cloke, R. R.; Perkins, W. S.; Fischer, F. R. *J. Am. Chem. Soc.* **2016**, *138* (19), 6234.

(7)     Madkour, A. E.; Koch, A. H. R.; Lienkamp, K.; Tew, G. N. *Macromolecules* **2010**, *43* (10), 4557.

(8)     Thompson, M. P.; Randolph, L. M.; James, C. R.; Davalos, A. N.; Hahn, M. E.; Gianneschi, N. C. *Polym Chem* **2014**, *5* (6), 1954.

(9)     Myers, S. B.; Register, R. A. *Macromolecules* **2008**, *41* (14), 5283.

(10)    Anslyn, E.; Dougherty, D. *Modern physical organic chemistry*; University Science Books: Sausalito, CA, 2006.

(11)    Collard-Motte, J.; Janousek, Z. *Top. Curr. Chem.* **2005**, *130*, 89.

(12)    Shi, D.; Liu, Z.; Zhang, Z.; Shi, W.; Chen, H. *ChemCatChem* **2015**, *7* (9), 1424.

(13)    Rezaei, H.; Normant, J. F.; *Synthesis* **2000**, *1*, 109.

(14)    Erver, F.; Hilt, G. *J. Org. Chem.* **2012**, *77* (11), 5215.

(15)    McCullough, L. G.; Schrock, R. R.; Dewan, J. C. *J. Am. Chem. Soc.* **1985**, *107* (21), 5993.

(16)    Mayer, J. M. *Inorg. Chem.* **1988**, *27*, 3899.

(17)    Sud, D.; Wigglesworth, T. J.; Branda, N. R. *Angew. Chem. Int. Ed.* **2007**, *46*, 8017

(18)    Benanti, T. L.; Saejueng, P.; Venkataraman, D. *Chem. Comm.* **2007**, 692.

# Supplemental Information
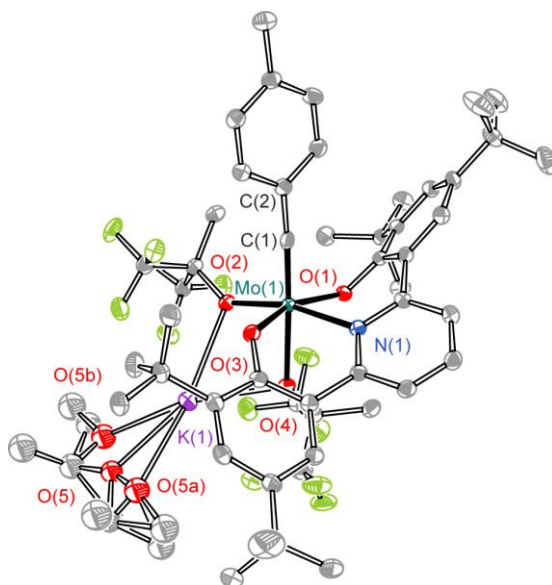


**Table S1.** Crystal data and structure refinement for **1**. ORTEP thermal ellipsoids are at the 50% probability level. Color coding: C (gray), O (red), F (green), N (blue), Mo (turquoise). Hydrogen atoms are omitted for clarity. Crystals obtained from slow evaporation of $^{i}Pr_2O$ contain disordered DME coordinated to the K ion. Disordered $^{i}Pr_2O$ and DME were refined isotropically.

| | |
|---|---|
| CCDC code | 998197 |
| Empirical formula | $C_{60.5}H_{83}F_{12}KMoNO_{6.25}$ |
| Formula weight | 1287.32 |
| Temperature | 100(2) K |
| Wavelength | 0.71073 Å |
| Crystal system | Monoclinic |
| Space group | P2(1)/n |
| Unit cell dimensions | $a$ = 12.751(5) Å          $\alpha$= 90.000(5)°. |
| | $b$ = 29.140(5) Å          $\beta$= 93.406(5)°. |
| | $c$ = 17.008(5) Å          $\gamma$= 90.000(5)°. |
| Volume | 6308(3) Å$^3$ |
| Z | 4 |
| Density (calculated) | 1.355 Mg/m$^3$ |
| Absorption coefficient | 0.358 mm$^{-1}$ |
| F(000) | 2688 |
| Crystal size | $0.08 \times 0.08 \times 0.01$ mm$^3$ |
| Theta range for data collection | 1.39 to 25.45°. |
| Index ranges | $-15 \leq h \leq 15, -35 \leq k \leq 35, -20 \leq l \leq 20$ |
| Reflections collected | 179115 |
| Independent reflections | 11663 [R(int) = 0.0688] |
| Completeness to theta = 25.00° | 100.0% |

| | |
|---|---|
| Absorption correction | Semi-empirical from equivalents |
| Max. and min. transmission | 0.9964 and 0.9720 |
| Refinement method | Full-matrix least-squares on $F^2$ |
| Data / restraints / parameters | 11663 / 0 / 748 |
| Goodness-of-fit on $F^2$ | 1.051 |
| Final R indices [I>2sigma(I)] | R1 = 0.0367, wR2 = 0.0818 |
| R indices (all data) | R1 = 0.0512, wR2 = 0.0885 |
| Largest diff. peak and hole | 0.615 and −0.439 e Å$^{-3}$ |

**Table S2.** Atomic coordinates ( $\times 10^4$) and equivalent isotropic displacement parameters ($\text{Å}^2 \times 10^3$) for **1**.  U(eq) is defined as one third of the trace of the orthogonalized $U^{ij}$ tensor.

|  | x | y | z | U(eq) |
|---|---|---|---|---|
| C(1) | −786(2) | 1324(1) | 4815(1) | 20(1) |
| C(2) | −1676(2) | 1039(1) | 4570(1) | 20(1) |
| C(3) | −1660(2) | 741(1) | 3922(1) | 24(1) |
| C(4) | −2514(2) | 466(1) | 3716(2) | 26(1) |
| C(5) | −3407(2) | 471(1) | 4143(1) | 22(1) |
| C(6) | −4307(2) | 154(1) | 3925(2) | 29(1) |
| C(7) | −3428(2) | 766(1) | 4783(1) | 24(1) |
| C(8) | −2581(2) | 1047(1) | 4995(1) | 24(1) |
| C(9) | 479(2) | 910(1) | 6507(1) | 23(1) |
| C(10) | 106(2) | 526(1) | 5948(2) | 26(1) |
| C(11) | −355(2) | 978(1) | 7109(2) | 26(1) |
| C(12) | 1528(2) | 771(1) | 6933(1) | 26(1) |
| C(13) | 2583(2) | 2234(1) | 5487(1) | 23(1) |
| C(14) | 2749(2) | 2300(1) | 4609(1) | 26(1) |
| C(15) | 3343(2) | 1860(1) | 5819(2) | 26(1) |
| C(16) | 2872(2) | 2691(1) | 5906(2) | 28(1) |
| C(17) | −633(2) | 2580(1) | 5711(1) | 20(1) |
| C(18) | −1111(2) | 2809(1) | 6337(1) | 22(1) |
| C(19) | −955(2) | 3278(1) | 6404(1) | 24(1) |
| C(20) | −371(2) | 3537(1) | 5887(1) | 24(1) |
| C(21) | −22(2) | 3311(1) | 5242(1) | 21(1) |
| C(22) | −188(2) | 2837(1) | 5121(1) | 19(1) |
| C(23) | −1796(2) | 2554(1) | 6908(2) | 27(1) |
| C(24) | −2683(2) | 2292(1) | 6442(2) | 37(1) |
| C(25) | −1132(2) | 2211(1) | 7400(2) | 35(1) |
| C(26) | −2315(2) | 2880(1) | 7474(2) | 30(1) |
| C(27) | −205(2) | 4053(1) | 6037(2) | 33(1) |
| C(28) | 333(3) | 4130(1) | 6858(2) | 48(1) |
| C(29) | −1270(3) | 4294(1) | 5990(2) | 59(1) |
| C(30) | 491(3) | 4269(1) | 5437(2) | 44(1) |
| C(31) | −33(2) | 2645(1) | 4328(1) | 17(1) |
| C(32) | −76(2) | 2952(1) | 3693(1) | 21(1) |
| C(33) | −30(2) | 2798(1) | 2937(1) | 23(1) |
| C(34) | 34(2) | 2333(1) | 2801(1) | 21(1) |
| C(35) | 74(2) | 2029(1) | 3435(1) | 17(1) |
| C(36) | 239(2) | 1539(1) | 3239(1) | 18(1) |
| C(37) | −187(2) | 1368(1) | 2522(1) | 19(1) |
| C(38) | 119(2) | 949(1) | 2229(1) | 20(1) |
| C(39) | 921(2) | 718(1) | 2660(1) | 20(1) |
| C(40) | 1381(2) | 870(1) | 3376(1) | 18(1) |

| | | | | |
|---|---|---|---|---|
| C(41) | 963(2) | 1275(1) | 3702(1) | 17(1) |
| C(42) | −361(2) | 771(1) | 1433(1) | 27(1) |
| C(43) | −1565(2) | 779(1) | 1438(2) | 52(1) |
| C(44) | −16(3) | 1086(1) | 783(2) | 47(1) |
| C(45) | −17(3) | 285(1) | 1250(2) | 42(1) |
| C(46) | 2364(2) | 632(1) | 3748(1) | 20(1) |
| C(47) | 3275(2) | 979(1) | 3745(2) | 25(1) |
| C(48) | 2211(2) | 479(1) | 4596(1) | 26(1) |
| C(49) | 2680(2) | 208(1) | 3286(2) | 26(1) |
| C(50) | 1845(3) | 2212(1) | 9291(2) | 44(1) |
| C(51) | 2201(4) | 1735(2) | 8998(3) | 44(1) |
| C(52) | 888(4) | 2136(2) | 9790(3) | 56(1) |
| C(53) | 1521(3) | 2963(1) | 8770(2) | 32(1) |
| C(54) | 2159(4) | 3200(2) | 8176(3) | 48(1) |
| C(55) | 406(4) | 3149(2) | 8696(3) | 59(1) |
| C(50A) | 1845(3) | 2212(1) | 9291(2) | 44(1) |
| C(51A) | 2199(10) | 1489(5) | 9215(8) | 55(4) |
| C(52A) | 2127(9) | 2741(4) | 8878(7) | 43(3) |
| C(53A) | 1356(10) | 3235(4) | 7912(8) | 53(3) |
| C(56) | 7183(2) | 982(1) | 8470(2) | 30(1) |
| C(57) | 7597(2) | 538(1) | 8833(2) | 37(1) |
| C(58) | 7520(2) | 1391(1) | 8961(2) | 41(1) |
| C(59) | 5556(2) | 718(1) | 7798(2) | 33(1) |
| C(60) | 4435(3) | 666(2) | 7999(2) | 64(1) |
| C(61) | 5671(3) | 937(1) | 6995(2) | 54(1) |
| N(1) | 53(1) | 2182(1) | 4194(1) | 17(1) |
| O(1) | 1280(1) | 1433(1) | 4421(1) | 17(1) |
| O(2) | 680(1) | 1332(1) | 6157(1) | 21(1) |
| O(3) | −681(1) | 2123(1) | 5658(1) | 21(1) |
| O(4) | 1579(1) | 2122(1) | 5659(1) | 20(1) |
| O(5) | 1538(2) | 2472(1) | 8609(2) | 32(1) |
| O(5A) | 1374(6) | 2777(3) | 8231(4) | 42(2) |
| O(5B) | 2171(6) | 1916(3) | 8782(5) | 42(2) |
| O(6) | 6055(1) | 991(1) | 8412(1) | 31(1) |
| F(1) | −1238(1) | 1148(1) | 6761(1) | 31(1) |
| F(2) | −615(1) | 586(1) | 7465(1) | 35(1) |
| F(3) | −48(1) | 1272(1) | 7692(1) | 32(1) |
| F(4) | 2247(1) | 671(1) | 6424(1) | 30(1) |
| F(5) | 1442(1) | 400(1) | 7400(1) | 34(1) |
| F(6) | 1940(1) | 1105(1) | 7404(1) | 32(1) |
| F(7) | 3253(1) | 1788(1) | 6601(1) | 34(1) |
| F(8) | 3148(1) | 1457(1) | 5477(1) | 35(1) |
| F(9) | 4364(1) | 1950(1) | 5743(1) | 39(1) |
| F(10) | 2763(1) | 2673(1) | 6692(1) | 38(1) |
| F(11) | 2255(1) | 3032(1) | 5637(1) | 40(1) |
| F(12) | 3867(1) | 2825(1) | 5829(1) | 40(1) |

| | | | | |
|---|---|---|---|---|
| K(1) | 1323(1) | 2047(1) | 7181(1) | 31(1) |
| Mo(1) | 267(1) | 1673(1) | 5164(1) | 16(1) |

**Table S3.** Bond lengths [Å] and angles [°] for **1**.

| | |
|---|---|
| C(1)–C(2) | 1.447(3) |
| C(1)–Mo(1) | 1.760(2) |
| C(2)–C(8) | 1.399(3) |
| C(2)–C(3) | 1.405(3) |
| C(3)–C(4) | 1.380(3) |
| C(3)–H(3) | 0.9500 |
| C(4)–C(5) | 1.386(4) |
| C(4)–H(4) | 0.9500 |
| C(5)–C(7) | 1.388(3) |
| C(5)–C(6) | 1.504(3) |
| C(6)–H(6A) | 0.9800 |
| C(6)–H(6B) | 0.9800 |
| C(6)–H(6C) | 0.9800 |
| C(7)–C(8) | 1.386(3) |
| C(7)–H(7) | 0.9500 |
| C(8)–H(8) | 0.9500 |
| C(9)–O(2) | 1.398(3) |
| C(9)–C(10) | 1.526(3) |
| C(9)–C(11) | 1.532(4) |
| C(9)–C(12) | 1.537(4) |
| C(10)–H(10A) | 0.9800 |
| C(10)–H(10B) | 0.9800 |
| C(10)–H(10C) | 0.9800 |
| C(11)–F(1) | 1.336(3) |
| C(11)–F(2) | 1.342(3) |
| C(11)–F(3) | 1.350(3) |
| C(12)–F(4) | 1.331(3) |
| C(12)–F(6) | 1.348(3) |
| C(12)–F(5) | 1.348(3) |
| C(13)–O(4) | 1.369(3) |
| C(13)–C(14) | 1.532(3) |
| C(13)–C(16) | 1.545(3) |
| C(13)–C(15) | 1.545(4) |
| C(13)–K(1) | 3.426(3) |
| C(14)–H(14A) | 0.9800 |
| C(14)–H(14B) | 0.9800 |
| C(14)–H(14C) | 0.9800 |
| C(15)–F(8) | 1.326(3) |
| C(15)–F(9) | 1.341(3) |
| C(15)–F(7) | 1.358(3) |
| C(16)–F(11) | 1.330(3) |
| C(16)–F(12) | 1.342(3) |
| C(16)–F(10) | 1.352(3) |
| C(17)–O(3) | 1.335(3) |

| | |
|---|---|
| C(17)–C(22) | 1.399(3) |
| C(17)–C(18) | 1.424(3) |
| C(18)–C(19) | 1.385(3) |
| C(18)–C(23) | 1.537(3) |
| C(19)–C(20) | 1.405(3) |
| C(19)–H(19) | 0.9500 |
| C(20)–C(21) | 1.376(3) |
| C(20)–C(27) | 1.536(3) |
| C(21)–C(22) | 1.411(3) |
| C(21)–H(21) | 0.9500 |
| C(22)–C(31) | 1.484(3) |
| C(23)–C(25) | 1.526(4) |
| C(23)–C(26) | 1.532(3) |
| C(23)–C(24) | 1.543(4) |
| C(24)–H(24A) | 0.9800 |
| C(24)–H(24B) | 0.9800 |
| C(24)–H(24C) | 0.9800 |
| C(25)–H(25A) | 0.9800 |
| C(25)–H(25B) | 0.9800 |
| C(25)–H(25C) | 0.9800 |
| C(26)–H(26A) | 0.9800 |
| C(26)–H(26B) | 0.9800 |
| C(26)–H(26C) | 0.9800 |
| C(27)–C(29) | 1.526(4) |
| C(27)–C(30) | 1.528(4) |
| C(27)–C(28) | 1.535(4) |
| C(28)–H(28A) | 0.9800 |
| C(28)–H(28B) | 0.9800 |
| C(28)–H(28C) | 0.9800 |
| C(29)–H(29A) | 0.9800 |
| C(29)–H(29B) | 0.9800 |
| C(29)–H(29C) | 0.9800 |
| C(30)–H(30A) | 0.9800 |
| C(30)–H(30B) | 0.9800 |
| C(30)–H(30C) | 0.9800 |
| C(31)–N(1) | 1.374(3) |
| C(31)–C(32) | 1.401(3) |
| C(32)–C(33) | 1.367(3) |
| C(32)–H(32) | 0.9500 |
| C(33)–C(34) | 1.378(3) |
| C(33)–H(33) | 0.9500 |
| C(34)–C(35) | 1.393(3) |
| C(34)–H(34) | 0.9500 |
| C(35)–N(1) | 1.368(3) |
| C(35)–C(36) | 1.486(3) |
| C(36)–C(37) | 1.395(3) |

| | |
|---|---|
| C(36)–C(41) | 1.406(3) |
| C(37)–C(38) | 1.386(3) |
| C(37)–H(37) | 0.9500 |
| C(38)–C(39) | 1.396(3) |
| C(38)–C(42) | 1.541(3) |
| C(39)–C(40) | 1.393(3) |
| C(39)–H(39) | 0.9500 |
| C(40)–C(41) | 1.419(3) |
| C(40)–C(46) | 1.535(3) |
| C(41)–O(1) | 1.347(3) |
| C(42)–C(45) | 1.520(4) |
| C(42)–C(44) | 1.523(4) |
| C(42)–C(43) | 1.536(4) |
| C(43)–H(43A) | 0.9800 |
| C(43)–H(43B) | 0.9800 |
| C(43)–H(43C) | 0.9800 |
| C(44)–H(44A) | 0.9800 |
| C(44)–H(44B) | 0.9800 |
| C(44)–H(44C) | 0.9800 |
| C(45)–H(45A) | 0.9800 |
| C(45)–H(45B) | 0.9800 |
| C(45)–H(45C) | 0.9800 |
| C(46)–C(49) | 1.531(3) |
| C(46)–C(48) | 1.533(3) |
| C(46)–C(47) | 1.540(3) |
| C(47)–H(47A) | 0.9800 |
| C(47)–H(47B) | 0.9800 |
| C(47)–H(47C) | 0.9800 |
| C(48)–H(48A) | 0.9800 |
| C(48)–H(48B) | 0.9800 |
| C(48)–H(48C) | 0.9800 |
| C(49)–H(49A) | 0.9800 |
| C(49)–H(49B) | 0.9800 |
| C(49)–H(49C) | 0.9800 |
| C(50)–O(5) | 1.421(4) |
| C(50)–C(52) | 1.544(6) |
| C(50)–C(51) | 1.554(6) |
| C(50)–H(50) | 1.0000 |
| C(51)–H(51A) | 0.9800 |
| C(51)–H(51B) | 0.9800 |
| C(51)–H(51C) | 0.9800 |
| C(52)–H(52A) | 0.9800 |
| C(52)–H(52B) | 0.9800 |
| C(52)–H(52C) | 0.9800 |
| C(53)–O(5) | 1.457(5) |
| C(53)–C(54) | 1.502(6) |

| | |
|---|---|
| C(53)–C(55) | 1.520(6) |
| C(53)–H(53) | 1.0000 |
| C(54)–H(54A) | 0.9800 |
| C(54)–H(54B) | 0.9800 |
| C(54)–H(54C) | 0.9800 |
| C(55)–H(55A) | 0.9800 |
| C(55)–H(55B) | 0.9800 |
| C(55)–H(55C) | 0.9800 |
| C(51A)–O(5B) | 1.447(15) |
| C(51A)–H(51D) | 0.9800 |
| C(51A)–H(51E) | 0.9800 |
| C(51A)–H(51F) | 0.9800 |
| C(52A)–O(5A) | 1.420(14) |
| C(52A)–H(52D) | 0.9900 |
| C(52A)–H(52E) | 0.9900 |
| C(53A)–O(5A) | 1.443(14) |
| C(53A)–H(53A) | 0.9800 |
| C(53A)–H(53B) | 0.9800 |
| C(53A)–H(53C) | 0.9800 |
| C(56)–O(6) | 1.437(3) |
| C(56)–C(58) | 1.505(4) |
| C(56)–C(57) | 1.515(4) |
| C(56)–H(56) | 1.0000 |
| C(57)–H(57A) | 0.9800 |
| C(57)–H(57B) | 0.9800 |
| C(57)–H(57C) | 0.9800 |
| C(58)–H(58A) | 0.9800 |
| C(58)–H(58B) | 0.9800 |
| C(58)–H(58C) | 0.9800 |
| C(59)–O(6) | 1.432(3) |
| C(59)–C(60) | 1.498(4) |
| C(59)–C(61) | 1.520(4) |
| C(59)–H(59) | 1.0000 |
| C(60)–H(60A) | 0.9800 |
| C(60)–H(60B) | 0.9800 |
| C(60)–H(60C) | 0.9800 |
| C(61)–H(61A) | 0.9800 |
| C(61)–H(61B) | 0.9800 |
| C(61)–H(61C) | 0.9800 |
| N(1)–Mo(1) | 2.2227(19) |
| O(1)–Mo(1) | 1.9876(16) |
| O(2)–Mo(1) | 2.0038(16) |
| O(2)–K(1) | 2.8068(17) |
| O(3)–Mo(1) | 2.0010(16) |
| O(4)–Mo(1) | 2.2475(16) |
| O(4)–K(1) | 2.6375(18) |

| | |
|---|---|
| O(5)–K(1) | 2.725(3) |
| O(5A)–K(1) | 2.773(8) |
| O(5B)–K(1) | 2.894(9) |
| F(3)–K(1) | 3.0166(17) |
| F(6)–K(1) | 2.8753(16) |
| F(7)–K(1) | 2.8097(19) |
| F(10)–K(1) | 2.7509(18) |
| K(1)–Mo(1) | 3.7715(11) |
| | |
| C(2)–C(1)–Mo(1) | 176.91(19) |
| C(8)–C(2)–C(3) | 117.8(2) |
| C(8)–C(2)–C(1) | 119.9(2) |
| C(3)–C(2)–C(1) | 122.3(2) |
| C(4)–C(3)–C(2) | 120.7(2) |
| C(4)–C(3)–H(3) | 119.7 |
| C(2)–C(3)–H(3) | 119.7 |
| C(3)–C(4)–C(5) | 121.4(2) |
| C(3)–C(4)–H(4) | 119.3 |
| C(5)–C(4)–H(4) | 119.3 |
| C(4)–C(5)–C(7) | 118.2(2) |
| C(4)–C(5)–C(6) | 120.2(2) |
| C(7)–C(5)–C(6) | 121.6(2) |
| C(5)–C(6)–H(6A) | 109.5 |
| C(5)–C(6)–H(6B) | 109.5 |
| H(6A)–C(6)–H(6B) | 109.5 |
| C(5)–C(6)–H(6C) | 109.5 |
| H(6A)–C(6)–H(6C) | 109.5 |
| H(6B)–C(6)–H(6C) | 109.5 |
| C(8)–C(7)–C(5) | 121.3(2) |
| C(8)–C(7)–H(7) | 119.4 |
| C(5)–C(7)–H(7) | 119.4 |
| C(7)–C(8)–C(2) | 120.6(2) |
| C(7)–C(8)–H(8) | 119.7 |
| C(2)–C(8)–H(8) | 119.7 |
| O(2)–C(9)–C(10) | 116.0(2) |
| O(2)–C(9)–C(11) | 108.77(19) |
| C(10)–C(9)–C(11) | 108.0(2) |
| O(2)–C(9)–C(12) | 104.86(19) |
| C(10)–C(9)–C(12) | 109.3(2) |
| C(11)–C(9)–C(12) | 109.8(2) |
| C(9)–C(10)–H(10A) | 109.5 |
| C(9)–C(10)–H(10B) | 109.5 |
| H(10A)–C(10)–H(10B) | 109.5 |
| C(9)–C(10)–H(10C) | 109.5 |
| H(10A)–C(10)–H(10C) | 109.5 |
| H(10B)–C(10)–H(10C) | 109.5 |

| | |
|---|---|
| F(1)–C(11)–F(2) | 106.9(2) |
| F(1)–C(11)–F(3) | 106.9(2) |
| F(2)–C(11)–F(3) | 106.02(19) |
| F(1)–C(11)–C(9) | 110.6(2) |
| F(2)–C(11)–C(9) | 113.0(2) |
| F(3)–C(11)–C(9) | 113.0(2) |
| F(4)–C(12)–F(6) | 106.5(2) |
| F(4)–C(12)–F(5) | 107.0(2) |
| F(6)–C(12)–F(5) | 105.78(19) |
| F(4)–C(12)–C(9) | 111.4(2) |
| F(6)–C(12)–C(9) | 112.8(2) |
| F(5)–C(12)–C(9) | 112.9(2) |
| O(4)–C(13)–C(14) | 115.1(2) |
| O(4)–C(13)–C(16) | 107.9(2) |
| C(14)–C(13)–C(16) | 107.4(2) |
| O(4)–C(13)–C(15) | 109.08(19) |
| C(14)–C(13)–C(15) | 109.0(2) |
| C(16)–C(13)–C(15) | 108.2(2) |
| O(4)–C(13)–K(1) | 44.81(10) |
| C(14)–C(13)–K(1) | 159.83(16) |
| C(16)–C(13)–K(1) | 81.91(14) |
| C(15)–C(13)–K(1) | 84.00(14) |
| C(13)–C(14)–H(14A) | 109.5 |
| C(13)–C(14)–H(14B) | 109.5 |
| H(14A)–C(14)–H(14B) | 109.5 |
| C(13)–C(14)–H(14C) | 109.5 |
| H(14A)–C(14)–H(14C) | 109.5 |
| H(14B)–C(14)–H(14C) | 109.5 |
| F(8)–C(15)–F(9) | 106.8(2) |
| F(8)–C(15)–F(7) | 105.6(2) |
| F(9)–C(15)–F(7) | 105.23(19) |
| F(8)–C(15)–C(13) | 111.6(2) |
| F(9)–C(15)–C(13) | 114.7(2) |
| F(7)–C(15)–C(13) | 112.3(2) |
| F(11)–C(16)–F(12) | 106.9(2) |
| F(11)–C(16)–F(10) | 106.1(2) |
| F(12)–C(16)–F(10) | 105.2(2) |
| F(11)–C(16)–C(13) | 111.3(2) |
| F(12)–C(16)–C(13) | 114.0(2) |
| F(10)–C(16)–C(13) | 112.7(2) |
| O(3)–C(17)–C(22) | 120.3(2) |
| O(3)–C(17)–C(18) | 119.9(2) |
| C(22)–C(17)–C(18) | 119.6(2) |
| C(19)–C(18)–C(17) | 117.3(2) |
| C(19)–C(18)–C(23) | 120.7(2) |
| C(17)–C(18)–C(23) | 121.9(2) |

| | |
|---|---|
| C(18)–C(19)–C(20) | 123.9(2) |
| C(18)–C(19)–H(19) | 118.0 |
| C(20)–C(19)–H(19) | 118.0 |
| C(21)–C(20)–C(19) | 116.7(2) |
| C(21)–C(20)–C(27) | 123.6(2) |
| C(19)–C(20)–C(27) | 119.6(2) |
| C(20)–C(21)–C(22) | 122.2(2) |
| C(20)–C(21)–H(21) | 118.9 |
| C(22)–C(21)–H(21) | 118.9 |
| C(17)–C(22)–C(21) | 118.9(2) |
| C(17)–C(22)–C(31) | 122.1(2) |
| C(21)–C(22)–C(31) | 118.3(2) |
| C(25)–C(23)–C(26) | 107.9(2) |
| C(25)–C(23)–C(18) | 110.2(2) |
| C(26)–C(23)–C(18) | 112.3(2) |
| C(25)–C(23)–C(24) | 109.0(2) |
| C(26)–C(23)–C(24) | 107.3(2) |
| C(18)–C(23)–C(24) | 110.0(2) |
| C(23)–C(24)–H(24A) | 109.5 |
| C(23)–C(24)–H(24B) | 109.5 |
| H(24A)–C(24)–H(24B) | 109.5 |
| C(23)–C(24)–H(24C) | 109.5 |
| H(24A)–C(24)–H(24C) | 109.5 |
| H(24B)–C(24)–H(24C) | 109.5 |
| C(23)–C(25)–H(25A) | 109.5 |
| C(23)–C(25)–H(25B) | 109.5 |
| H(25A)–C(25)–H(25B) | 109.5 |
| C(23)–C(25)–H(25C) | 109.5 |
| H(25A)–C(25)–H(25C) | 109.5 |
| H(25B)–C(25)–H(25C) | 109.5 |
| C(23)–C(26)–H(26A) | 109.5 |
| C(23)–C(26)–H(26B) | 109.5 |
| H(26A)–C(26)–H(26B) | 109.5 |
| C(23)–C(26)–H(26C) | 109.5 |
| H(26A)–C(26)–H(26C) | 109.5 |
| H(26B)–C(26)–H(26C) | 109.5 |
| C(29)–C(27)–C(30) | 109.0(3) |
| C(29)–C(27)–C(28) | 109.2(3) |
| C(30)–C(27)–C(28) | 107.5(2) |
| C(29)–C(27)–C(20) | 109.2(2) |
| C(30)–C(27)–C(20) | 111.9(2) |
| C(28)–C(27)–C(20) | 110.1(2) |
| C(27)–C(28)–H(28A) | 109.5 |
| C(27)–C(28)–H(28B) | 109.5 |
| H(28A)–C(28)–H(28B) | 109.5 |
| C(27)–C(28)–H(28C) | 109.5 |

| | |
|---|---|
| H(28A)–C(28)–H(28C) | 109.5 |
| H(28B)–C(28)–H(28C) | 109.5 |
| C(27)–C(29)–H(29A) | 109.5 |
| C(27)–C(29)–H(29B) | 109.5 |
| H(29A)–C(29)–H(29B) | 109.5 |
| C(27)–C(29)–H(29C) | 109.5 |
| H(29A)–C(29)–H(29C) | 109.5 |
| H(29B)–C(29)–H(29C) | 109.5 |
| C(27)–C(30)–H(30A) | 109.5 |
| C(27)–C(30)–H(30B) | 109.5 |
| H(30A)–C(30)–H(30B) | 109.5 |
| C(27)–C(30)–H(30C) | 109.5 |
| H(30A)–C(30)–H(30C) | 109.5 |
| H(30B)–C(30)–H(30C) | 109.5 |
| N(1)–C(31)–C(32) | 119.9(2) |
| N(1)–C(31)–C(22) | 122.4(2) |
| C(32)–C(31)–C(22) | 117.4(2) |
| C(33)–C(32)–C(31) | 120.9(2) |
| C(33)–C(32)–H(32) | 119.6 |
| C(31)–C(32)–H(32) | 119.6 |
| C(32)–C(33)–C(34) | 119.2(2) |
| C(32)–C(33)–H(33) | 120.4 |
| C(34)–C(33)–H(33) | 120.4 |
| C(33)–C(34)–C(35) | 119.6(2) |
| C(33)–C(34)–H(34) | 120.2 |
| C(35)–C(34)–H(34) | 120.2 |
| N(1)–C(35)–C(34) | 121.5(2) |
| N(1)–C(35)–C(36) | 122.4(2) |
| C(34)–C(35)–C(36) | 115.9(2) |
| C(37)–C(36)–C(41) | 120.2(2) |
| C(37)–C(36)–C(35) | 119.0(2) |
| C(41)–C(36)–C(35) | 119.9(2) |
| C(38)–C(37)–C(36) | 121.7(2) |
| C(38)–C(37)–H(37) | 119.2 |
| C(36)–C(37)–H(37) | 119.2 |
| C(37)–C(38)–C(39) | 116.7(2) |
| C(37)–C(38)–C(42) | 120.5(2) |
| C(39)–C(38)–C(42) | 122.7(2) |
| C(40)–C(39)–C(38) | 124.2(2) |
| C(40)–C(39)–H(39) | 117.9 |
| C(38)–C(39)–H(39) | 117.9 |
| C(39)–C(40)–C(41) | 117.3(2) |
| C(39)–C(40)–C(46) | 120.4(2) |
| C(41)–C(40)–C(46) | 122.1(2) |
| O(1)–C(41)–C(36) | 118.2(2) |
| O(1)–C(41)–C(40) | 122.6(2) |

| | |
|---|---|
| C(36)–C(41)–C(40) | 119.0(2) |
| C(45)–C(42)–C(44) | 108.2(2) |
| C(45)–C(42)–C(43) | 108.4(2) |
| C(44)–C(42)–C(43) | 109.1(3) |
| C(45)–C(42)–C(38) | 112.8(2) |
| C(44)–C(42)–C(38) | 108.6(2) |
| C(43)–C(42)–C(38) | 109.6(2) |
| C(42)–C(43)–H(43A) | 109.5 |
| C(42)–C(43)–H(43B) | 109.5 |
| H(43A)–C(43)–H(43B) | 109.5 |
| C(42)–C(43)–H(43C) | 109.5 |
| H(43A)–C(43)–H(43C) | 109.5 |
| H(43B)–C(43)–H(43C) | 109.5 |
| C(42)–C(44)–H(44A) | 109.5 |
| C(42)–C(44)–H(44B) | 109.5 |
| H(44A)–C(44)–H(44B) | 109.5 |
| C(42)–C(44)–H(44C) | 109.5 |
| H(44A)–C(44)–H(44C) | 109.5 |
| H(44B)–C(44)–H(44C) | 109.5 |
| C(42)–C(45)–H(45A) | 109.5 |
| C(42)–C(45)–H(45B) | 109.5 |
| H(45A)–C(45)–H(45B) | 109.5 |
| C(42)–C(45)–H(45C) | 109.5 |
| H(45A)–C(45)–H(45C) | 109.5 |
| H(45B)–C(45)–H(45C) | 109.5 |
| C(49)–C(46)–C(48) | 107.4(2) |
| C(49)–C(46)–C(40) | 112.79(19) |
| C(48)–C(46)–C(40) | 111.86(19) |
| C(49)–C(46)–C(47) | 107.8(2) |
| C(48)–C(46)–C(47) | 109.4(2) |
| C(40)–C(46)–C(47) | 107.52(19) |
| C(46)–C(47)–H(47A) | 109.5 |
| C(46)–C(47)–H(47B) | 109.5 |
| H(47A)–C(47)–H(47B) | 109.5 |
| C(46)–C(47)–H(47C) | 109.5 |
| H(47A)–C(47)–H(47C) | 109.5 |
| H(47B)–C(47)–H(47C) | 109.5 |
| C(46)–C(48)–H(48A) | 109.5 |
| C(46)–C(48)–H(48B) | 109.5 |
| H(48A)–C(48)–H(48B) | 109.5 |
| C(46)–C(48)–H(48C) | 109.5 |
| H(48A)–C(48)–H(48C) | 109.5 |
| H(48B)–C(48)–H(48C) | 109.5 |
| C(46)–C(49)–H(49A) | 109.5 |
| C(46)–C(49)–H(49B) | 109.5 |
| H(49A)–C(49)–H(49B) | 109.5 |

| | |
|---|---|
| C(46)–C(49)–H(49C) | 109.5 |
| H(49A)–C(49)–H(49C) | 109.5 |
| H(49B)–C(49)–H(49C) | 109.5 |
| O(5)–C(50)–C(52) | 109.7(3) |
| O(5)–C(50)–C(51) | 106.7(3) |
| C(52)–C(50)–C(51) | 107.6(3) |
| O(5)–C(50)–H(50) | 110.9 |
| C(52)–C(50)–H(50) | 110.9 |
| C(51)–C(50)–H(50) | 110.9 |
| O(5)–C(53)–C(54) | 108.0(3) |
| O(5)–C(53)–C(55) | 111.1(3) |
| C(54)–C(53)–C(55) | 108.8(4) |
| O(5)–C(53)–H(53) | 109.6 |
| C(54)–C(53)–H(53) | 109.6 |
| C(55)–C(53)–H(53) | 109.6 |
| O(5B)–C(51A)–H(51D) | 109.5 |
| O(5B)–C(51A)–H(51E) | 109.5 |
| H(51D)–C(51A)–H(51E) | 109.5 |
| O(5B)–C(51A)–H(51F) | 109.5 |
| H(51D)–C(51A)–H(51F) | 109.5 |
| H(51E)–C(51A)–H(51F) | 109.5 |
| O(5A)–C(52A)–H(52D) | 111.1 |
| O(5A)–C(52A)–H(52E) | 111.1 |
| H(52D)–C(52A)–H(52E) | 109.0 |
| O(5A)–C(53A)–H(53A) | 109.5 |
| O(5A)–C(53A)–H(53B) | 109.5 |
| H(53A)–C(53A)–H(53B) | 109.5 |
| O(5A)–C(53A)–H(53C) | 109.5 |
| H(53A)–C(53A)–H(53C) | 109.5 |
| H(53B)–C(53A)–H(53C) | 109.5 |
| O(6)–C(56)–C(58) | 105.9(2) |
| O(6)–C(56)–C(57) | 111.5(2) |
| C(58)–C(56)–C(57) | 111.7(2) |
| O(6)–C(56)–H(56) | 109.2 |
| C(58)–C(56)–H(56) | 109.2 |
| C(57)–C(56)–H(56) | 109.2 |
| C(56)–C(57)–H(57A) | 109.5 |
| C(56)–C(57)–H(57B) | 109.5 |
| H(57A)–C(57)–H(57B) | 109.5 |
| C(56)–C(57)–H(57C) | 109.5 |
| H(57A)–C(57)–H(57C) | 109.5 |
| H(57B)–C(57)–H(57C) | 109.5 |
| C(56)–C(58)–H(58A) | 109.5 |
| C(56)–C(58)–H(58B) | 109.5 |
| H(58A)–C(58)–H(58B) | 109.5 |
| C(56)–C(58)–H(58C) | 109.5 |

| | |
|---|---|
| H(58A)–C(58)–H(58C) | 109.5 |
| H(58B)–C(58)–H(58C) | 109.5 |
| O(6)–C(59)–C(60) | 106.1(2) |
| O(6)–C(59)–C(61) | 111.2(2) |
| C(60)–C(59)–C(61) | 113.1(3) |
| O(6)–C(59)–H(59) | 108.8 |
| C(60)–C(59)–H(59) | 108.8 |
| C(61)–C(59)–H(59) | 108.8 |
| C(59)–C(60)–H(60A) | 109.5 |
| C(59)–C(60)–H(60B) | 109.5 |
| H(60A)–C(60)–H(60B) | 109.5 |
| C(59)–C(60)–H(60C) | 109.5 |
| H(60A)–C(60)–H(60C) | 109.5 |
| H(60B)–C(60)–H(60C) | 109.5 |
| C(59)–C(61)–H(61A) | 109.5 |
| C(59)–C(61)–H(61B) | 109.5 |
| H(61A)–C(61)–H(61B) | 109.5 |
| C(59)–C(61)–H(61C) | 109.5 |
| H(61A)–C(61)–H(61C) | 109.5 |
| H(61B)–C(61)–H(61C) | 109.5 |
| C(35)–N(1)–C(31) | 118.87(19) |
| C(35)–N(1)–Mo(1) | 118.38(15) |
| C(31)–N(1)–Mo(1) | 122.62(15) |
| C(41)–O(1)–Mo(1) | 121.79(14) |
| C(9)–O(2)–Mo(1) | 138.65(14) |
| C(9)–O(2)–K(1) | 116.36(13) |
| Mo(1)–O(2)–K(1) | 101.96(6) |
| C(17)–O(3)–Mo(1) | 130.80(15) |
| C(13)–O(4)–Mo(1) | 137.97(14) |
| C(13)–O(4)–K(1) | 113.73(13) |
| Mo(1)–O(4)–K(1) | 100.77(6) |
| C(50)–O(5)–C(53) | 112.2(3) |
| C(50)–O(5)–K(1) | 119.54(19) |
| C(53)–O(5)–K(1) | 127.7(2) |
| C(52A)–O(5A)–C(53A) | 110.7(9) |
| C(52A)–O(5A)–K(1) | 115.6(6) |
| C(53A)–O(5A)–K(1) | 118.0(7) |
| C(51A)–O(5B)–K(1) | 126.1(7) |
| C(59)–O(6)–C(56) | 116.0(2) |
| C(11)–F(3)–K(1) | 114.28(13) |
| C(12)–F(6)–K(1) | 121.22(13) |
| C(15)–F(7)–K(1) | 115.44(14) |
| C(16)–F(10)–K(1) | 115.79(13) |
| O(4)–K(1)–O(5) | 145.60(7) |
| O(4)–K(1)–F(10) | 61.58(5) |
| O(5)–K(1)–F(10) | 86.27(7) |

| | |
|---|---|
| O(4)–K(1)–O(5A) | 124.66(16) |
| O(5)–K(1)–O(5A) | 23.23(15) |
| F(10)–K(1)–O(5A) | 72.34(16) |
| O(4)–K(1)–O(2) | 60.07(5) |
| O(5)–K(1)–O(2) | 154.24(7) |
| F(10)–K(1)–O(2) | 118.65(5) |
| O(5A)–K(1)–O(2) | 164.37(16) |
| O(4)–K(1)–F(7) | 60.98(5) |
| O(5)–K(1)–F(7) | 113.03(7) |
| F(10)–K(1)–F(7) | 57.12(5) |
| O(5A)–K(1)–F(7) | 116.38(16) |
| O(2)–K(1)–F(7) | 79.17(5) |
| O(4)–K(1)–F(6) | 99.14(5) |
| O(5)–K(1)–F(6) | 107.74(7) |
| F(10)–K(1)–F(6) | 119.32(5) |
| O(5A)–K(1)–F(6) | 130.65(16) |
| O(2)–K(1)–F(6) | 55.96(5) |
| F(7)–K(1)–F(6) | 63.29(5) |
| O(4)–K(1)–O(5B) | 150.79(17) |
| O(5)–K(1)–O(5B) | 37.77(18) |
| F(10)–K(1)–O(5B) | 98.82(17) |
| O(5A)–K(1)–O(5B) | 60.2(2) |
| O(2)–K(1)–O(5B) | 124.39(18) |
| F(7)–K(1)–O(5B) | 90.51(16) |
| F(6)–K(1)–O(5B) | 70.51(18) |
| O(4)–K(1)–F(3) | 116.89(5) |
| O(5)–K(1)–F(3) | 96.52(6) |
| F(10)–K(1)–F(3) | 172.81(5) |
| O(5A)–K(1)–F(3) | 112.39(16) |
| O(2)–K(1)–F(3) | 57.95(4) |
| F(7)–K(1)–F(3) | 115.75(5) |
| F(6)–K(1)–F(3) | 53.52(5) |
| O(5B)–K(1)–F(3) | 79.69(17) |
| O(4)–K(1)–C(13) | 21.46(5) |
| O(5)–K(1)–C(13) | 130.53(7) |
| F(10)–K(1)–C(13) | 44.36(5) |
| O(5A)–K(1)–C(13) | 115.16(16) |
| O(2)–K(1)–C(13) | 74.35(5) |
| F(7)–K(1)–C(13) | 44.17(5) |
| F(6)–K(1)–C(13) | 97.12(5) |
| O(5B)–K(1)–C(13) | 130.14(17) |
| F(3)–K(1)–C(13) | 132.07(5) |
| O(4)–K(1)–Mo(1) | 35.83(4) |
| O(5)–K(1)–Mo(1) | 162.48(6) |
| F(10)–K(1)–Mo(1) | 97.15(4) |
| O(5A)–K(1)–Mo(1) | 143.16(16) |

| | |
|---|---|
| O(2)–K(1)–Mo(1) | 31.32(3) |
| F(7)–K(1)–Mo(1) | 82.85(4) |
| F(6)–K(1)–Mo(1) | 85.63(3) |
| O(5B)–K(1)–Mo(1) | 155.63(18) |
| F(3)–K(1)–Mo(1) | 82.18(3) |
| C(13)–K(1)–Mo(1) | 55.96(5) |
| C(1)–Mo(1)–O(1) | 95.37(9) |
| C(1)–Mo(1)–O(3) | 92.97(9) |
| O(1)–Mo(1)–O(3) | 158.41(6) |
| C(1)–Mo(1)–O(2) | 98.84(9) |
| O(1)–Mo(1)–O(2) | 102.29(7) |
| O(3)–Mo(1)–O(2) | 96.03(7) |
| C(1)–Mo(1)–N(1) | 94.50(9) |
| O(1)–Mo(1)–N(1) | 79.58(7) |
| O(3)–Mo(1)–N(1) | 79.93(7) |
| O(2)–Mo(1)–N(1) | 166.27(7) |
| C(1)–Mo(1)–O(4) | 177.51(8) |
| O(1)–Mo(1)–O(4) | 86.90(6) |
| O(3)–Mo(1)–O(4) | 85.25(7) |
| O(2)–Mo(1)–O(4) | 79.64(6) |
| N(1)–Mo(1)–O(4) | 86.92(6) |
| C(1)–Mo(1)–K(1) | 134.23(7) |
| O(1)–Mo(1)–K(1) | 118.02(5) |
| O(3)–Mo(1)–K(1) | 67.70(5) |
| O(2)–Mo(1)–K(1) | 46.73(5) |
| N(1)–Mo(1)–K(1) | 120.27(5) |
| O(4)–Mo(1)–K(1) | 43.39(4) |

Symmetry transformations used to generate equivalent atoms:

**Table S4.** Anisotropic displacement parameters ($\text{Å}^2 \times 10^3$) for **1**. The anisotropic displacement factor exponent takes the form: $-2\pi^2$ [ $h^2 a^2 U^{11} + ... + 2\,h\,k\,a^*\,b^*\,U^{12}$]

| | $U^{11}$ | $U^{22}$ | $U^{33}$ | $U^{23}$ | $U^{13}$ | $U^{12}$ |
|---|---|---|---|---|---|---|
| C(1) | 27(1) | 17(1) | 16(1) | 3(1) | 7(1) | 1(1) |
| C(2) | 24(1) | 17(1) | 20(1) | 1(1) | 1(1) | −1(1) |
| C(3) | 25(1) | 23(1) | 24(1) | −2(1) | 8(1) | −3(1) |
| C(4) | 32(2) | 18(1) | 27(1) | −5(1) | 1(1) | −2(1) |
| C(5) | 22(1) | 17(1) | 25(1) | 4(1) | −2(1) | −1(1) |
| C(6) | 26(1) | 26(1) | 36(2) | 0(1) | −2(1) | −4(1) |
| C(7) | 21(1) | 25(1) | 25(1) | 1(1) | 4(1) | −1(1) |
| C(8) | 26(1) | 23(1) | 22(1) | −2(1) | 3(1) | −3(1) |
| C(9) | 30(1) | 18(1) | 22(1) | 4(1) | 3(1) | −3(1) |
| C(10) | 34(2) | 18(1) | 28(1) | 2(1) | 4(1) | −6(1) |
| C(11) | 33(2) | 21(1) | 24(1) | 6(1) | 3(1) | 1(1) |
| C(12) | 37(2) | 19(1) | 23(1) | 4(1) | 5(1) | −2(1) |
| C(13) | 24(1) | 20(1) | 23(1) | 0(1) | 0(1) | −4(1) |
| C(14) | 26(1) | 26(1) | 26(1) | 3(1) | 2(1) | −7(1) |
| C(15) | 26(1) | 27(1) | 25(1) | −1(1) | 1(1) | −6(1) |
| C(16) | 28(2) | 26(1) | 30(2) | 1(1) | −4(1) | −7(1) |
| C(17) | 19(1) | 20(1) | 21(1) | −3(1) | 0(1) | −1(1) |
| C(18) | 21(1) | 25(1) | 19(1) | −2(1) | 1(1) | 1(1) |
| C(19) | 25(1) | 24(1) | 21(1) | −4(1) | 4(1) | 4(1) |
| C(20) | 28(1) | 20(1) | 24(1) | −5(1) | 4(1) | 2(1) |
| C(21) | 24(1) | 19(1) | 21(1) | 0(1) | 3(1) | 1(1) |
| C(22) | 19(1) | 19(1) | 21(1) | 0(1) | 1(1) | 2(1) |
| C(23) | 29(1) | 28(1) | 24(1) | −5(1) | 8(1) | −1(1) |
| C(24) | 34(2) | 48(2) | 31(2) | −12(1) | 14(1) | −13(1) |
| C(25) | 47(2) | 32(2) | 27(2) | 3(1) | 13(1) | 4(1) |
| C(26) | 31(2) | 36(2) | 25(1) | −4(1) | 11(1) | −1(1) |
| C(27) | 47(2) | 20(1) | 33(2) | −8(1) | 14(1) | −3(1) |
| C(28) | 77(2) | 37(2) | 32(2) | −11(1) | 13(2) | −23(2) |
| C(29) | 68(2) | 26(2) | 84(3) | −9(2) | 17(2) | 12(2) |
| C(30) | 77(2) | 18(1) | 39(2) | −8(1) | 18(2) | −11(2) |
| C(31) | 16(1) | 17(1) | 19(1) | −1(1) | 2(1) | −1(1) |
| C(32) | 25(1) | 15(1) | 24(1) | 1(1) | 3(1) | 1(1) |
| C(33) | 26(1) | 20(1) | 21(1) | 4(1) | 2(1) | 1(1) |
| C(34) | 21(1) | 23(1) | 18(1) | −1(1) | 0(1) | 2(1) |
| C(35) | 13(1) | 19(1) | 18(1) | −1(1) | −1(1) | 1(1) |
| C(36) | 19(1) | 18(1) | 18(1) | 1(1) | 3(1) | −1(1) |
| C(37) | 19(1) | 19(1) | 19(1) | 2(1) | 1(1) | 3(1) |
| C(38) | 25(1) | 20(1) | 16(1) | −1(1) | 2(1) | 1(1) |
| C(39) | 25(1) | 15(1) | 20(1) | −2(1) | 3(1) | 2(1) |
| C(40) | 18(1) | 16(1) | 19(1) | 1(1) | 3(1) | −1(1) |
| C(41) | 16(1) | 17(1) | 17(1) | 0(1) | 2(1) | −4(1) |

| | | | | | |
|---|---|---|---|---|---|
| C(42) | 36(2) | 24(1) | 21(1) | −6(1) | −5(1) | 6(1) |
| C(43) | 42(2) | 68(2) | 44(2) | −26(2) | −12(2) | 2(2) |
| C(44) | 87(3) | 29(2) | 24(2) | 1(1) | −4(2) | 10(2) |
| C(45) | 68(2) | 28(2) | 29(2) | −6(1) | −13(1) | 7(2) |
| C(46) | 21(1) | 16(1) | 22(1) | 0(1) | 3(1) | 1(1) |
| C(47) | 21(1) | 21(1) | 33(1) | −2(1) | 2(1) | 2(1) |
| C(48) | 30(2) | 22(1) | 26(1) | 4(1) | −2(1) | 4(1) |
| C(49) | 25(1) | 23(1) | 30(1) | −2(1) | −2(1) | 5(1) |
| C(56) | 29(2) | 32(2) | 30(1) | 1(1) | 7(1) | 2(1) |
| C(57) | 37(2) | 32(2) | 41(2) | −2(1) | 5(1) | 4(1) |
| C(58) | 34(2) | 33(2) | 57(2) | 0(1) | 6(1) | −6(1) |
| C(59) | 40(2) | 27(2) | 31(2) | −7(1) | 1(1) | 2(1) |
| C(60) | 40(2) | 94(3) | 57(2) | −37(2) | −5(2) | −5(2) |
| C(61) | 86(3) | 39(2) | 35(2) | −3(1) | −13(2) | −11(2) |
| N(1) | 16(1) | 16(1) | 19(1) | −1(1) | 2(1) | 0(1) |
| O(1) | 19(1) | 16(1) | 17(1) | −1(1) | 0(1) | −1(1) |
| O(2) | 27(1) | 17(1) | 19(1) | 2(1) | 2(1) | −4(1) |
| O(3) | 27(1) | 16(1) | 21(1) | −1(1) | 7(1) | −2(1) |
| O(4) | 23(1) | 18(1) | 20(1) | −1(1) | 1(1) | −5(1) |
| O(6) | 31(1) | 32(1) | 30(1) | −9(1) | 3(1) | 3(1) |
| F(1) | 30(1) | 32(1) | 31(1) | 6(1) | 6(1) | 2(1) |
| F(2) | 43(1) | 27(1) | 36(1) | 13(1) | 15(1) | −2(1) |
| F(3) | 42(1) | 32(1) | 22(1) | −1(1) | 6(1) | 2(1) |
| F(4) | 31(1) | 33(1) | 28(1) | 2(1) | 6(1) | 4(1) |
| F(5) | 43(1) | 29(1) | 31(1) | 14(1) | 4(1) | 6(1) |
| F(6) | 37(1) | 28(1) | 28(1) | −2(1) | −6(1) | 3(1) |
| F(7) | 38(1) | 38(1) | 25(1) | 5(1) | −5(1) | 4(1) |
| F(8) | 42(1) | 24(1) | 37(1) | −5(1) | −10(1) | 5(1) |
| F(9) | 22(1) | 47(1) | 49(1) | 7(1) | −1(1) | −2(1) |
| F(10) | 53(1) | 32(1) | 28(1) | −8(1) | 0(1) | −12(1) |
| F(11) | 45(1) | 20(1) | 51(1) | −2(1) | −12(1) | −2(1) |
| F(12) | 33(1) | 36(1) | 51(1) | −8(1) | 1(1) | −18(1) |
| K(1) | 42(1) | 27(1) | 24(1) | −5(1) | 6(1) | −6(1) |
| Mo(1) | 20(1) | 14(1) | 15(1) | 0(1) | 2(1) | −2(1) |

**Table S5.** Hydrogen coordinates ( $\times 10^4$ ) and isotropic displacement parameters ($\text{Å}^2 \times 10^3$) for **1**.

| | x | y | z | U(eq) |
|---|---|---|---|---|
| H(3) | −1055 | 729 | 3622 | 29 |
| H(4) | −2489 | 269 | 3272 | 31 |
| H(6A) | −4851 | 189 | 4304 | 44 |
| H(6B) | −4056 | −164 | 3934 | 44 |
| H(6C) | −4602 | 229 | 3395 | 44 |
| H(7) | −4034 | 775 | 5081 | 29 |
| H(8) | −2616 | 1247 | 5434 | 28 |
| H(10A) | −620 | 585 | 5755 | 40 |
| H(10B) | 142 | 232 | 6229 | 40 |
| H(10C) | 558 | 513 | 5502 | 40 |
| H(14A) | 2602 | 2012 | 4328 | 39 |
| H(14B) | 3478 | 2392 | 4543 | 39 |
| H(14C) | 2273 | 2540 | 4395 | 39 |
| H(19) | −1260 | 3434 | 6824 | 28 |
| H(21) | 342 | 3480 | 4866 | 26 |
| H(24A) | −2377 | 2081 | 6070 | 56 |
| H(24B) | −3141 | 2512 | 6152 | 56 |
| H(24C) | −3094 | 2118 | 6808 | 56 |
| H(25A) | −575 | 2375 | 7707 | 52 |
| H(25B) | −815 | 1989 | 7051 | 52 |
| H(25C) | −1578 | 2049 | 7758 | 52 |
| H(26A) | −2769 | 2704 | 7809 | 45 |
| H(26B) | −2737 | 3107 | 7171 | 45 |
| H(26C) | −1771 | 3037 | 7805 | 45 |
| H(28A) | −115 | 4010 | 7259 | 72 |
| H(28B) | 446 | 4459 | 6943 | 72 |
| H(28C) | 1010 | 3970 | 6894 | 72 |
| H(29A) | −1603 | 4257 | 5459 | 88 |
| H(29B) | −1170 | 4621 | 6104 | 88 |
| H(29C) | −1720 | 4159 | 6376 | 88 |
| H(30A) | 1166 | 4108 | 5448 | 66 |
| H(30B) | 611 | 4593 | 5569 | 66 |
| H(30C) | 143 | 4246 | 4909 | 66 |
| H(32) | −137 | 3272 | 3789 | 26 |
| H(33) | −43 | 3008 | 2510 | 27 |
| H(34) | 52 | 2220 | 2278 | 25 |
| H(37) | −700 | 1545 | 2229 | 23 |
| H(39) | 1169 | 438 | 2452 | 24 |
| H(43A) | −1868 | 666 | 931 | 78 |
| H(43B) | −1804 | 1093 | 1523 | 78 |

| | | | | |
|---|---|---|---|---|
| H(43C) | −1791 | 581 | 1862 | 78 |
| H(44A) | 753 | 1089 | 785 | 70 |
| H(44B) | −271 | 1398 | 872 | 70 |
| H(44C) | −308 | 975 | 272 | 70 |
| H(45A) | −381 | 182 | 758 | 63 |
| H(45B) | −191 | 80 | 1680 | 63 |
| H(45C) | 744 | 280 | 1194 | 63 |
| H(47A) | 3098 | 1252 | 4046 | 37 |
| H(47B) | 3395 | 1066 | 3202 | 37 |
| H(47C) | 3914 | 838 | 3987 | 37 |
| H(48A) | 1647 | 251 | 4596 | 39 |
| H(48B) | 2023 | 745 | 4911 | 39 |
| H(48C) | 2865 | 344 | 4821 | 39 |
| H(49A) | 3318 | 74 | 3541 | 39 |
| H(49B) | 2815 | 297 | 2746 | 39 |
| H(49C) | 2110 | −18 | 3276 | 39 |
| H(50) | 2428 | 2368 | 9607 | 53 |
| H(51A) | 1599 | 1576 | 8738 | 66 |
| H(51B) | 2478 | 1553 | 9448 | 66 |
| H(51C) | 2750 | 1775 | 8624 | 66 |
| H(52A) | 615 | 2433 | 9953 | 83 |
| H(52B) | 1103 | 1954 | 10258 | 83 |
| H(52C) | 340 | 1971 | 9477 | 83 |
| H(53) | 1836 | 3023 | 9312 | 38 |
| H(54A) | 2878 | 3079 | 8214 | 72 |
| H(54B) | 2174 | 3530 | 8281 | 72 |
| H(54C) | 1843 | 3144 | 7645 | 72 |
| H(55A) | 107 | 3099 | 8159 | 88 |
| H(55B) | 415 | 3479 | 8812 | 88 |
| H(55C) | −23 | 2991 | 9070 | 88 |
| H(50A) | 2227 | 2174 | 9811 | 53 |
| H(50B) | 1082 | 2179 | 9354 | 53 |
| H(51D) | 2437 | 1242 | 8877 | 82 |
| H(51E) | 1494 | 1417 | 9380 | 82 |
| H(51F) | 2685 | 1517 | 9681 | 82 |
| H(52D) | 2043 | 2993 | 9259 | 51 |
| H(52E) | 2851 | 2747 | 8698 | 51 |
| H(53A) | 833 | 3253 | 7467 | 79 |
| H(53B) | 2050 | 3312 | 7732 | 79 |
| H(53C) | 1172 | 3453 | 8320 | 79 |
| H(56) | 7449 | 1016 | 7931 | 36 |
| H(57A) | 7301 | 493 | 9346 | 55 |
| H(57B) | 8365 | 553 | 8903 | 55 |
| H(57C) | 7394 | 281 | 8485 | 55 |
| H(58A) | 7240 | 1672 | 8708 | 62 |
| H(58B) | 8289 | 1407 | 9008 | 62 |

| | | | | |
|---|---|---|---|---|
| H(58C) | 7250 | 1362 | 9486 | 62 |
| H(59) | 5893 | 408 | 7803 | 39 |
| H(60A) | 4410 | 535 | 8528 | 96 |
| H(60B) | 4068 | 462 | 7616 | 96 |
| H(60C) | 4092 | 967 | 7985 | 96 |
| H(61A) | 5339 | 1240 | 6983 | 81 |
| H(61B) | 5330 | 742 | 6586 | 81 |
| H(61C) | 6418 | 969 | 6901 | 81 |
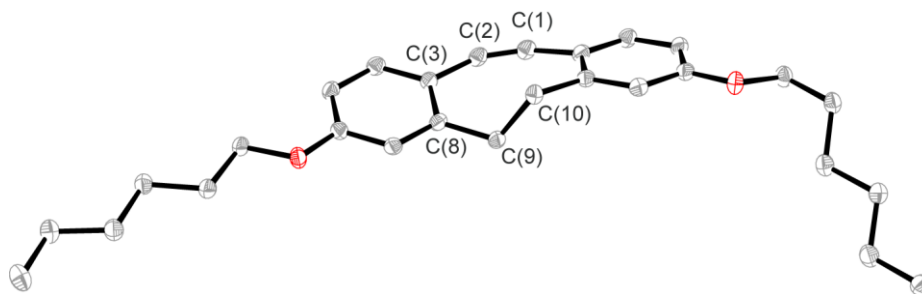
**Table S6.** Crystal data and structure refinement for **2a** (Chapter 2). ORTEP thermal ellipsoids are at the 50% probability level. Color coding: C (gray), O (red). Hydrogen atoms are omitted for clarity.

| | |
|---|---|
| CCDC code | 998198 |
| Empirical formula | $C_{28}H_{36}O_2$ |
| Formula weight | 404.57 |
| Temperature | 100(2) K |
| Wavelength | 1.54178 Å |
| Crystal system | Monoclinic |
| Space group | P2(1)/c |
| Unit cell dimensions | $a$ = 22.8625(8) Å      $\alpha$= 90° |
| | $b$ = 6.7348(2) Å      $\beta$= 97.153(2)° |
| | $c$ = 15.0755(5) Å      $\gamma$ = 90° |
| Volume | 2303.17(13) Å$^3$ |
| Z | 4 |
| Density (calculated) | 1.167 Mg/m$^3$ |
| Absorption coefficient | 0.547 mm$^{-1}$ |
| F(000) | 880 |
| Crystal size | $0.08 \times 0.04 \times 0.01$ mm$^3$ |
| Theta range for data collection | 3.90 to 68.26°. |
| Index ranges | $-27 \leq h \leq 27$, $0 \leq k \leq 8$, $0 \leq l \leq 18$ |
| Reflections collected | 4188 |
| Independent reflections | 4188 [R(int) = 0.0000] |
| Completeness to theta = 67.00° | 99.8% |
| Absorption correction | Semi-empirical from equivalents |
| Max. and min. transmission | 0.995 and 0.974 |
| Refinement method | Full-matrix least-squares on F$^2$ |
| Data / restraints / parameters | 4188 / 0 / 274 |
| Goodness-of-fit on F$^2$ | 1.024 |
| Final R indices [I>2sigma(I)] | R1 = 0.0292, wR2 = 0.0756 |
| R indices (all data) | R1 = 0.0331, wR2 = 0.0779 |
| Largest diff. peak and hole | 0.179 and –0.150 e Å$^{-3}$ |

**Table S7.** Atomic coordinates ($\times 10^4$) and equivalent isotropic displacement parameters ($\text{Å}^2 \times 10^3$) for **2a**. U(eq) is defined as one third of the trace of the orthogonalized $U^{ij}$ tensor.

|        | x          | y         | z         | U(eq)  |
|--------|-----------|-----------|-----------|--------|
| O(2)   | 9790(1)   | 1394(1)   | 8722(1)   | 25(1)  |
| O(1)   | 5384(1)   | −3728(1)  | 6967(1)   | 24(1)  |
| C(3)   | 8728(1)   | −3418(2)  | 7922(1)   | 20(1)  |
| C(17)  | 4964(1)   | −4943(2)  | 6424(1)   | 23(1)  |
| C(6)   | 9474(1)   | −272(2)   | 8464(1)   | 21(1)  |
| C(13)  | 5959(1)   | −4333(2)  | 7070(1)   | 21(1)  |
| C(23)  | 10409(1)  | 1237(2)   | 9049(1)   | 21(1)  |
| C(7)   | 8884(1)   | 93(2)     | 8142(1)   | 20(1)  |
| C(14)  | 6153(1)   | −6175(2)  | 6807(1)   | 22(1)  |
| C(16)  | 7157(1)   | −5230(2)  | 7338(1)   | 21(1)  |
| C(8)   | 8506(1)   | −1445(2)  | 7865(1)   | 20(1)  |
| C(5)   | 9694(1)   | −2196(2)  | 8509(1)   | 21(1)  |
| C(12)  | 6363(1)   | −2952(2)  | 7475(1)   | 21(1)  |
| C(15)  | 6752(1)   | −6604(2)  | 6939(1)   | 23(1)  |
| C(1)   | 7786(1)   | −5445(2)  | 7462(1)   | 23(1)  |
| C(10)  | 7395(1)   | −1867(2)  | 8069(1)   | 20(1)  |
| C(26)  | 11417(1)  | 5824(2)   | 9630(1)   | 26(1)  |
| C(2)   | 8283(1)   | −4884(2)  | 7676(1)   | 22(1)  |
| C(24)  | 10615(1)  | 3360(2)   | 9165(1)   | 22(1)  |
| C(9)   | 7869(1)   | −1055(2)  | 7494(1)   | 20(1)  |
| C(4)   | 9317(1)   | −3762(2)  | 8240(1)   | 22(1)  |
| C(11)  | 6960(1)   | −3358(2)  | 7615(1)   | 20(1)  |
| C(27)  | 12058(1)  | 6262(2)   | 9954(1)   | 28(1)  |
| C(19)  | 4457(1)   | −1831(2)  | 5752(1)   | 25(1)  |
| C(20)  | 3868(1)   | −824(2)   | 5463(1)   | 23(1)  |
| C(22)  | 3359(1)   | 2292(2)   | 4792(1)   | 29(1)  |
| C(21)  | 3936(1)   | 1172(2)   | 5014(1)   | 28(1)  |
| C(18)  | 4395(1)   | −3780(2)  | 6245(1)   | 24(1)  |
| C(25)  | 11260(1)  | 3623(2)   | 9551(1)   | 23(1)  |
| C(28)  | 12191(1)  | 8468(2)   | 10044(1)  | 34(1)  |

**Table S8.** Bond lengths [Å] and angles [°] for **2a**.

| | |
|---|---|
| O(2)–C(6) | 1.3648(16) |
| O(2)–C(23) | 1.4420(15) |
| O(1)–C(13) | 1.3656(15) |
| O(1)–C(17) | 1.4391(16) |
| C(3)–C(4) | 1.3925(18) |
| C(3)–C(8) | 1.4208(18) |
| C(3)–C(2) | 1.4322(19) |
| C(17)–C(18) | 1.5123(18) |
| C(6)–C(5) | 1.3893(19) |
| C(6)–C(7) | 1.3979(17) |
| C(13)–C(14) | 1.3917(19) |
| C(13)–C(12) | 1.3969(19) |
| C(23)–C(24) | 1.5089(18) |
| C(7)–C(8) | 1.3793(19) |
| C(14)–C(15) | 1.3910(19) |
| C(16)–C(15) | 1.3912(19) |
| C(16)–C(11) | 1.4198(19) |
| C(16)–C(1) | 1.4327(17) |
| C(8)–C(9) | 1.5163(17) |
| C(5)–C(4) | 1.3900(19) |
| C(12)–C(11) | 1.3821(17) |
| C(1)–C(2) | 1.2038(19) |
| C(10)–C(11) | 1.5141(18) |
| C(10)–C(9) | 1.5687(17) |
| C(26)–C(27) | 1.5155(18) |
| C(26)–C(25) | 1.5264(19) |
| C(24)–C(25) | 1.5269(17) |
| C(27)–C(28) | 1.5195(19) |
| C(19)–C(18) | 1.5237(19) |
| C(19)–C(20) | 1.5236(18) |
| C(20)–C(21) | 1.521(2) |
| C(22)–C(21) | 1.5203(19) |
| | |
| C(6)–O(2)–C(23) | 119.97(10) |
| C(13)–O(1)–C(17) | 117.40(10) |
| C(4)–C(3)–C(8) | 119.95(12) |
| C(4)–C(3)–C(2) | 126.84(12) |
| C(8)–C(3)–C(2) | 113.12(11) |
| O(1)–C(17)–C(18) | 107.77(11) |
| O(2)–C(6)–C(5) | 125.22(11) |
| O(2)–C(6)–C(7) | 114.14(11) |
| C(5)–C(6)–C(7) | 120.64(12) |
| O(1)–C(13)–C(14) | 124.72(12) |
| O(1)–C(13)–C(12) | 115.20(11) |

| | |
|---|---|
| C(14)–C(13)–C(12) | 120.08(12) |
| O(2)–C(23)–C(24) | 104.48(10) |
| C(8)–C(7)–C(6) | 120.94(12) |
| C(15)–C(14)–C(13) | 119.16(12) |
| C(15)–C(16)–C(11) | 119.96(12) |
| C(15)–C(16)–C(1) | 126.29(12) |
| C(11)–C(16)–C(1) | 113.65(11) |
| C(7)–C(8)–C(3) | 118.59(11) |
| C(7)–C(8)–C(9) | 121.20(11) |
| C(3)–C(8)–C(9) | 120.21(11) |
| C(6)–C(5)–C(4) | 119.01(12) |
| C(11)–C(12)–C(13) | 121.50(12) |
| C(14)–C(15)–C(16) | 121.00(12) |
| C(2)–C(1)–C(16) | 154.40(14) |
| C(11)–C(10)–C(9) | 116.19(11) |
| C(27)–C(26)–C(25) | 114.97(11) |
| C(1)–C(2)–C(3) | 154.44(13) |
| C(23)–C(24)–C(25) | 115.33(11) |
| C(8)–C(9)–C(10) | 115.73(11) |
| C(5)–C(4)–C(3) | 120.87(12) |
| C(12)–C(11)–C(16) | 118.30(12) |
| C(12)–C(11)–C(10) | 121.18(12) |
| C(16)–C(11)–C(10) | 120.51(11) |
| C(26)–C(27)–C(28) | 113.20(12) |
| C(18)–C(19)–C(20) | 112.99(11) |
| C(21)–C(20)–C(19) | 112.59(11) |
| C(20)–C(21)–C(22) | 113.68(11) |
| C(17)–C(18)–C(19) | 113.76(11) |
| C(24)–C(25)–C(26) | 110.39(11) |

Symmetry transformations used to generate equivalent atoms:

**Table S9.** Anisotropic displacement parameters ($\mathring{A}^2 \times 10^3$) for **2a**. The anisotropic displacement factor exponent takes the form: $-2\pi^2$ [ $h^2a^2U^{11} + ... + 2\,h\,k\,a^*\,b^*\,U^{12}$]

|       | $U^{11}$ | $U^{22}$ | $U^{33}$ | $U^{23}$ | $U^{13}$ | $U^{12}$ |
|-------|----------|----------|----------|----------|----------|----------|
| O(2)  | 18(1)    | 20(1)    | 37(1)    | 1(1)     | −2(1)    | −1(1)    |
| O(1)  | 17(1)    | 26(1)    | 27(1)    | −6(1)    | 0(1)     | 1(1)     |
| C(3)  | 20(1)    | 20(1)    | 20(1)    | 0(1)     | 1(1)     | 0(1)     |
| C(17) | 20(1)    | 22(1)    | 27(1)    | −4(1)    | −1(1)    | −2(1)    |
| C(6)  | 19(1)    | 23(1)    | 20(1)    | 1(1)     | 3(1)     | −2(1)    |
| C(13) | 20(1)    | 24(1)    | 19(1)    | 2(1)     | 2(1)     | 0(1)     |
| C(23) | 16(1)    | 25(1)    | 24(1)    | 2(1)     | 2(1)     | 2(1)     |
| C(7)  | 20(1)    | 17(1)    | 24(1)    | 2(1)     | 2(1)     | 2(1)     |
| C(14) | 21(1)    | 21(1)    | 22(1)    | 0(1)     | −1(1)    | −2(1)    |
| C(16) | 21(1)    | 19(1)    | 21(1)    | 1(1)     | 0(1)     | 1(1)     |
| C(8)  | 19(1)    | 23(1)    | 17(1)    | 2(1)     | 2(1)     | 3(1)     |
| C(5)  | 18(1)    | 24(1)    | 22(1)    | 2(1)     | 1(1)     | 3(1)     |
| C(12) | 22(1)    | 21(1)    | 19(1)    | 0(1)     | 4(1)     | 2(1)     |
| C(15) | 23(1)    | 19(1)    | 25(1)    | −1(1)    | 0(1)     | 2(1)     |
| C(1)  | 25(1)    | 17(1)    | 27(1)    | −2(1)    | 0(1)     | 4(1)     |
| C(10) | 19(1)    | 19(1)    | 22(1)    | −3(1)    | 2(1)     | 1(1)     |
| C(26) | 23(1)    | 24(1)    | 29(1)    | −1(1)    | 1(1)     | 0(1)     |
| C(2)  | 22(1)    | 18(1)    | 26(1)    | −1(1)    | 0(1)     | 6(1)     |
| C(24) | 19(1)    | 24(1)    | 23(1)    | 1(1)     | 2(1)     | 1(1)     |
| C(9)  | 19(1)    | 17(1)    | 24(1)    | 2(1)     | 0(1)     | 1(1)     |
| C(4)  | 23(1)    | 20(1)    | 24(1)    | 0(1)     | 2(1)     | 3(1)     |
| C(11) | 20(1)    | 22(1)    | 17(1)    | 1(1)     | 2(1)     | 0(1)     |
| C(27) | 24(1)    | 29(1)    | 29(1)    | −4(1)    | 1(1)     | −3(1)    |
| C(19) | 20(1)    | 25(1)    | 29(1)    | −3(1)    | 3(1)     | −1(1)    |
| C(20) | 21(1)    | 25(1)    | 24(1)    | −3(1)    | 2(1)     | 0(1)     |
| C(22) | 27(1)    | 33(1)    | 29(1)    | 6(1)     | 6(1)     | 3(1)     |
| C(21) | 23(1)    | 27(1)    | 36(1)    | −1(1)    | 4(1)     | −2(1)    |
| C(18) | 19(1)    | 24(1)    | 28(1)    | −2(1)    | 1(1)     | −2(1)    |
| C(25) | 19(1)    | 26(1)    | 24(1)    | −1(1)    | 2(1)     | −1(1)    |
| C(28) | 31(1)    | 33(1)    | 37(1)    | −7(1)    | 6(1)     | −9(1)    |

**Table S10.** Hydrogen coordinates ( $\times 10^4$) and isotropic displacement parameters ($\mathring{A}^2 \times 10^3$) for **2a**.

|         | x      | y      | z      | U(eq) |
|---------|--------|--------|--------|-------|
| H(17A)  | 4897   | −6171  | 6732   | 28    |
| H(17B)  | 5110   | −5268  | 5864   | 28    |
| H(23A)  | 10620  | 547    | 8623   | 26    |
| H(23B)  | 10466  | 532    | 9615   | 26    |
| H(7)    | 8743   | 1390   | 8115   | 25    |
| H(14)   | 5885   | −7108  | 6546   | 26    |
| H(5)    | 10088  | −2434  | 8716   | 25    |
| H(12)   | 6228   | −1732  | 7653   | 25    |
| H(15)   | 6885   | −7828  | 6759   | 27    |
| H(10A)  | 7598   | −2479  | 8603   | 24    |
| H(10B)  | 7174   | −747   | 8259   | 24    |
| H(26A)  | 11317  | 6439   | 9049   | 31    |
| H(26B)  | 11175  | 6440   | 10038  | 31    |
| H(24A)  | 10371  | 4031   | 9554   | 26    |
| H(24B)  | 10553  | 4012   | 8588   | 26    |
| H(9A)   | 7796   | −1642  | 6903   | 24    |
| H(9B)   | 7815   | 367    | 7425   | 24    |
| H(4)    | 9460   | −5056  | 8274   | 27    |
| H(27A)  | 12302  | 5685   | 9538   | 33    |
| H(27B)  | 12163  | 5630   | 10530  | 33    |
| H(19A)  | 4652   | −2086  | 5228   | 30    |
| H(19B)  | 4705   | −937   | 6138   | 30    |
| H(20A)  | 3627   | −1688  | 5051   | 28    |
| H(20B)  | 3663   | −630   | 5982   | 28    |
| H(22A)  | 3102   | 1550   | 4361   | 44    |
| H(22B)  | 3436   | 3568   | 4548   | 44    |
| H(22C)  | 3176   | 2464   | 5325   | 44    |
| H(21A)  | 4110   | 958    | 4467   | 34    |
| H(21B)  | 4207   | 1987   | 5406   | 34    |
| H(18A)  | 4252   | −3498  | 6811   | 29    |
| H(18B)  | 4103   | −4596  | 5895   | 29    |
| H(25A)  | 11511  | 2972   | 9166   | 28    |
| H(25B)  | 11329  | 3007   | 10136  | 28    |
| H(28A)  | 12095  | 9101   | 9474   | 50    |
| H(28B)  | 12603  | 8654   | 10246  | 50    |
| H(28C)  | 11961  | 9043   | 10468  | 50    |